



LUND UNIVERSITY

Blue-green stormwater systems for citywide flood mitigation

Monitoring, conceptualization, modeling, and evaluation

Haghighatafshar, Salar

2019

Document Version:

Publisher's PDF, also known as Version of record

[Link to publication](#)

Citation for published version (APA):

Haghighatafshar, S. (2019). *Blue-green stormwater systems for citywide flood mitigation: Monitoring, conceptualization, modeling, and evaluation*. [Doctoral Thesis (compilation), Division of Chemical Engineering]. Lund University, Faculty of Engineering.

Total number of authors:

1

General rights

Unless other specific re-use rights are stated the following general rights apply:

Copyright and moral rights for the publications made accessible in the public portal are retained by the authors and/or other copyright owners and it is a condition of accessing publications that users recognise and abide by the legal requirements associated with these rights.

- Users may download and print one copy of any publication from the public portal for the purpose of private study or research.
- You may not further distribute the material or use it for any profit-making activity or commercial gain
- You may freely distribute the URL identifying the publication in the public portal

Read more about Creative commons licenses: <https://creativecommons.org/licenses/>

Take down policy

If you believe that this document breaches copyright please contact us providing details, and we will remove access to the work immediately and investigate your claim.

LUND UNIVERSITY

PO Box 117
221 00 Lund
+46 46-222 00 00



Blue-green stormwater systems for citywide flood mitigation

Monitoring, conceptualization, modeling, and evaluation

SALAR HAGHIGHATAFSHAR | CHEMICAL ENGINEERING | LUND UNIVERSITY



Blue-green stormwater systems for citywide flood mitigation

Blue-green stormwater systems for citywide flood mitigation

Monitoring, conceptualization, modeling, and evaluation

Salar Haghighatafshar



LUND
UNIVERSITY

DOCTORAL DISSERTATION

by due permission of the Faculty of Engineering, Lund University, Sweden.
To be defended at Lecture Hall K:C at the Centre for Chemistry and Chemical
Engineering, Naturvetarvägen 14, Lund, on Friday, October 25, 2019, 9:15 AM.


Faculty opponent

Professor Wolfgang Rauch

Department of Infrastructure Engineering, University of Innsbruck

| | | |
|---|---|-------------------------------------|
| Organization LUND UNIVERSITY Water and Environmental Engineering, Department of Chemical Engineering P.O. Box 124, SE-221 00 Lund, Sweden Author(s) Salar Haghighatafshar | Document name DOCTORAL THESIS | |
| | Date of issue 2019-09-16 | |
| | Sponsoring organizations Sweden Water Research AB, The Swedish Water and Wastewater Association via VA-teknik Södra, VINNOVA, J. Gust. Richert Foundation (at SWECO), VA SYD, DHI, Skånska Ingenjörsklubben | |
| Title and subtitle Blue-green stormwater systems for citywide flood mitigation <i>Monitoring, conceptualization, modeling, and evaluation</i> | | |
| Abstract <p>Considering the growth in urbanization, leading to an increase in impervious surfaces, and the changing climate, enhancing the intensity and frequency of rainfall events, existing urban drainage networks—separate or combined sewer systems—are presumed to face substantially elevated hydraulic loads, causing pluvial floods in urban areas.</p> <p>There are several ways to address these challenges. Cities can invest in replacing existing pipes with new larger pipes to enhance the hydraulic capacity of the drainage network. This solution is considered to be extremely expensive and unsustainable. An alternative solution is to manipulate urban surfaces by constructing blue-green (open) stormwater systems. These systems are built on urban surfaces and include approaches that mimic natural processes, such as infiltration, evaporation, transpiration, pond storage, and slow transport of stormwater through ditches. The implementation of blue-green stormwater systems in dense cities would, to some extent, relieve the overload. However, the method for identifying urban areas in which the implementation of blue-green stormwater systems would have a larger effect hydraulically on the existing sewer network is unestablished.</p> <p>Thus, general aim of this thesis was to develop a method for studying the interactions between piped drainage networks and blue-green stormwater systems on the city-scale, performed in four steps, which shape the backbone of this thesis:</p> <ul style="list-style-type: none"> • An existing blue-green stormwater system—i.e. the Eco-city of Augustenborg in Malmö—was examined to understand how such systems work, locally and regarding the surrounding neighborhoods. • A simple conceptual model for blue-green stormwater systems was proposed. • Based on the proposed concept, a fast, easy-to-use, and robust modeling tool was developed, making it possible to simulate the interaction between blue-green stormwater systems and sewer networks. • The modeling tool was supplemented with a hydroeconomic optimization algorithm and evaluated on the city-scale to identify the most effective site and size for blue-green stormwater systems throughout the catchment of the sewer network. <p>The developed method and toolchain constitute a new platform for increasing our understanding of complex urban drainage networks. This platform is also a starting point for the development of a more reliable tool for the initial screening of urban catchments to identify urban areas in which it is hydraulically and economically efficient to construct neighborhood-scale blue-green stormwater systems.</p> | | |
| Keywords: blue-green measures, drainage system, flooding, flood mitigation, hydrodynamic modeling, rainfall-runoff, stormwater | | |
| Classification system and/or index terms (if any) | | |
| Supplementary bibliographical information | | Language: English |
| ISBN 978-91-7422-681-2 (print) | | ISBN 978-91-7422-682-9 (pdf) |
| Recipient's notes | Number of pages: 133 | Price |
| | Security classification | |

I, the undersigned, being the copyright owner of the abstract of the aforementioned dissertation, hereby grant to all reference sources permission to publish and disseminate the abstract of the aforementioned dissertation.

Signature  Date 2019-09-16

Blue-green stormwater systems for citywide flood mitigation

Monitoring, conceptualization, modeling, and evaluation

Salar Haghighatafshar



LUND
UNIVERSITY

Front cover photo by Salar Haghighatafshar
Back cover photo by ©Fotokon | Adobe Stock

Copyright pp 1-46 (Salar Haghighatafshar)

Paper 1 © Elsevier B.V.

Paper 2 © by the Authors (Open access)

Paper 3 © Elsevier B.V.

Paper 4 © Elsevier B.V.

Lund University
Faculty of Engineering
Water and Environmental Engineering, Department of Chemical Engineering

ISBN 978-91-7422-681-2 (print)

ISBN 978-91-7422-682-9 (pdf)

Printed in Sweden by Media-Tryck, Lund University
Lund 2019



Media-Tryck is an environmentally
certified and ISO 14001:2015 certified
provider of printed material.
Read more about our environmental
work at www.mediatryck.lu.se

MADE IN SWEDEN 

The difference between state and knowledge - in questions of belief - is the same as that between talking [about qualities] and having them.

The Muqaddimah – Ibn Khaldun (1332-1406 A.D.)

Table of Contents

| | |
|--|-----------|
| Acknowledgments | i |
| Summary..... | iii |
| چکیده‌ی رساله (Abstract in Persian) | vii |
| Populärvetenskaplig sammanfattning (Popular science summary in Swedish) | ix |
| List of papers | xi |
| My contribution to the papers | xiii |
| Related publications | xv |
| Nomenclature and abbreviations | xvii |
| 1 Introduction | 1 |
| 1.1 Why blue and green? | 2 |
| 1.2 Aim | 5 |
| 1.3 Outline of the thesis | 5 |
| 2 Eco-city Augustenborg: A blue-green retrofit..... | 7 |
| 2.1 Stormwater management | 9 |
| 2.2 Rainfall-runoff measurements | 11 |
| 2.2.1 Error sources..... | 14 |
| 2.3 When it rains in Augustenborg | 15 |
| 2.3.1 Local effects of a blue-green system..... | 15 |
| 2.3.2 Downstream effects of a blue-green system | 17 |
| 3 Model development | 19 |
| 3.1 Concept development | 20 |
| 3.2 Mathematical formulation of the concept | 21 |
| 3.3 Joint model architecture..... | 25 |
| 4 From meso- to macroscale: Upscaling and optimization | 29 |
| 4.1 Hydroeconomic optimization | 30 |

| | | |
|-----|--------------------------------------|----|
| 4.2 | Implementation of the toolchain..... | 33 |
| 5 | Conclusions | 37 |
| 6 | Future research..... | 39 |
| 7 | References..... | 41 |

Acknowledgments

The story of this PhD project was initiated long ago by *Henrik Aspegren* and *Jes la Cour Jansen* and has continued with my participation in this project and the pursuit of its goals. Therefore, I thank *Henrik* and *Jes* for conceiving of such a bright research idea and maintaining all of the required financing.

I owe the realization of this thesis to many people with whom I have had the honor to work. I express my sincere gratitude to my main supervisor, *Karin Jönsson*, and my assistant supervisors—*Jes la Cour Jansen*, *Henrik Aspegren*, and *Maria Roldin*—who have made essential contributions throughout all of the stages of my PhD study. Thank you for all of the fruitful discussions and professional and emotional support. Your encouraging attitudes and trust in me were indeed major driving forces for my progress and development in research.

I also thank the personnel at VA SYD—namely, *Tomas Wolf*, *John Hägg*, *Åsa Sönnér*, *Leif Johansson*, *Jan Hyvönen*, *Tom Almén*, *Engin Alioğlu*, and *Timmy Kristensson*—for their invaluable help with practicalities with regard to field measurements. I also thank *Hans Bertil Wittgren*, *Marianne Beckmann*, *Susanne Steen Kronborg*, *Emma Falk*, and *Kristina Hall*, also at VA SYD, for their support during the course of this PhD project.

I am grateful to all of my co-authors, especially *Mikael Yamanee-Nolin* and *Anders Klinting*, for their vital contributions of Python coding and programming. Thanks to *Lars-Göran Gustafsson* and *Magnus Larson* for generously sharing their long experience and invaluable expertise in hydrodynamic modeling with me. I thank *Per Becker*, who has been a source of inspiration and unconditional help and support.

I am grateful to my ex-officemate, research partner, discussion comrade, and, above all, dear friend, *Hamse Kjerstadius*, or *Hamsman* (as some call him), to whom I owe much. You have no idea how all of those moments of exchanging ideas and reflecting over countless socio-political, cultural, and sometimes scientific issues provided me with new perspectives on life and the world.

I thank my dear colleagues and fellow PhD students in the Department of Chemical Engineering at LTH, Lund University, especially in the Water and Environmental Engineering group, for creating a lovely, comfortable, and constructive work environment.

Thank you, *Gertrud Persson*, for being a nice and helpful friend to me and my family all of this time.

I have also had the honor of supervising several talented and smart students in their master's theses, whom I sincerely acknowledge.

I am thankful to my project partners in the Sustainable Urban Flood Management project (SUrF) at Lund University and the Future City Flow project at Sweden Water Research for all of the interesting and constructive discussions over the past several years. I sincerely thank *Misagh Mottaghi* for helping me develop illustrations for this thesis. Thanks to *Henrik Thorén* for allowing me to use his photo, taken at Augustenborg under extreme rainfall on August 31, 2014 (Figure 8).

During my PhD project, I have had the opportunity of receiving financial support from Sweden Water Research AB, VINNOVA (Future City Flow project), the Swedish Water and Wastewater Association (*Svenskt Vatten*) through *VA-teknik Södra*, J. Gust. Richert Foundation at SWECO, and *Skånska Ingenjörsklubben*.

Many thanks to DHI Sweden and DHI Denmark for giving me access to their commercial software products—MIKE Urban, MIKE 21, MIKE Flood, and MIKE Operations—throughout my tenure.

I express my deep gratitude to my dear brother, *Sina Haghighatafshar*, for proofreading the whole thesis. I am very grateful to my dear friends, *Kurosh Aliyani*, *Mehdi Mousavi*, and *Saeed Edalatjou*, who kindly proofread and revised the Persian abstract of this dissertation. I also thank *Michael Cimbritz* for proofreading the Swedish popular science summary of this thesis.

Finally, my most intimate gratitude goes to my lovely family. I am truly grateful to my parents, who have always supported me with love, care, encouragement, and passion throughout my life. I am also deeply indebted to *Mana*, my beautiful wife, and my sweet children, *Sam* and *Elsa*. I would have barely made it to the end of this road without your love and dedication. I love you all!

Summary

Based on the growth in urbanization, which has increased the amount in impervious surfaces, and the changing climate, which has intensified the extent and frequency of rainfall events, existing urban drainage networks—separate or combined sewer systems—are presumed to face substantially greater hydraulic loads, causing pluvial floods in urban areas.

There are several means of addressing these challenges. Cities can invest in replacing existing pipes with newer, larger pipes to improve the hydraulic capacity of the drainage network, but this option would be extremely expensive and unsustainable. An alternative solution is to alter urban surfaces by constructing blue-green (open) stormwater systems, which include approaches that mimic natural processes, such as infiltration, evaporation, transpiration, pond storage, and slow transport of stormwater through ditches. The implementation of blue-green stormwater systems in dense cities would, to a certain extent, mitigate this overload. However, there is no method for identifying urban areas in which the implementation of blue-green stormwater systems would have a larger effect hydraulically on the existing sewer network.

Thus, general aim of this thesis was to develop a method for studying the interactions between piped drainage networks and blue-green stormwater systems on the city scale, comprising four steps:

- An existing blue-green stormwater system—i.e. the Eco-city of Augustenborg in Malmö—was examined to understand how such systems work, locally and regarding the surrounding neighborhoods.
- A simple conceptual model for blue-green stormwater systems was proposed.
- Based on the proposed concept, a rapid, easy-to-use, and robust modeling tool was developed, making it possible to simulate the interaction between blue-green stormwater systems and sewer networks.
- The modeling tool was complemented by a hydroeconomic optimization algorithm and evaluated on the city scale to identify the most effective site and size for blue-green stormwater systems throughout the catchment of the sewer networks.

This thesis examined a specific setup of blue-green stormwater systems, suggested to be called *mesoscale blue-green stormwater systems*. These systems consist of multiple interconnected blue-green measures for retaining and detaining runoff that have a pronounced role in the transformation of neighborhoods into large blue-green

retention cells. The Eco-city of Augustenborg is an archetype of mesoscale blue-green stormwater systems.

A case study in Augustenborg was performed, encompassing onsite rainfall-runoff measurements and extensive 1D/2D modeling. This study revealed that the mesoscale blue-green systems in Augustenborg are effective in controlling and confining surface floods at the local level. The influence of the mesoscale systems was not limited to the local boundaries, also affecting the surrounding pipe-bound catchments.

The case study in Augustenborg illustrated that the outflow hydrograph from a mesoscale blue-green stormwater system under a 100-year rainfall is equivalent to that of a 6.5-year rainfall from a conventional pipe-bound catchment. This substantial downsizing can relieve the hydraulic pressure that builds up in receiving sewer systems that are designed to handle rainfalls of up to a specific recurrence interval. Also, the spatial distribution of constituent retention components (i.e., blue-green measures) in a mesoscale blue-green stormwater system governs the hydrographical characteristics of the final discharge from the system. This observation then formed the basis for the conceptualization of mesoscale blue-green stormwater systems.

The concept of mesoscale blue-green systems was further developed into a mathematical model that simulated the final outflow from the system. This model used the mass conservation principle, but for greater simplicity and simulation speed, it did not include a detailed description of the flow process that follows the conservation of momentum. Thus, a nonlinear reservoir model was introduced to generate the detention effects in the outflow hydrograph. The model successfully simulated the peak flow, lag time, and overall characteristics of the resulting hydrograph. The rapid simulation speed of the mathematical model facilitated city-scale simulations in studying how the interaction between blue-green implementations and existing sewer networks can be optimized for sustainable flood mitigation.

Subsequently, a software program for cosimulation of mesoscale systems and sewer networks was architected, and a multiobjective optimization algorithm was docked with the cosimulation model. The software was applied to the large catchment area of a combined sewer system in Malmö, Sweden, encompassing an area of over 950 ha, to hydroeconomically identify the optimal sizes and locations of mesoscale systems to be retrofitted in the catchment. The optimization was based solely on flooding costs and the outlays for construction and maintenance of blue-green systems. Consequently, the results tentatively implied that the safety margins for economic justification of mesoscale retrofits in the framework of a large-scale combined sewer network are relatively small. This finding encourages a more detailed and thorough survey of the costs and benefits of blue-green systems. It is

anticipated that monetizing the advantages of blue-green systems, such as improved biodiversity, mitigation of urban heat islands, enhanced quality of runoff, and greater neighborhood amenities (by juxtaposing water and greenery), will have a considerable impact on the outcome of the optimization.

The results from the model also imply that when blue-green retrofits are drained into the original sewer network, there are blue-green retrofit scenarios in which the overall flood performance of the sewer network deteriorates in terms of the number of flooded manholes. This conclusion is tentatively associated with the high complexity of networks on the city scale, through which even retained and detained blue-green discharges can coincide with peak flows in the pipe, giving rise to hydraulic head and, hence, flooding. Thus, the discharge from mesoscale blue-green retrofits should preferably not be connected to the original network if the economy and local circumstances allow. In other words, it is hydraulically safer and more beneficial, with regard to the underlying sewer network, to eliminate the impact of the catchment than to discharge detained and delayed flow to the downstream network.

The more stringent demands for flood mitigation in the context of combined sewer networks and the large areas of city-scale catchments (leading to high dimensionality and complexity) render optimization a challenging issue. Thus, further enhancement of the method is required to screen urban catchments to identify areas in which it would be hydraulically and economically efficient to retrofit blue-green stormwater systems. The resulting platform will help users better understand the complex nature of sewer networks in their interaction with mesoscale blue-green stormwater systems.

سطح شهر به صورت کلان تعبیه می‌شود، به نحوی که تأثیری مثبت روی ارتقای کارکرد و کاهش بار هیدرولیکی شبکه‌ی زهکشی شهری بگذارد.

فرضیه‌ی اصلی رساله‌ی حاضر این است که ارتقای تمهیدات آبی-سبز کنترل رواناب از میان‌مقیاس به کلان‌مقیاس - یا به عبارتی پیاده‌سازی تمهیدات میان‌مقیاس در سطح شبکه‌ی زهکشی شهری به صورت کلان - منجر به کاهش چشم‌گیر آب‌گرفتگی معابر، پس‌زدگی فاضلاب و خسارت‌های ناشی از آن خواهد شد. بنا بر این فرضیه، هدف کلی این رساله، توسعه‌ی روشی کارآمد و قابل‌استفاده برای مطالعه‌ی اثرات سیستم‌های آبی-سبز کنترل رواناب بر میزان بار هیدرولیکی وارد بر شبکه‌ی زهکشی شهری است. چهار مرحله‌ی زیر برای دستیابی به این هدف در قالب این رساله تعریف و اجرا شده است:

- **مطالعه‌ی میدانی و شناخت:** سیستم کنترل رواناب آبی-سبز میان‌مقیاس منحصر به فرد در محله‌ی آگوستنبوری (Augustenborg) در شهر مالمو (Malmö) سوئد، مورد مطالعه و ارزیابی قرار گرفت. این مطالعه به اثرات محلی سیستم موجود، بازدهی آن تحت بارندگی‌های شدیدتر از بار طراحی و نحوه‌ی تعامل هیدرولیکی آن با حوضه‌ها و مناطق اطراف در بالادست و پایین‌دست توجه داشت (مقاله‌ی پیوست I).
- **مفهوم‌سازی:** بر اساس دانش و شناخت به دست آمده در مرحله‌ی فوق، یک مدل مفهومی ساده و کارکردی برای سیستم‌های کنترل رواناب آبی-سبز تعریف و پیشنهاد شد (مقاله‌ی پیوست II).
- **مدل‌سازی:** بر اساس مدل مفهومی پیشنهادی در مرحله‌ی قبل، یک ابزار مدل‌سازی هیدرولوژیکی و هیدرولیکی کاربرپسند، سریع و قابل اعتماد برای شبیه‌سازی هیدروگراف جریان خروجی از سیستم‌های آبی-سبز میان‌مقیاس ساخته شد. مدل پیشنهادی فوق طی یک الگوریتم خاص به نرم‌افزار تک-بعدی MIKE Urban (محصول شرکت DHI) متصل شد. مدل ترکیبی حاصله، امکان شبیه‌سازی و مطالعه‌ی تعامل و برهم‌کنش بین سیستم‌های آبی-سبز و شبکه‌ی زهکشی شهری را در مقیاس کلان (کل شهر) امکان‌پذیر نمود (مقاله‌های پیوست III و IV).
- **بهینه‌سازی:** الگوریتم بهینه‌سازی با تقریب خطی و قابلیت محدودسازی به مدل ترکیبی ساخته شده در مرحله‌ی پیشین اضافه شد. مدل بهینه‌سازی پیشنهادی در این رساله، از محاسبات و تخمین‌های اقتصادی هزینه-فایده، برای تعیین محل بهینه‌ی ساخت و تعبیه‌ی تمهیدات کنترل رواناب آبی-سبز (مناطق بالقوه) و همچنین تعیین ظرفیت بهینه‌ی مورد نیاز برای این تمهیدات استفاده می‌کند (مقاله‌ی پیوست IV).

بر اساس یافته‌های این رساله، سیستم‌های کنترل رواناب آبی-سبز می‌توانند جریان خروجی از یک منطقه به شبکه‌ی زهکشی شهری را به حد قابل ملاحظه‌ای کاهش دهند. اندازه‌گیری‌های میدانی و مدل مفهومی توسعه داده شده در این پژوهش نشان داد که جریان خروجی از یک سیستم آبی-سبز تابع چیدمان و نحوه‌ی قرارگیری عناصر تشکیل‌دهنده‌ی آن است. همچنین نشان داده شد که انتخاب تصادفی و بدون مطالعه‌ی محل پیاده‌سازی این سیستم‌ها در سطح شهر می‌تواند منجر به افزایش بار هیدرولیکی شبکه‌ی زهکشی شود. روش و زنجیره‌ی ابزار¹ توسعه داده شده در این پژوهش بستر جدیدی برای شناخت بیشتر و بهتر سیستم‌های پیچیده‌ی زهکشی شهری فراهم می‌کند.

¹ Toolchain

چکیده رساله (Abstract in Persian)

طبق برآورد سازمان ملل متحد، بیش از دو سوم جمعیت کره‌ی زمین در سال ۲۰۵۰ ساکن مناطق شهری خواهند بود. هر قدر فضاهای شهری و جمعیت ساکن در شهرها بیش‌تر شوند، سطوح نفوذناپذیر هم افزایش می‌یابد. از سویی دیگر، تغییرات اقلیمی هم عدم قطعیت‌های زیادی را به الگوهای بارندگی تحمیل می‌کند که به شکل بارندگی‌های بسیار شدید و با فواصل زمانی نسبتاً کوتاه - به‌خصوص در مناطق اروپای شمالی - بروز پیدا می‌کند. این دو مسأله‌ی عمده، به همراه عوامل متعدد دیگر سبب خواهد شد که ظرفیت هیدرولیکی شبکه‌ی زهکشی شهری - که در اروپا و بسیاری از شهرهای جهان به صورت شبکه‌ی لوله‌های زیرزمینی طراحی و ساخته شده است - پاسخگوی حجم رواناب تولید شده در این شرایط جدید نباشد. این افزایش شدید رواناب نسبت به ظرفیت هیدرولیکی نسبتاً ثابت شبکه‌ی زهکشی شهری، منجر به وقوع آب‌گرفتگی‌های پی‌درپی در معابر شهری و پس‌زدگی فاضلاب در ساختمان‌های مسکونی و اداری متصل به شبکه‌ی جمع‌آوری فاضلاب در هم^۱ خواهد شد.

یکی از رهیافت‌های مواجهه با چالش‌های فوق‌الذکر، استفاده از زیرساخت‌های آبی-سبز^۲ در مدیریت رواناب شهری است. رهیافت آبی-سبز کنترل رواناب به دسته‌ای از تمهیدات و سازه‌ها اطلاق می‌شود که در آن‌ها، رواناب شهری مشابه آن‌چه در طبیعت برای آب باران رخ می‌دهد، مدیریت می‌شود. برای مثال، تمهیداتی مانند حوضچه‌های نفوذپذیر کنترل سیلاب (حوضچه‌های خشک)، حوضچه‌های نفوذناپذیر برای کاهش سرعت جریان (حوضچه‌های تر)، بام‌های سبز، باغچه‌ی باران^۳ و کانال‌ها یا نهرهای باز، همه جزو عناصر آبی-سبز کنترل رواناب هستند که در سطح شهر و به‌صورت روباز تعبیه می‌شوند.

این رساله، انواع پیاده‌سازی تمهیدات آبی-سبز در محیط‌های شهری را به سه دسته‌ی مختلف تقسیم می‌کند:

- «تمهیدات آبی-سبز خردمقیاس» - *Microscale* - که به صورت عناصری پراکنده و منفرد از یکدیگر در سطوح شهری تعبیه و خروجی‌های آن‌ها مستقیماً به شبکه زهکشی شهری متصل می‌شوند.
- «تمهیدات آبی-سبز میان‌مقیاس» - *Mesoscale* - که در آن مجموعه‌ای از انواع عناصر آبی-سبز کنترل رواناب در یک منطقه/محله‌ی شهری از بالادست تا پایین‌دست به‌صورت زنجیره‌ای ایجاد می‌شوند، به‌نحوی که جریان خروجی از اجزای بالادستی تشکیل‌دهنده‌ی سیستم آبی-سبز میان‌مقیاس به اجزای پایین‌دستی سیستم سرریز می‌شود. جریان خروجی نهایی بعد از سرریز از پایین‌دست‌ترین عنصر آبی-سبز سیستم وارد شبکه‌ی زهکشی شهری یا آب‌پذیرنده^۴ می‌شود.
- «تمهیدات آبی-سبز کلان‌مقیاس» - *Macroscale* - که در آن تعداد معتدلی از تمهیدات میان‌مقیاس در

^۱ Combined Sewer Network

^۲ Blue-green infrastructure

^۳ Rain garden

^۴ Receiving water

Populärvetenskaplig sammanfattning (Popular science summary in Swedish)

Enligt FN kommer mer än två tredjedelar av världens befolkning år 2050 att bo i urbana områden. Detta betyder att vi kommer att ha större städer vilket in sin tur innebär fler hårdgjorda ytor som tak och asfalterade ytor. Klimatförändringarna medför också mer frekventa och kraftigare regn. Kombinationen av allt fler hårdgjorda ytor och ökande regnintensitet gör att de befintliga ledningsnäten i våra städer som ska ta hand om dagvattnet blir överbelastade och därför kommer vi att få urbana översvämningar oftare än vad systemen dimensionerats för. *Dagvatten* är det vatten som rinner av markytan vid nederbörd.

Det finns olika sätt att möta de här svårigheterna. Man kan utöka ledningsnätets kapacitet genom att bygga fördröjningsmagasin och genom att ersätta de befintliga nedgrävda ledningarna med nya större ledningar. Dessa lösningar blir både dyra och ohållbara eftersom de inte ger den flexibilitet som behövs för att hantera framtidens osäkra klimatförhållanden. Oavsett hur stor ledning eller hur stort fördröjningsmagasin som byggs, kommer systemet att ha en begränsad kapacitet som kan överskridas vid något regntillfälle. Dessutom fungerar alltför stora ledningar dåligt vid låga flöden, vilket trots allt kommer att vara fallet merparten av tiden. Den alternativa lösningen är att förändra urbana ytor genom att anlägga blå-gröna (öppna) dagvattensystem. Blågröna dagvattensystem anläggs på ytan och härmar naturens processer för avrinningshantering, genom infiltration, avdunstning, transpiration (avdunstning via växter), magasinering i dammar och långsam avledning av vattenflöden i diken. Exempel på sådana lösningar är gröna tak, dammar, kanaler och svackdiken. När man inför de här blågröna lösningarna i den täta staden, avlastar man det befintliga ledningsnätet, men det är svårt att veta *hur stora* blågröna dagvattensystem som behövs och *var* i staden de bör anläggas för att uppnå bästa effekt. Det generella målet med denna avhandling var därför att utveckla en metodik och ett verktyg för att studera hur vi med blågröna lösningar kan minska risken för och konsekvenserna av översvämningar i en hel stad.

För att kunna uppnå detta mål togs fyra viktiga steg:

- Flöden från ett blågrönt dagvattensystem i Ekostaden Augustenborg i Malmö, undersöktes och utvärderades för att förstå hur sådana system fungerar lokalt och i samspel med andra stadsdelar.
- En enkel beskrivning av blågröna dagvattensystem föreslogs.

- Baserat på det föreslagna konceptet utvecklades ett förenklat modelleringsverktyg - lätt att använda, snabbt och robust - vilket möjliggör simulering av interaktionen mellan blågröna dagvattensystem och ledningsnät.
- Modelleringsverktyget kompletterades med en storskalig, flödesbaserad och ekonomisk optimeringsfunktion för att kunna ta fram bästa placering och utformning av blågröna dagvattensystem.

Studien visade att blågröna dagvattensystem kraftigt kan minska utflödet från ett område till ett ledningsnät. Det visades också att utflödet beror på i vilken ordning de blågröna lösningarna är placerade i systemet. Men det kan vara så att översvämningsrisken till och med ökar om de blågröna systemen inte införs på ett genomtänkt sätt i städer.

List of papers

The backbone of this thesis consists of the following papers, which are referred to in the text by Roman numerals I-IV:

Paper I Haghighatafshar, S., Nordlöf, B., Roldin, M., Gustafsson, L.-G., la Cour Jansen, J. & Jönsson, K. (2018). Efficiency of blue-green stormwater retrofits for flood mitigation – Conclusions drawn from a case study in Malmö, Sweden. *Journal of Environmental Management*, 207, 60–69.

Paper II Haghighatafshar, S., la Cour Jansen, J., Aspegren, H. & Jönsson, K. (2018). Conceptualization and schematization of mesoscale sustainable drainage systems: a full-scale study. *Water*, 10(8), 1041.

Paper III Haghighatafshar, S., Yamanee-Nolin, M. & Larson, M. (2019). A physically based model for mesoscale SuDS – an alternative to large-scale urban drainage simulations. *Journal of Environmental Management*, 240, 527-536.

Paper IV Haghighatafshar, S., Yamanee-Nolin, M., Klinting, A., Roldin, M., Gustafsson, L.-G., Aspegren, H. & Jönsson, K. (2019). Hydroeconomic optimization of mesoscale blue-green stormwater systems at the city level. *Journal of Hydrology*, 578, Article 124125.

Paper I and **Paper III**, published in the *Journal of Environmental Management*, as well as **Paper IV**, published in the *Journal of Hydrology*, are reprinted in this thesis according to the right that is granted in Elsevier's publishing agreement. **Paper II**, published in *MDPI Water*, is reprinted under the Creative Common Attribution License, CC BY 4.0, for open-access publishing.

My contribution to the papers

Paper I *Henrik Aspegren* owned the original idea of the research question regarding the in-depth investigation of *Augustenborg* through onsite rainfall-runoff measurements. I designed the technical framework of the study, with input from my supervisors, and applied for supplementary funding to build a research team. I took part in discussions on appropriate locations for the installation of flowmeters. I helped *Tomas Wolf* (VA SYD) program and install the flowmeters at the designated locations. I carried out the field work regarding the maintenance of the flowmeters and the data acquisition. I participated in the model setup, analyzed the results, and wrote the final manuscript with input from my supervisors and co-authors.

Paper II I generated the idea of the paper; carried out the field work, including installing and maintaining the flowmeters; and performed the data acquisition. I analyzed and interpreted the data, developed the conceptual model, and wrote the final manuscript with input from my supervisors.

Paper III I developed the concept and the mathematical representation of the model with input from *Magnus Larson*. I carried out the required field work and data acquisition. With *Mikael Yamanee-Nolin*, I analyzed and evaluated the model output compared with the observed data and wrote the final manuscript with input from my co-authors.

Paper IV I introduced the idea of the study, formulated the research project, applied for supplementary funding, built a research team, and contributed to the final method. All authors took part equally in the discussions regarding the development of the software logics and algorithm. *Mikael Yamanee-Nolin* and *Anders Klinting* contributed substantially to programming, coding, and implementing the developed algorithm. I analyzed and interpreted the results of the study and composed the final manuscript with input from my co-authors.

Related publications

Berndtsson, R., Becker, P., Persson, A., Aspegren, H., **Haghighatafshar, S.**, Jönsson, K., Larsson, R., Mobini, S., Mottaghi, M., Nilsson, J., Nordström, J., Pilesjö, P., Scholz, M., Sternudd, C., Sörensen, J. & Tussupova, K. (2019). Drivers of changing urban flood risk: a framework for action. *Journal of Environmental Management*, 240, pp. 47-56.

Haghighatafshar, S., la Cour Jansen, J., Aspegren, H., Lidström, V., Mattsson, A. & Jönsson, K. (2014). Storm-water management in Malmö and Copenhagen with regard to climate change scenarios. *Journal of Water Management and Research* (Tidskriften Vatten), 70 (3), pp. 159-168.

Haghighatafshar, S. (2014). Malmö and Copenhagen: Similar climate – different strategies. *Teknik & Miljö* (December 2014, Denmark), pp. 30-31.

Nomenclature and abbreviations

| Item | Description | Unit |
|--------------|---|----------|
| A_{BG} | The area of the blue-green retrofit in the sub-catchment | ha |
| A_{SC} | Total area of the target sub-catchment | ha |
| $A_{Tot,BG}$ | Total area of the blue-green retrofit in the model | ha |
| C_{act} | Uniform annual cost of flood-mitigating actions | SEK/year |
| c_{BG} | Construction cost of blue-green systems per hectare | SEK/ha |
| CDS | Chicago Design Storm | - |
| C_{flood} | Uniform annual cost of flood damage | SEK/year |
| c_{fi} | Damage cost per flooded node (manhole) | SEK/node |
| $COBYLA$ | Constrained Optimization by Linear Approximation | - |
| CP_N | Connection point between the Northern blue-green system and the sewer network | - |
| CP_P | Connection point between the stormwater pipe system and the sewer network | - |
| CP_S | Connection point between the Southern blue-green system and the pipe network | - |
| $DCIA$ | Directly Connected Impervious Area | ha |
| DHI | Danish Hydraulic Institute | - |
| EIA | Effective Impervious Area | ha |
| F_{BG} | Fraction of the sub-catchment converted to blue-green system | - |
| H | Hydraulic head in the model nodes | m |
| H_{max} | Maximum hydraulic head in the model nodes | m |
| i | Interest rate | % |

| | | |
|-------------|---|---------------------|
| <i>IPCC</i> | Intergovernmental Panel on Climate Change | - |
| k | Nonlinear reservoir routing parameter (<i>coefficient</i>) | 1/min |
| L | Technical lifespan of constructed systems | year |
| M | Net annual wage for maintenance per hectare blue-green system | SEK/(year.ha) |
| m | Nonlinear reservoir routing parameter (<i>exponent</i>) | - |
| n_{fn} | Number of flooded nodes | - |
| PI | Performance indicator (also optimization multiobjective) | - |
| Q | Flow in the pipes | m ³ /min |
| Q_{FRC} | Fast runoff component | m ³ /min |
| Q_{MU} | Calculated runoff in MIKE Urban | m ³ /min |
| Q_{BG} | Calculated runoff in the mesoscale blue-green model | m ³ /min |
| Q_{SRC} | Slow runoff component | m ³ /min |
| Q_{TR} | Total runoff generated | m ³ /min |
| Q_{WW} | Domestic wastewater flow | m ³ /min |
| R | Rainfall depth | mm |
| $R^{acc,t}$ | Accumulated rainfall depth at time step t | mm |
| R_e | Effective retention | mm |
| $R_{e,i}$ | Effective retention for component i | mm |
| $REIA$ | Runoff-Equivalent Impervious Area | ha |
| $r_{i,t}$ | Direct runoff into blue-green component | m ³ /min |
| S | Dynamic storage in the reservoir model | m ³ |
| SC | Sub-catchment | - |
| SCM | Stormwater Control Measure | - |
| SEK | Swedish krona (the official currency of Sweden) | - |
| S_t | Dynamic storage in the reservoir model at time step t | m ³ |

| | | |
|-----------------|--|----------|
| $SuDS$ | Sustainable Drainage Systems | |
| $SWMM$ | Storm Water Management Model | - |
| T | Number of periods in Sinking Fund equation | - |
| TIA | Total Impervious Area | ha |
| u | Blue-green scenario (distribution of \mathbf{F}_{BG}) | - |
| $UNDRR$ | United Nations' Office for Disaster Risk Reduction | - |
| $US\ EPA$ | United States Environmental Protection Agency | - |
| V_{fb} | Volume stored in the freeboard | m^3 |
| V_{inf} | Volume in the infiltration zone | m^3 |
| V_{out} | Discharged volume | m^3 |
| $V_{out}^{i,t}$ | Discharged volume from component i at time step t | m^3 |
| $\Phi(u)$ | Scalarized total cost function | SEK/year |
| α | Annual average pay raise | - |

1 Introduction

Climate change is anticipated to have tremendous impacts on human health and quality of life through its potential effects on natural ecosystems. A study by Thomas *et al.* (2004) shows that a mid-range rise in temperature of 1.8-2 °C by 2050 might raise the risk of extinction for at least 24% of species. This rate becomes more dramatic if the average temperature rises by more than 2 °C or if the projection period is extended to 2100, putting most ecosystems in danger. These changes would endanger the well-being of humans through increased food insecurity as a result of the extinctions and the loss of 7% to 10% of rangeland livestock (Hoegh-Guldberg *et al.*, 2018).

The consequences of climate change on humans are not merely limited to disturbances in natural ecosystems. Urban areas are also prone to climate change due to increased risks for landslides, air pollution, drought, water scarcity, inland and coastal flooding, heat stress, sea level rise, storm surges, and storms and extreme precipitation (IPCC, 2014). Consequently, additional vulnerabilities—primarily water-related—might prevail, depending on the efficiency and function of the infrastructure on which cities rely.

The urban drainage system has been a crucial infrastructural element in urban areas since the middle of the 19th century. Already at the beginning of the 20th century, discussions arose, questioning the sufficiency of urban drainage capacity due to frequent basement flooding (Lloyd-Davies, 1906):

“Owing to the rapid and continuous growth of towns and cities under modern conditions, the accurate estimation of storm-water in main-sewerage systems and its adequate elimination therefrom has become an important and difficult problem. Serious flooding of basements and cellars connected with sewers in low-lying districts is of frequent occurrence during heavy rainfall; whilst the failure of culverts due to water-ram from the storm-wave, particularly in ground of a yielding nature, is by no means rare.”

Today, flooding problems have escalated due to, inter alia, climate change (e.g., higher risk for extreme precipitation), intensified urbanization, and densification of cities (Berndtsson *et al.*, 2019). According to the United Nations Office for Disaster

Risk Reduction, flood disasters¹ have experienced a dramatic increase in number and frequency since 1980 (UNDRR, 2018). Figure 1 shows the number of various natural disasters that occurred globally between 1980 and 2011. The situation is anticipated to deteriorate, because the urban population of the world is projected to rise to 68% by 2050 (UN, 2018) compared with today's 55%, substantially boosting urbanization and vulnerability. According to the World Economic Forum Global Risks Perception Survey 2017-2018, extreme weather events, natural disasters, and failure of climate change mitigation and adaptation are the top three high impact-high likelihood risks in the global risks landscape (Schwab and Brende, 2018). Increased urbanization in an enormously uncertain future climate will subject urban infrastructures and urban ecosystems to greater economic, social, environmental, and biophysical tension and insecurity (DellaSala and Goldstein, 2017).

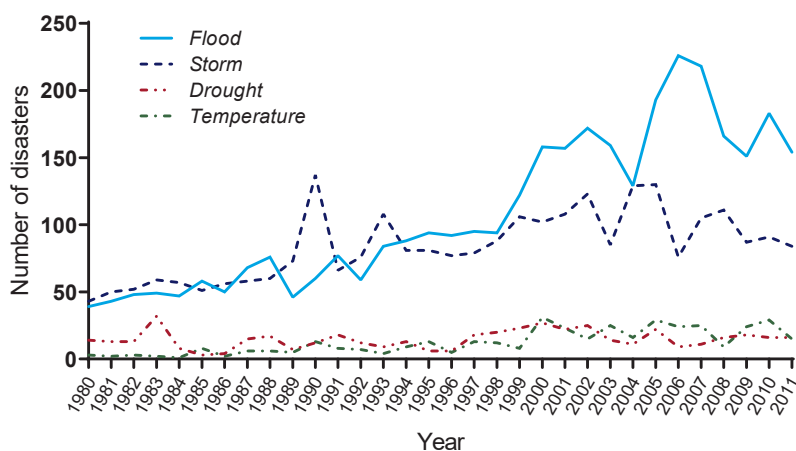


Figure 1.

Total number of natural disasters worldwide caused by floods, storms, droughts and temperature between 1980 and 2011 [after source data from UNDRR (2018)].

1.1 Why blue and green?

Flooding, in the context of this thesis, is the result of an overwhelmed drainage system due to the overload of precipitation, known as pluvial flooding. Overloading due to rain, however, is not the only cause of flooding. Clogged street drains, blocked

¹ A *disaster*, according to UNDRR, is “a serious disruption of the functioning of a community or a society at any scale due to hazardous events interacting with conditions of exposure, vulnerability and capacity, leading to one or more of the following: human, material, economic and environmental losses and impacts.”

gully pots, and malfunctioning pumps can also cause flooding, underscoring the importance of maintenance in urban drainage.

The conventional drainage system, based on pipes, pumps, and manholes, is designed through a deterministic approach—i.e., the hydraulic capacity of a drainage network suffices for a specific hydraulic load. This load is calculated, based on the catchment characteristics and design storm, the latter of which, at least in Sweden, is a block rain or Chicago Design Storm (CDS) (Keifer and Chu, 1957) with a given recurrence interval.

The deterministic approach in the design of urban drainage networks is practiced globally as the heritage of an old engineering culture (Rauch *et al.*, 2002; Butler and Davies, 2011). An outcome of the deterministic design method is that the designed structure will fail as soon as the imposed load exceeds the design load. Such designs have their roots in the fail-safe design mindset, also known as engineering resilience, which is based on efficiency, constancy, and predictability (Holling, 1996). A problem that emerges is that in future scenarios that are based on climate change and anthropogenic variations, constancy and predictability are severely undermined, introducing large uncertainties regarding future meteorological scenarios. This argument has been broached and discussed by researchers, who have advocated new, alternative design paradigms and appropriate solutions for urban water management, including urban runoff (Milly *et al.*, 2008; Carpenter *et al.*, 2009).

The deterministic approach also affects the way that we design local drainage networks. In many cases, the comprehensive plans of municipalities for cities take landownership into account in delineating urban districts. A direct consequence of this approach is that during the detail-planning phase of a district, the planners realize that the drainage area is not limited to the boundaries of the target district. Thus, designing a drainage system requires deterministic assumptions with regard to the land use of the unplanned proportions of the drainage area. These assumptions might be realized in future detail plans (or not), introducing another source of uncertainty to the design process (Becker, 2018).

Intensifying urbanization, an uncertain and changing climate, and the current rigid design practice have necessitated an urgent transition in how urban infrastructure—namely, urban drainage systems—should be designed and developed for future scenarios. One alternative to alleviate the future pressure on drainage systems is to introduce blue-green stormwater systems to urban catchments. These systems add flexibility and adaptability to the drainage system compared with piped drainage (Ashley *et al.*, 2016). The blue-green stormwater system is a concept in the context of sustainable drainage systems (SuDS), emphasizing the deliberately designed presence of water on urban surfaces (*blue*) and the inclusion of vegetation (*green*) through interactive relationships (Walmsley, 1995; Stahre, 2006, 2008; Fletcher *et al.*, 2015). This setup is an implicit indication that blue-green stormwater systems

are those that are implemented on urban surfaces, contrary to underground detention basins and storage units, which, in some cases, are also classified as SuDS (Cunha *et al.*, 2016).

Blue-green stormwater measures, termed stormwater control measures (SCMs) in the appended papers, can be implemented on various scales. As discussed in **Paper I** and **Paper II**, three scales of implementation can be defined:

- *Microscale measures*, which consist of single, discrete blue-green measures that are locally retrofitted, from which discharges run directly into the receiving system (e.g., piped network and natural body of water).
- *Mesoscale measures (systems)*, comprising multiple interconnected microscale blue-green measures in which the discharge from the upstream measure is diverted to the next immediate downstream measure. In mesoscale blue-green systems, the discharge from the most downstream measure is connected to the receiving system.
- *Macroscale measure* is the upscaled implementation of mesoscale blue-green systems that cover a broader urban area.

Figure 2 shows schematics of the various implementation scales of blue-green measures with respect to the piped drainage network.

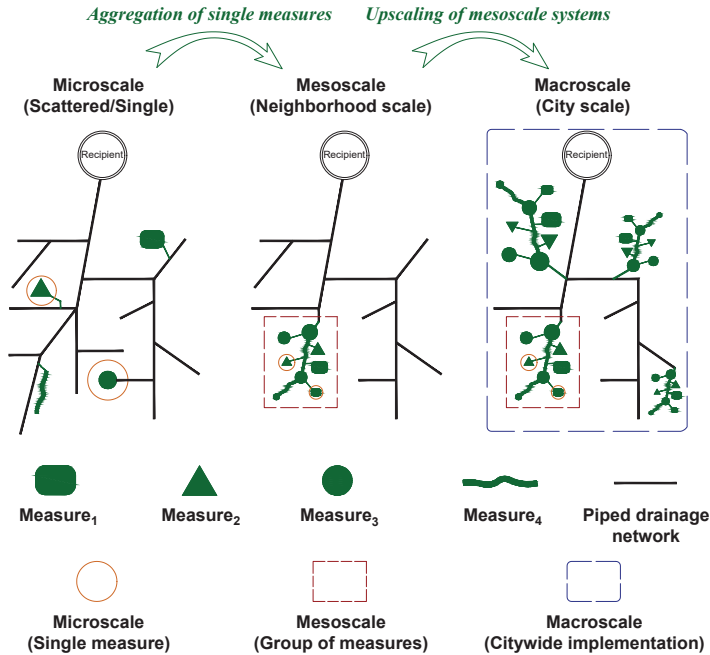


Figure 2.

Micro-, meso-, and macroscale blue-green stormwater measures within the scope of this thesis (adapted from **Paper II**).

1.2 Aim

It is anticipated that optimized retrofits of mesoscale systems throughout the entire piped catchment will have significant effects on flood mitigation. The general aim of this thesis is therefore to develop a method and tool to study the citywide effects of blue-green stormwater systems on the loading and performance of traditional pipe-based sewer networks.

However, to fulfill this aim, four crucial steps must be taken:

- *Understanding*: A full-scale existing mesoscale blue-green stormwater system must be studied and evaluated with respect to its local effects and how the surrounding catchments, upstream and downstream, interact with the blue-green system.
- *Conceptualization*: A simple, representative conceptual model for mesoscale blue-green stormwater systems must be developed.
- *Mathematical formulation*: Based on the proposed concept above, a suitable modeling tool—fast, easy-to-use, and robust—with the ability to simulate the interaction between blue-green stormwater systems and the pipe network, has to be developed.
- *Evaluation*: The developed method and tool should be evaluated against an actual large-scale drainage context, providing us with lessons on and a deeper understanding of how complex drainage systems behave under various blue-green scenarios.

1.3 Outline of the thesis

The thesis is structured to reflect the aim of the study, as stated above, which is also consistent with the appended papers (**Papers I, II, III, and IV**). In the following chapter, the study area, Augustenborg, is presented, as is the measurement network that was set up in the area. In the same chapter, the results from **Paper I** on the efficiency of the local blue-green stormwater system in Augustenborg and its potential impacts on surrounding catchments are discussed.

Next, **Paper II** and **Paper III**, in which the development of the model—from conceptualization to mathematical implementation—are discussed. **Paper II** conceptualizes the definition of the mesoscale blue-green stormwater system and provides a better understanding of the dynamics through which discharge from the system is initiated. **Paper III** is built on the concept and scheme in **Paper II** and

suggests a rapid, physically based rainfall-runoff model for mesoscale blue-green stormwater systems.

The findings in **Paper I** and **Paper II** are combined with the rapid model that is introduced in **Paper III**, together forming the basis for the upscaling/optimization study that was performed and presented in **Paper IV**.

2 Eco-city Augustenborg: A blue-green retrofit

The implementation of blue-green stormwater systems in the outskirts of cities in new developments, where land and available space are less limited, is relatively established and is being practiced. However, the circumstances in inner-city catchments differ. Most cities are highly urbanized in central districts and suffer from limited space for implementation of blue-green stormwater retrofits. Moreover, other factors, such as the roles and responsibilities of land owners, legal and institutional frameworks, political will and interest, economic stress, and lack of knowledge, are obstacles that impact the feasibility of retrofitting blue-green stormwater systems in such areas (Wihlborg *et al.*, 2019).

Due to these issues, there are few full-scale examples of mesoscale blue-green stormwater systems in densely populated inner-city catchments. Augustenborg, in Malmö, Sweden, is one of the few successful implementations of a blue-green stormwater system in a central urban catchment (see Figure 3).

This area, constructed in the 1940s and 1950s, encompasses approximately 33 ha, consisting primarily of 3- to 6-story residential buildings (Stahre, 2008; VA SYD, 2008). Augustenborg was originally part of the combined sewer catchment that suffered from frequent basement flooding as a result of its hydraulically overloaded sewer system during heavy rainfall events (Stahre, 2008). In the 1970s, due to social and economic problems and degraded buildings and outdoor spaces, the inhabitants of Augustenborg began their egress from the area, further deteriorating the social status of Augustenborg.

Since the mid-1990s, city authorities had been developing action plans to restore the social, economic, ecological, and physical status of the area, eventually deciding to upgrade its overall status by transforming it into an eco-city prototype (Stahre, 2008; Bernstad Saraiva Schott *et al.*, 2013; Malmö stad, 2017). The required funding was provided by the municipality of Malmö, the municipal housing company in Malmö (MKB), EU Life Fund, and the Swedish government. Paralleling fundamental changes in the area, such as solid waste management, improved energy efficiency, and increased urban biodiversity, the stormwater management system in Augustenborg underwent substantial transformation. The runoff from the area was

disconnected from the combined sewer network and instead was led through mesoscale blue-green stormwater systems.

Since the implementation of blue-green retrofits in Augustenborg in the late 1990s, it has been generally believed and claimed repeatedly in the urban water sector that the new stormwater system has had a tremendous impact on flood reduction in the area. However, because the area was a real-life urban project for everyday use (not a research facility), performing hydraulic and hydrologic research in the area encountered serious hurdles with regard to the installation, maintenance, and safety of the equipment. Despite these difficulties, several studies on the hydraulic efficiency of the blue-green stormwater measures in Augustenborg have been published (Villarreal *et al.*, 2004; Bengtsson *et al.*, 2005; Villarreal and Bengtsson, 2005; Villarreal, 2007; Shukri, 2010; Kibirige and Tan, 2013), but none has addressed its full-scale performance with respect to flood mitigation capacity and its impacts on the surrounding catchments and neighborhoods.

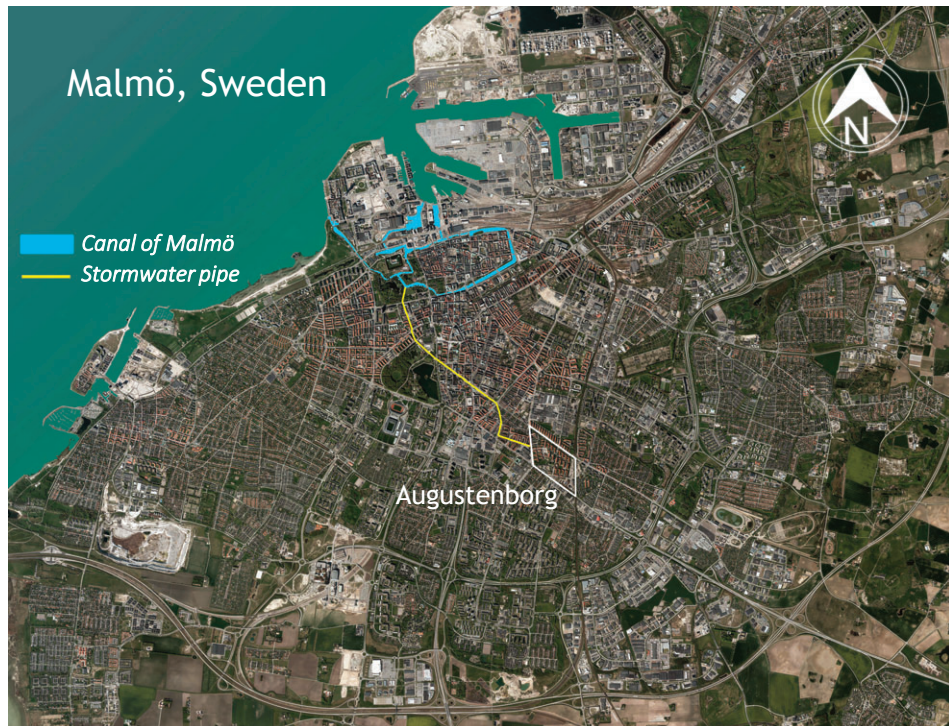


Figure 3.

Location of Augustenborg in the city of Malmö, Sweden, is illustrated in the aerial photo of the city. The path of the separate stormwater pipe (the yellow polyline) that carries the stormwater discharge from all of the subsystems of Augustenborg directly to the canals of Malmö (the light blue surfaces) is also shown (the background orthophoto is courtesy of the Swedish Mapping, Cadastral and Land Registration Authority, ©Lantmäteriet).

2.1 Stormwater management

Augustenborg, as it exists today, comprises two major blue-green stormwater systems: one each in the south (Southern retrofit, implemented 1999-2001), with a drainage area of roughly 9.6 ha, and north (Northern retrofit, implemented 2002-2003), with a drainage area of approximately 6.3 ha. In addition, a separate local stormwater pipe system was constructed in 2003, covering a drainage area of about 3.5 ha. These three subsystems of Augustenborg are illustrated in Figure 4.

The Southern retrofit was constructed ambitiously. It is more diverse and consists of various types and designs of blue-green stormwater measures. Approximately 1 ha of green roofs was installed in the southeast corner of the retrofit, primarily in the area that belongs to the municipality of Malmö. The open channels and wet and dry ponds of the retrofit were designed aesthetically to match the typical character of the area. In addition, all downpipes were disconnected from the pipe network and instead were led down to concrete open gutters that were incorporated in walkways. Generally, the presence and visibility of water are noticeable throughout the Southern retrofit. This part of Eco-city Augustenborg is reportedly designed to be able to manage rainfall with a recurrence interval of about 25 years.

The Northern retrofit, in contrast, encompasses a smaller area and was designed to handle a 10-year rainfall. The diversity of the implemented blue-green measures is low, consisting of swales, channels, and wet ponds. The downpipes in this section of the Eco-city lead straight down into the ground, connecting to a nearby ditch. Unlike the Southern retrofit, there are no open gutters in the walkways of the Northern retrofit; rather, grated channels are used. The specific design of the Northern retrofit has decreased the visibility of water over the drainage area, compared with that of the Southern retrofit.

A separate local stormwater pipe system receives runoff primarily from asphalt street surfaces and parking lots. Topographical circumstances and issues with available space have rendered conventionally piped drainage an appropriate choice for this part of the area.

The remaining sections of the Augustenborg area are drained directly into the combined sewer network or have a local blue-green stormwater system that is not connected to the major systems. Notably, this thesis focuses on the Northern and Southern blue-green stormwater systems, whereas the separate stormwater sewer was used solely as a reference for comparison in **Paper I** and **Paper II**. The untransformed areas within the boundaries of Augustenborg and small, local blue-green stormwater systems are not included in this thesis.

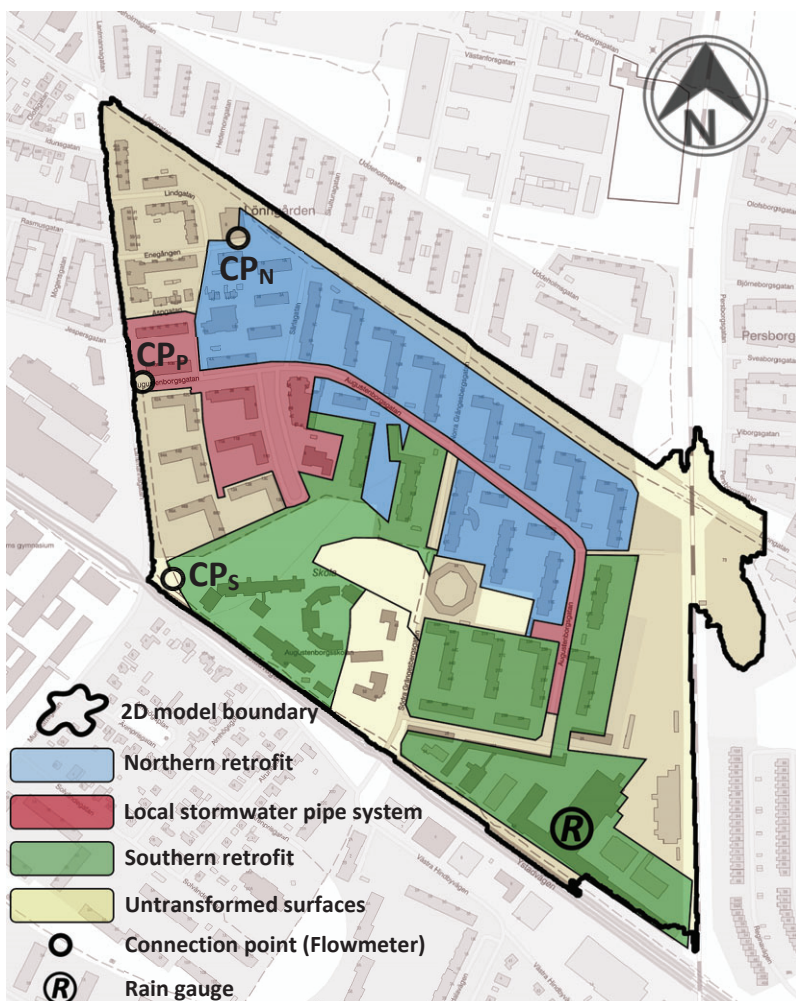


Figure 4.

Subsystems of Augustenborg, including two blue-green stormwater retrofits and the local pipe system. The figure also shows the connection points between the subsystems and sewer network, into which the discharge from the subsystems are drained. All rainfall measurements are based on a single tipping bucket rain gauge that was installed in the southeast corner of the area, marked ®.

The transformation of the stormwater management system in Augustenborg is, in principle, a complete separation project, in that the runoff from the area is disconnected from the combined sewer network. The discharge that leaves the Augustenborg area—as surcharge from the blue-green systems or the flow in the separate stormwater system—is led to the closest receiving water body—i.e., the canal in Malmö—through a separate stormwater pipe that was installed in 2001–2002 (shown in Figure 3). The separate stormwater pipe was also constructed to complement the Augustenborg-retrofit.

2.2 Rainfall-runoff measurements

The discharge from the three subsystems of Augustenborg and rainfall were monitored over the course of the study. The rain gauge—a Casella CEL tipping bucket gauge with 0.2 mm resolution—had already been installed and was present in the area, as part of the rainfall monitoring network that was owned and operated by the local water utility company (VA SYD). The flowmeters, *Mainstream™ Portable AV-Flowmeters* (Figure 5), however, were selected specifically for the project and placed at various points in the area.

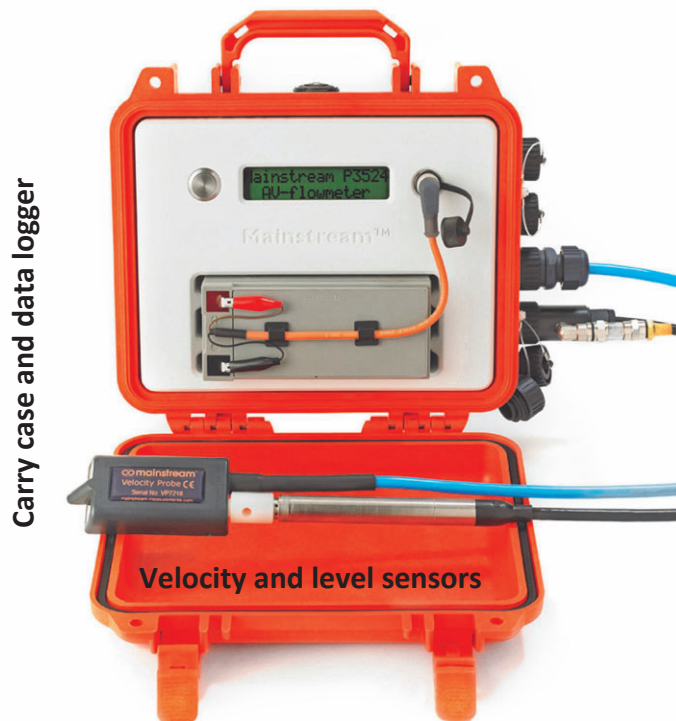


Figure 5. Mainstream™ Portable AV-Flowmeters used in this study. Picture is courtesy of Mainstream™ measurements LTD.

Mainstream flowmeters use the area-velocity method for estimating flow. These meters have velocity and level probes that are submerged in the incoming flow toward the manhole—i.e., the upstream pipe of the manhole. The probes are mounted on an adjustable curved metal sheet—i.e., a mounting sheet—that can be fastened to the inner wall of the pipe. It is also preferable to tilt the probe 5°-10°

from the quadrant of the pipe section, as shown in Figure 6, to avoid or decrease the accumulation of sediment in front of the probe. This requires that the flow depth measurements be corrected by a constant offset value. The probe in the pipe communicates with the data logger, which resides in the upper section of the manhole, just beneath the manhole lid. The positions of the velocity and level sensors and data logger are shown in Figure 7.

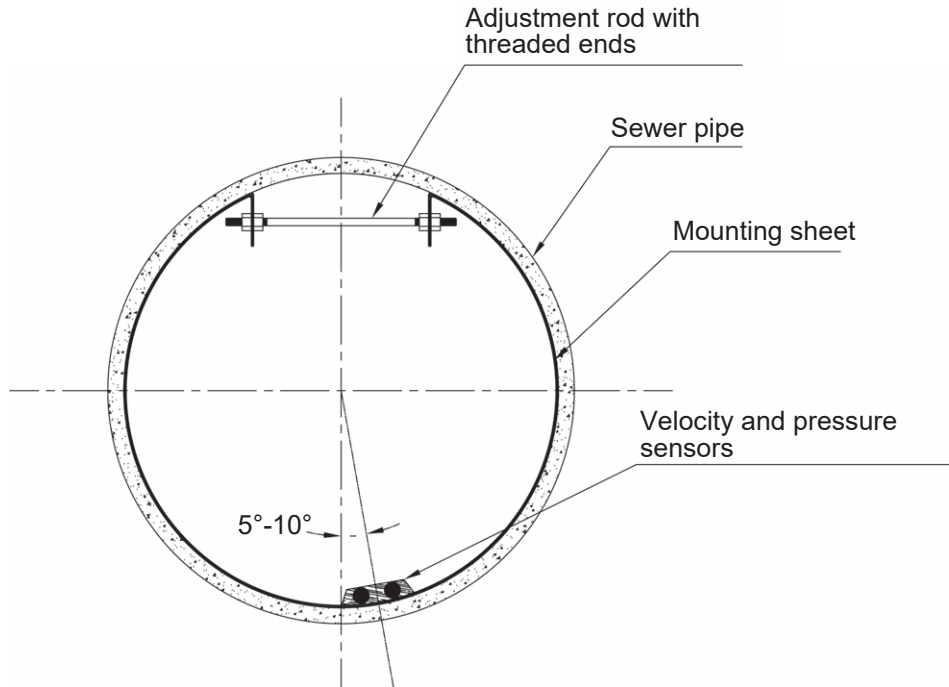


Figure 6.
Cross-sectional view of the velocity-pressure probe in the pipe.

The probe transmits ultrasound waves into the flow and, based on the reflected waves from the solid particles and bubbles in the liquid, creates a histogram of flow velocities. The histogram is used by the meter to calculate the mean flow velocity. The flow depth is estimated using the pressure transmitter, which senses the water pressure. Mainstream™ combines the velocity data, flow depth, and geometry of the pipe (or channel) cross-section to deduce the flow.

Monitoring the flow in a blue-green stormwater system that is located in a residential neighborhood in the center of the city is a challenge. The chief obstacle in this respect is exposure of the meters in the open channels, ponds, and ditches of the system, which entails physical damage due to environmental factors, such as humidity, and places them at high risk for vandalism, unintended damage, and theft. Such solutions

as constructing enclosed measurement huts with sufficient protection might be possible, but these alternatives are rarely feasible, considering the time and economic resources that are required with respect to the budget of the project. Thus, few options remain for monitoring blue-green catchments—i.e., manholes and the pipe system.

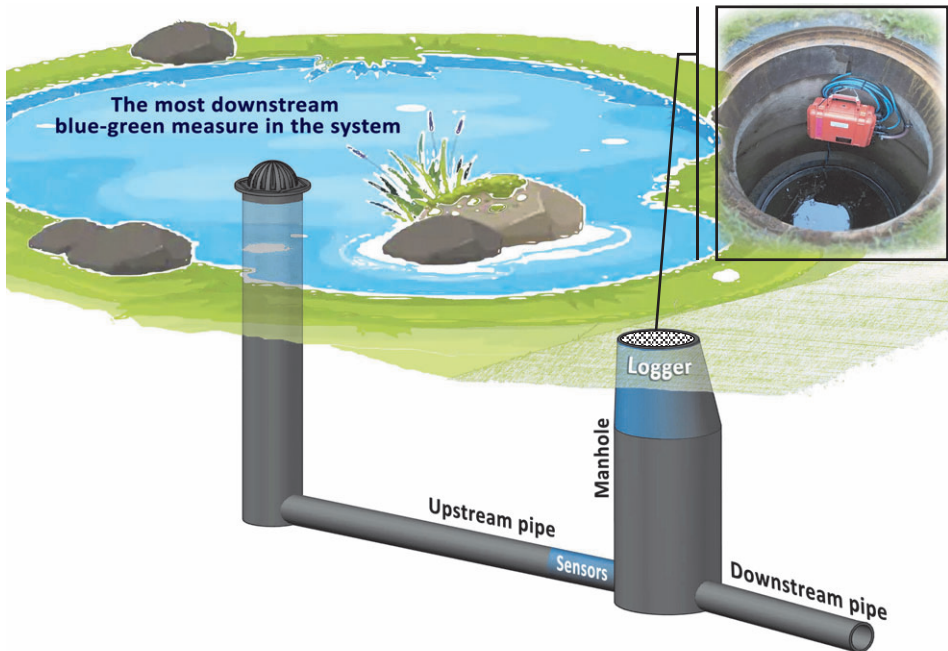


Figure 7.

Schematic of connection points linking blue-green stormwater systems to the municipal pipe network. This connection occurs at the most downstream blue-green stormwater measure (or stormwater control measure, SCM) of the mesoscale blue-green stormwater system. The discharge flow is measured in the pipe section connected to the first manhole of the sewer network (illustration: Salar Haghighatafshar and Misagh Mottaghi).

Consequently, the connection points (CP_N , CP_S , and CP_P , as shown in Figure 4), through which the subsystems of Augustenborg were connected to the separate stormwater pipe that carries the total stormwater discharge from Augustenborg to the canal of Malmö (see Figure 3), were selected for the installation of flowmeters. Figure 7 illustrates how these connection points, linking the most downstream blue-green measure to the pipe network, were constructed.

The measurements were made for approximately 3 years, with occasional interruptions due to maintenance and recalibration. Flow and rainfall data were downloaded monthly from the flowmeters and rain gauge. Ten rainfall events with relatively larger depths, for which the corresponding runoff measurements were also

available, were selected within the context of this thesis. These responses were presented in **Paper II** and used for the calibration and validation of the model in **Paper III**.

2.2.1 Error sources

Rainfall measurements

All rainfall data were acquired from a single tipping bucket rain gauge that was installed at the southeast corner of the Augustenborg area. This step intrinsically introduces a degree of uncertainty and error in the rainfall-runoff measurements (Fiener and Auerswald, 2009), because the recorded rainfall data are primarily locally valid for the installation point of the rain gauge, whereas the spatial variation in rainfall pattern across the entire catchment is overlooked and ignored. A single fixed rain gauge also misses the rainfall dynamics as the rainfall moves over the catchment. The movement of a rainfall peak affects the resulting hydrograph (Singh, 1997). However, considering that the longest distance within the catchment from the rain gauge is approximately 750 meters, the error that is introduced into the calculations and simulations is anticipated to be small.

Flow measurements

The flow measurements in this study were also subject to errors and uncertainty. One possible source of error originates from the minimum operating depth of the velocity sensor, which is approximately 30 mm (MainstreamTM, 2017). Thus, the velocity measurements for flows that are shallower than 30 mm are invalid or completely missed, leading to unreliable flow calculation or zero flow, respectively. This error is magnified due to the tilted position of the probe in the cross-section of the pipe (shown in Figure 6), which, in principle, means that a larger proportion of smaller flows—e.g., base flow, start of the rising limb, and end of the falling limb—is missed. Such a phenomenon might affect the studies in this thesis, but the effects are considered to be minor, because the focus is on peak flow and lag time.

In addition, decalibration due to abrupt environmental changes (e.g., ambient temperature), installation errors, offset estimation, turbulence in the flow, and insufficient maintenance are sources of uncertainty and error in the flow data. In this thesis, all data that were suspected of inaccuracy due to decalibration or invalidity due to other sources of error were excluded from the study, leading to loss of long-term continuity in the rainfall-runoff data at various measurement stations.

2.3 When it rains in Augustenborg

To better understand the blue-green stormwater system in Augustenborg, a model-based study was set up, as published in **Paper I**, using: the MIKE Flood system by DHI, which is a coupled one-dimensional (1D) sewer and two-dimensional (2D) overland hydrodynamic model. This model allows surcharge from the sewer system to be distributed over the surface and return to the sewer when hydraulic capacity is available.

Paper I focused on the efficiency of the blue-green stormwater system in Augustenborg for flood mitigation. Two models were built for this purpose:

- i- 1D-2D model of Augustenborg before implementation of the blue-green stormwater system (reference case).
- ii- 1D-2D model of Augustenborg as it exists today.

The details of the model concept, logic, and structure and parameter estimation are discussed in **Paper I**.

2.3.1 Local effects of a blue-green system

An extreme rainfall event that struck Malmö on August 31, 2014 was simulated in both models. The simulation results showed that Augustenborg manages extreme rainfall events efficiently through the cascade of retrofitted blue-green measures. The flood maps that were generated by the models in **Paper I** differed considerably. Spatially, the flooding in the reference case (i.e., before implementation of the blue-green stormwater system) was extensive and scattered. The flood stretched to the main street of the district, having surrounded some of the residential buildings. The modeled surface flood in the reference case does not represent reality. In actuality, most flood volume is accommodated by the basements of the buildings, because the area is connected entirely to the combined sewer network.

In contrast to the reference case, the extreme rainfall in a blue-green Augustenborg did not precipitate any extreme flooding. The flooding occurred primarily on surfaces, which, through the design and implementation of the blue-green stormwater system, were intended to be flooded. The model output is consistent with onsite observations at Augustenborg on the day of the simulated rainfall. Figure 8 shows the actual flooding situation in Augustenborg on August 31, 2014, in which the lawn that was connected to the final swale and pond in the Southern retrofit was flooded, as designed (compare the photo with Fig. 5b in **Paper I**).

Although the results indicate that the blue-green stormwater system in Augustenborg substantially alleviated the flooding problem, a closer and critical look into the

existing flow streams in and through the area shows that the hydraulic load that was exerted on the systems in the simulation scenarios differed substantially. On examining the water balance for both scenarios, the amount of water that was required to have been managed by the system in the reference case (before blue-green implementation) was over 2-fold the water volume that entered the blue-green stormwater system, as it exists today. Figure 9, adapted from **Paper I**, illustrates the flows that must be managed by the stormwater system in each case. In Figure 9a, the stormwater system is the municipal combined sewer system, which is a pipe network. Thus, in addition to the direct precipitation volume on the area ($=30\,300\text{ m}^3$), the network beneath the Augustenborg area had to manage the inflow from the adjacent neighborhoods ($=33\,800\text{ m}^3$), whereas the latter is inapplicable and irrelevant in the case of blue-green stormwater systems.



Figure 8.

The downstream section of the Southern blue-green retrofit in Augustenborg on August 31, 2014, right after the extreme rainfall. The situation in this photo is comparable with the simulation result in **Fig. 5b** in **Paper I**, in which the designated flood area in Augustenborg is covered with water. Photo: Henrik Thorén.

Thus, a blue-green stormwater system has the advantage of having a larger hydraulic capacity and benefits from receiving a reduced load due to catchment isolation—i.e., it is segregated from the remainder of the surrounding catchments in a decentralized manner. In summary, a blue-green-retrofitted (isolated) area is solely responsible for handling the rainfall that arrives within its boundaries. This pattern is opposite to

the process that takes place in pipe systems, in which the flow aggregates constantly along the drainage network as it propagates from upstream to downstream.

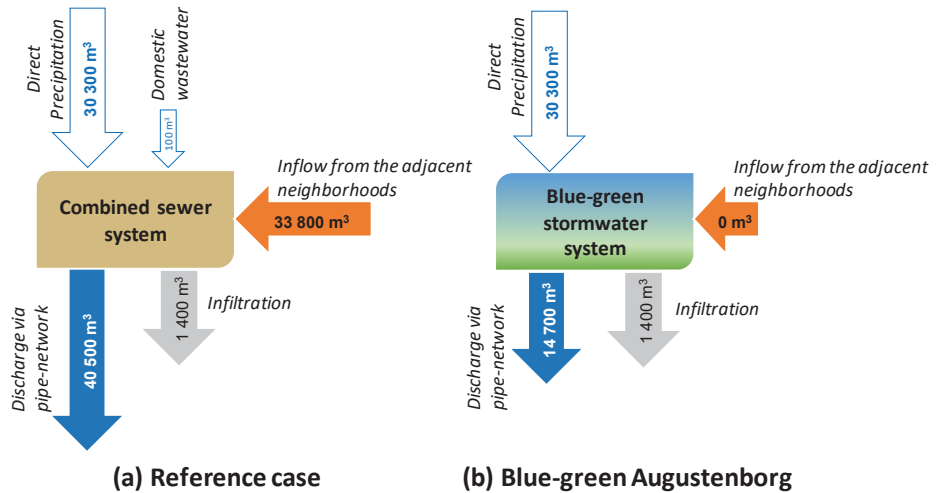


Figure 9.

Water balances in Augustenborg under the extreme rainfall scenario (cloudburst on August 31, 2014) (a) for the reference case—i.e., before implementation of the blue-green stormwater system—and (b) after installation of the blue-green stormwater system. Adapted from **Paper I** with permission from Elsevier.

Further, the considerable volume of runoff that is generated in the upstream catchments must still pass through the underground sewer network in the retrofitted area. Depending on the magnitude of the rainfall, the flow that is generated in upstream catchments can cause basement flooding (in a combined sewer network) in the retrofitted area if backwater valves are not installed. There is also a risk that the flooding problem is shifted downstream in the aftermath of retrofitting the target catchment. This likely shift is especially important if the discharge from the blue-green stormwater system enters the same pipe network at a downstream point. Thus, with regard to sustainability, it is advised, via **Paper I**, that the process of retrofitting blue-green stormwater systems be prioritized in the upstream catchments of the drainage network.

2.3.2 Downstream effects of a blue-green system

Blue-green stormwater systems, when implemented in inner-city catchments, interact constantly with existing pipe networks—combined or separate sewer systems—because the discharge from the blue-green stormwater system must be diverted into the existing pipe network, when no natural water body is nearby. Thus,

it is important to study the downstream effects of blue-green stormwater systems on an existing pipe network.

To this end, **Paper I** quantified an arbitrary rainfall that would have produced a similar hydrograph from a conventional catchment with a pipe network as a 100-year CDS on a blue-green stormwater system. In the case of Augustenborg (Southern retrofit), detention in the blue-green stormwater system rendered the effects of the 100-year rainfall event similar to those of a 6.5-year rainfall event on a conventional pipe network, as illustrated in Figure 10. This improvement is attributed to the reduction in peak flow and runoff volume through the retention-detention measures that constitute components of the blue-green stormwater systems, as reported frequently in the literature (Damodaram *et al.*, 2013; Locatelli *et al.*, 2015; Sahoo and Pekkat, 2018).

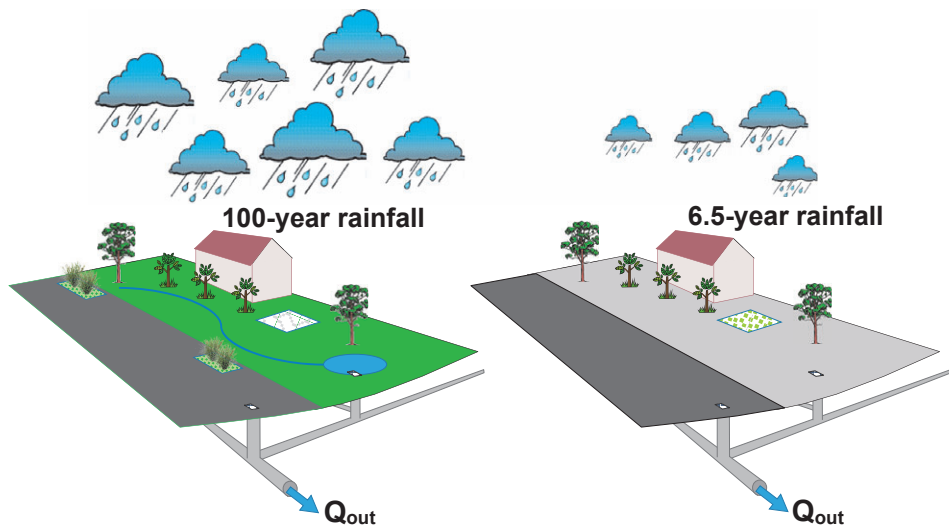


Figure 10.

Two rainfalls with similar discharge hydrographs, illustrating that blue-green stormwater systems downgrade the runoff from an intense rainfall event to a runoff corresponding to a milder rainfall.

The lower runoff volume and runoff peak through blue-green stormwater systems have potential positive impacts on the downstream catchments, such as decreased combined sewer overflow in a combined sewer network and reduced hydraulic loads, which could be advantageous for the recipient—e.g., a pipe network, wastewater treatment plant, and natural water body. Whether this dramatic downgrade in rainfall magnitude, with respect to the resulting hydrograph, could be used to relieve the overloading of a pipe-network under heavy rainfall events needs to be determined. An example of such use is the replication of Augustenborg-like retrofits, from which the discharge is connected to the original pipe-based sewer system, throughout the city (see Section 1.2).

3 Model development

Mesoscale blue-green stormwater systems, as defined in this thesis, are not the most common scale in real-world implementations or research studies. The significant potential of the mesoscale blue-green system in flood mitigation renders it an interesting case study with respect to its local and citywide effects. The findings with the MIKE Flood models that were built in **Paper I** demonstrated this potential, as discussed in Section 2.3. However, the adopted modeling approach was demanding in terms of parameter estimation and computational cost.

Such models as the MUSIC model (by eWater) and Adaptation Support Tool (AST) (van de Ven *et al.*, 2016) were developed specifically for blue-green stormwater systems in larger and complex systems, but they do not incorporate the simulation of traditional pipe-based sewer systems (van de Ven *et al.*, 2016; Lerer, 2019). Moreover, other commercially available models, such as MIKE Urban (by DHI) and the US EPA Storm Water Management Model (SWMM), have modules that cosimulate traditional pipe-based sewers and blue-green stormwater measures interactively. These models partly bridge the gap that was identified by Fletcher *et al.* (2013) regarding the need for communicative modeling of blue-green stormwater measures and catchment-scale network hydraulic behaviors. However, MIKE Urban and SWMM merely integrate single blue-green measures—so-called *microscale measures* in the framework of this thesis (see Section 1.1).

Thus, a gap in the need for a model for cosimulation of mesoscale blue-green stormwater systems, in connection with hydrodynamic modeling of traditional pipe-based sewers, was identified. In this chapter, the development of a new, rapid, and easy-to-use model system, developed in the following three stages, is presented:

- i. Conceptualization of mesoscale blue-green stormwater systems (**Paper II**)
- ii. Mathematical implementation of the introduced model concept (**Paper III**)
- iii. Coupling the mesoscale model and 1D sewer network model (**Paper IV**)

3.1 Concept development

In conventional urban planning, in which local retention and detention structures are negligible, the total volume of the discharge from a pipe-based drainage system can be used to quantify the contributing area (mainly impervious surfaces) to the runoff. This value, calculated based on the rainfall-runoff response, is referred to as *effective impervious area* (EIA), which is the proportion of the *total impervious area* (TIA) that is hydraulically connected to the pipe-based drainage system (Alley and Veenhuis, 1983). *Directly connected impervious area* (DCIA) also represents the hydraulically connected portion of TIA; however, DCIA is viewed primarily as a measurable (rather than computable) parameter, based on on-site investigations, surveys, and maps (Ebrahimian *et al.*, 2016).

In conventional urban planning with small retention and detention capacities, the EIA is 80% to 90% of the measured DCIA (Melanen and Laukkanen, 1980; Boyd *et al.*, 1993). This difference—i.e., 10% to 20%—can be due to uncertainties in DCIA, leading to losses in runoff, such as surface cracks, undiscovered vegetative interception, and surface depression storage (Albrecht, 1974; Ebrahimian *et al.*, 2016).

In catchments with blue-green implementation, the relationship between EIA and DCIA above does not necessarily hold, due primarily to the considerable retention capacity on the surface, which is also extremely case-specific. Thus, in the case of blue-green stormwater systems, it is not possible to quantify EIA, based on the observed runoff. In other words, the EIA for a blue-green catchment will not be a constant value but rather a function of rainfall depth. Consequently, a similar concept was introduced in **Paper II**, referred to as *runoff-equivalent impervious area* (REIA). Equation-wise, REIA is calculated as EIA (Eq. 1), but what they represent differs. EIA is assumed to be the portion of TIA that contributes to the runoff, whereas REIA is an imaginary impervious area that results in the observed runoff if no loss (e.g., retention, infiltration, and evapotranspiration) is taken into account.

$$EIA \cong REIA = \frac{V_{out}}{R} \quad \text{Eq. 1}$$

where V_{out} is the total discharge volume (m^3) from the drainage system and R is the rainfall depth (m).

Eq. 1 was applied to 10 individual rainfall-runoff responses of the three subsystems in Augustenborg: the Northern blue-green retrofit, the Southern blue-green retrofit, and the local separate stormwater pipe system (see Figure 4). The results showed that REIA was generally constant for the sub-catchment with the local separate stormwater pipe system at various rainfall depths (Figure 11a). In contrast, the blue-

green retrofits (Northern and Southern) demonstrated more dynamic behavior with regard to REIA at various rainfall depths (Figure 11b and 11c).

The REIA grew linearly in relation to rainfall depth in the Northern retrofit (Figure 11b) but consisted of two clear phases for the Southern retrofit, as seen in Figure 11c. In the first phase of the process, REIA remained nearly 0 for all rain depths up to roughly 17 mm, after which it jumped abruptly from 0 to 0.8 ha. These behaviors can be explained by the sequence of retention volumes. As demonstrated in **Paper II**, if a blue-green stormwater measure with relatively large retention capacity is placed at the most downstream point of a blue-green stormwater system, the system will behave similarly to the Southern retrofit in Augustenborg (Figure 11c). In contrast, if the retention capacity of the most downstream blue-green measure is small, the REIA response will be similar to the Northern retrofit in Augustenborg (Figure 11b).

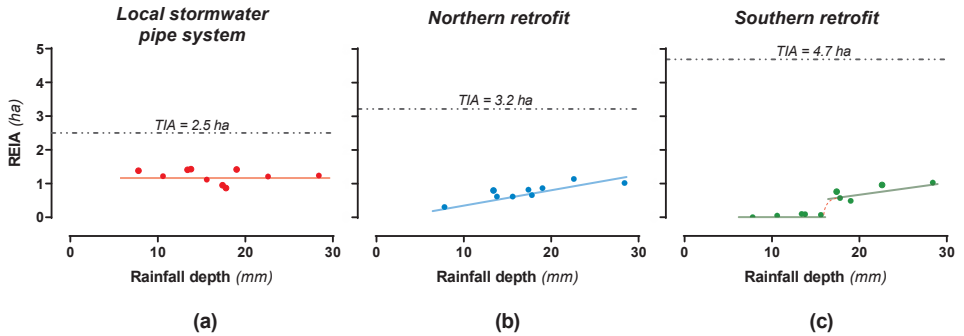


Figure 11.

The relationship between REIA and rainfall depth for the various subsystems of Augustenborg.

Subsequently, a mesoscale blue-green stormwater system was conceptualized as a series of retention volumes, wherein the distribution of retention units (blue-green stormwater measures) leads to various REIAs (or different total discharge volumes) under a given rainfall event.

3.2 Mathematical formulation of the concept

Initially, a basic scheme was proposed to express the retention characteristics of a single blue-green stormwater measure. It was assumed that every blue-green measure that receives runoff from the connected catchment can be schematized as the available volume under the overflow threshold (i.e., storage at the freeboard level:

V_{fb}) and infiltration capacity (i.e., storage in the infiltration layer: V_{inf}). It was also presumed that the immediate evapotranspiration during the rainfall was negligible, considering the Swedish climate, and that the entire connected catchment could be represented by DCIA within the framework of this thesis. Based on this fixed scheme, the *effective retention capacity* (R_e) for any blue-green measure is calculated per Eq. 2:

$$R_e = \frac{V_{fb} + V_{inf}}{DCIA} \quad \text{Eq. 2}$$

where DCIA is the impervious area that is connected directly to the blue-green measure. This scheme was subsequently applied on the mesoscale, consisting of multiple blue-green measures, as shown in Figure 12 (adapted from **Paper III**).

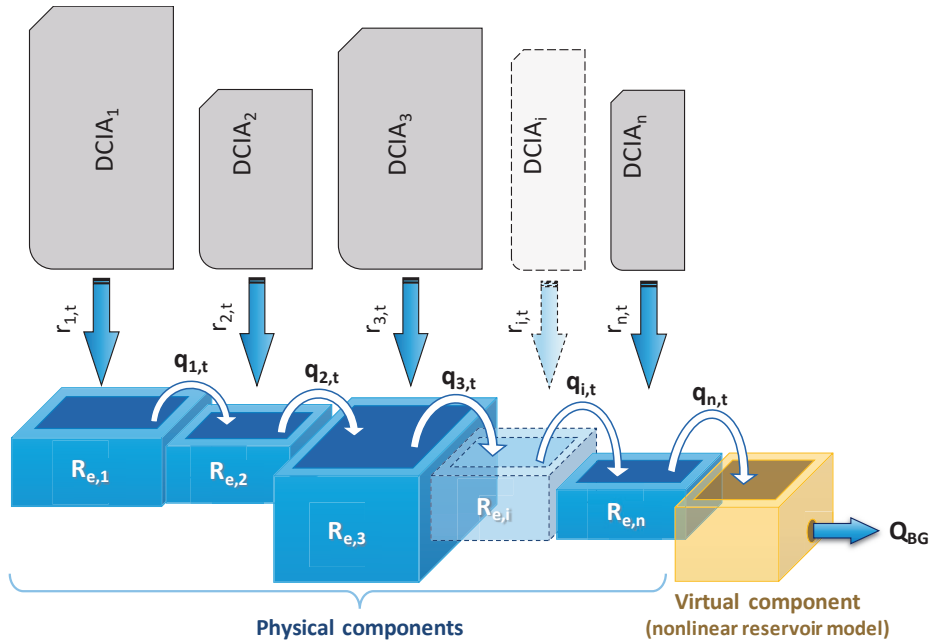


Figure 12.

Flow dynamics, as described by the conceptual model for mesoscale description of blue-green stormwater systems – based on **Paper III** – resulting in a discharge (Q_{BG}) from system. $r_{i,t}$ and $q_{i,t}$ and defined in Eq. 3.

The mesoscale scheme, presented in Figure 12, illustrates the flow dynamics in the conceptual model, in which all blue-green measures receive runoff from their corresponding DCIA, whereas downstream measures can also receive flows from upstream measures. Note that although Figure 12 depicts a simple linear cascade of blue-green measures from upstream to downstream, the concept and mathematical model incorporate and handle branched configurations of mesoscale blue-green

systems, in which two or more measures are connected directly to a single measure in the immediate downstream as a tree structure. This flow scheme is expressed mathematically in Eq. 3 using explicit discretization.

$$\begin{aligned}
 q_{i,t} &= \frac{V_{out}^{i,t} - V_{out}^{i,t-1}}{\Delta t} = \overset{q_{i,t-1} \text{ acc. to Figure 12}}{\frac{V_{out}^{i,t-1} - V_{out}^{i,t-2}}{\Delta t}} + \underbrace{\frac{(R_{acc,t} - R_{e,i}) \times DCIA_i}{\Delta t}}_{\substack{\text{Runoff from DCIA} \\ (r_{i,t}) \text{ acc. to Figure 12}}} + \underbrace{\sum_{j=1}^n \frac{V_{out}^{i-j,t}}{\Delta t} - \frac{V_{out}^{i,t-1}}{\Delta t}}_{\substack{\text{Inflow from upstream} \\ \text{component(s), } q_{i-1,t}}} , \text{ for } i = 1 \dots n
 \end{aligned} \tag{Eq. 3}$$

in which $q_{i,t}$ is the flow from component i at time step t , $V_{out}^{i,t}$ is the total discharged volume by time step t , $V_{out}^{i,t-1}$ is the total discharged volume by time step $t-1$, $R_{acc,t}$ is the accumulated rainfall depth at time step t , $R_{e,i}$ is the effective retention capacity in component i , and n is the number of components that is discharged directly to component i .

The calculated flow ($q_{i,t}$) through Eq. 3 follows the form of an instantaneous hydrograph (Nash, 1957), because it does not take the detention effect into account. In other words, the model is based on the mass conservation principle (continuity equation), but for increased simplicity and rapid simulation, it does not include a detailed description of a runoff process that follows momentum conservation (Rauch *et al.*, 2001). Thus, to introduce the detention effects, a nonlinear reservoir model (Butler and Davies, 2011) was applied through a virtual component at the most downstream point of the mesoscale blue-green stormwater system (see Figure 12). The virtual component receives flow from the last physical component of the system (i.e., q_n) and generates outflow Q_{BG} from the nonlinear reservoir model (Eq. 4).

$$\frac{dS}{dt} = q_n - Q_{BG} \xrightarrow{Q_{BG} = kS^m} \frac{dS}{dt} = q_n - kS^m \tag{Eq. 4}$$

where S (m^3) is the dynamic storage volume in the virtual reservoir, q_n is the inflow to the virtual component from the most downstream blue-green measure (i.e., the most downstream physical component, as illustrated in Figure 12), and k (1/min) and m (unitless) are the reservoir coefficients. The ordinary differential equation in Eq. 4 was solved using an explicit numerical method—namely, the *forward Euler method*—for which finite difference approximation was used per Eq. 5.

$$\frac{dS}{dt} \approx \frac{S_{t+\Delta t} - S_t}{\Delta t} \tag{Eq. 5}$$

$$\xrightarrow{\text{Eq.4 \& Eq.5}} S_{t+\Delta t} = S_t + \Delta t \cdot (q_{n,t} - kS_t^m) \quad \text{Eq. 6}$$

where $S_0 = 0$

$$S_1 = \Delta t \cdot q_{n,0}$$

$$S_2 = S_1 + \Delta t \cdot (q_{n,1} - kS_1^m)$$

$$S_3 = S_2 + \Delta t \cdot (q_{n,2} - kS_2^m)$$

\vdots

$$Q_{BG,t} = kS_t^m \quad \text{Eq. 7}$$

The entire model (Eq. 2-7) was set up in Python™, an open-source programming tool (Python, 2019). Application of the reservoir model converts the instantaneous hydrograph to a detained hydrograph, as illustrated in Figure 13.

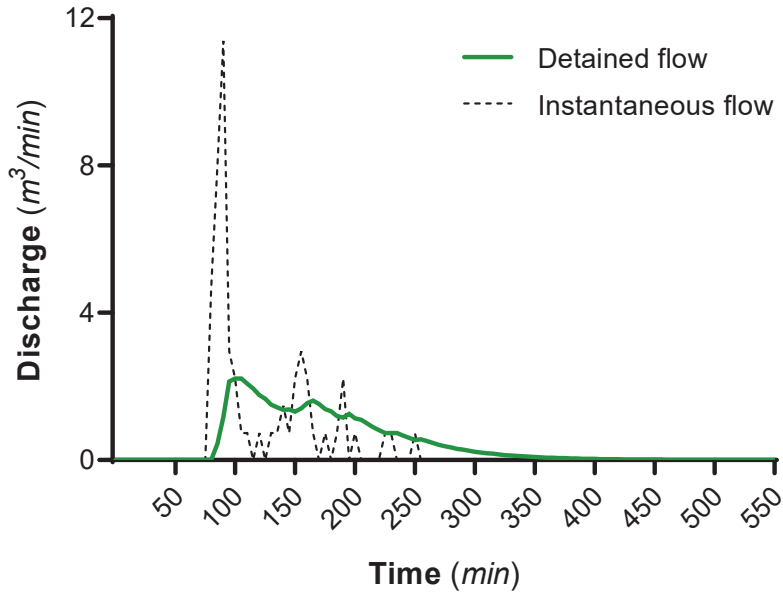


Figure 13.

Transformation of an instantaneous hydrograph (without detention) to a detained hydrograph using a nonlinear reservoir model.

After Q_{BG} (Eq. 7) was derived using the calculated S_t , based on Eq. 6, the nonlinear reservoir model was calibrated, and the reservoir routing parameters k and m were optimized—also in Python[™]—using four single rainfall events, as presented in **Paper III**. Six additional rainfall events were used to validate the model with respect to the simulated peak discharge and lag time.

The applicability, validity, and sensitivity of the developed model for mesoscale blue-green stormwater systems are fully discussed and presented in **Paper III**. However, it is an event-based model and incapable of simulating long-term (continuous) scenarios due to the lack of sink functions, such as dynamic infiltration and evapotranspiration, in the retention and detention units.

3.3 Joint model architecture

The developed model for mesoscale blue-green stormwater systems had to be coupled to a pipe network model to facilitate the study of interactions between blue-green systems and municipal combined/separate sewer networks. For this purpose, DHI's MIKE Urban was adopted for coupling with the mesoscale blue-green model (**Paper IV**).

The models were coupled in DHI's MIKE Operations, which builds on the MIKE Workbench data management framework (DHI, 2019). The MIKE Operations platform enables communication between two models (MIKE Urban and mesoscale blue-green model) via Python[™]. The software architecture for the coupled models and cosimulation is presented in Figure 14.

The logic consists of three major blocks, as follows:

- i. The characterization block (input data)
- ii. The hydrological module, including two rainfall-runoff models
- iii. The hydraulic module, including a hydrodynamic simulation engine

System parameters and catchment definitions, such as the configuration of the blue-green system and the position and size of the mesoscale blue-green systems with respect to the sewer network, are defined and registered in the characterization block. In the hydrological module, catchment definitions, system parameters, and rainfall data are fed into both rainfall-runoff models—i.e., MIKE Urban and the mesoscale blue-green model. The catchment definition for the rainfall-runoff module in MIKE Urban includes the drainage area for the pipe network, excluding the catchments (areas) with mesoscale blue-green stormwater systems that are modeled separately in

the mesoscale blue-green model. As a result, the two models generate two sets of flow series: Q_{BG} (simulated according to Eq. 7) and Q_{MU} (simulated in MIKE Urban).

These flow series cumulate and form the total runoff load (Q_{TR}) per Eq. 8. In contrast to the case in Augustenborg, in which the discharge from the blue-green system is connected to a separate stormwater pipe system (and not to the original combined sewer), this study assumes that mesoscale blue-green retrofits are still discharged into the original sewer network (in this case, the combined sewer network) after applied retention and detention. This step is designed to determine whether flow detention alone—which often is the case for blue-green retrofits—rather than flow elimination from the original sewer network, also relieves flooding situations.

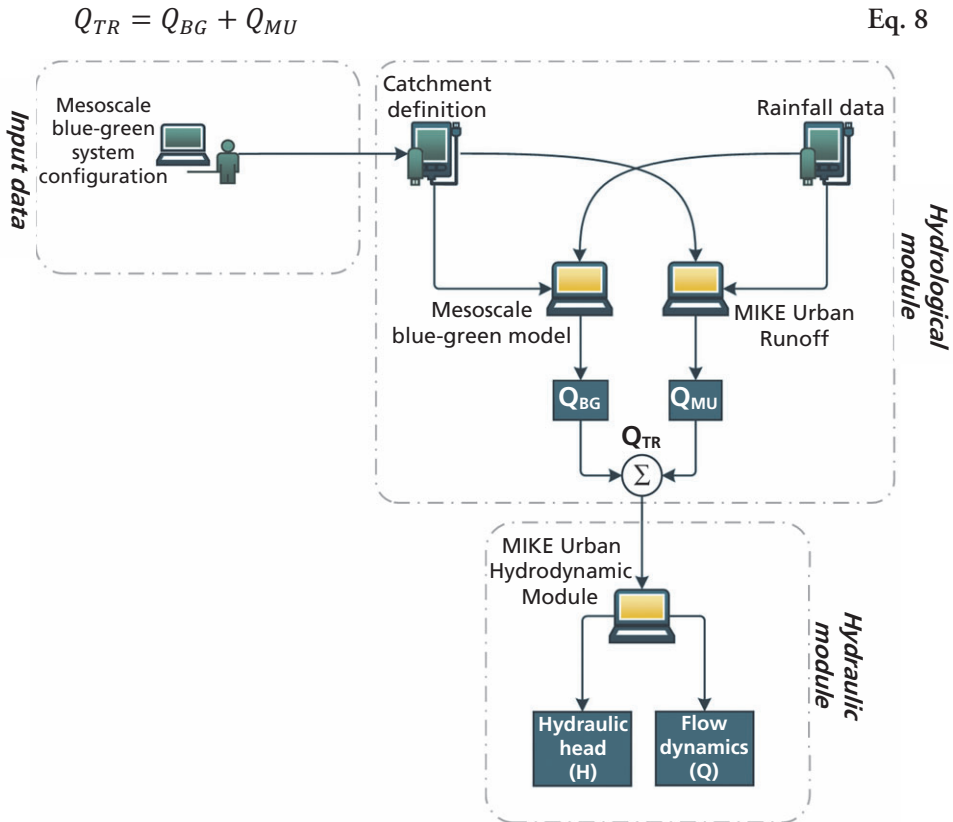


Figure 14.

The logic implemented in MIKE Operations through which the mesoscale blue-green model and MIKE Urban are coupled (adapted from **Paper IV**).

Moreover, Q_{MU} consists of several components, such as the fast runoff component, (Q_{FRC}), the slow runoff component (Q_{SRC}), and the domestic wastewater flow (Q_{WW}) in the case of combined sewer systems. Because the MIKE Urban model incorporates sub-catchments, each of which is connected to a node, mesoscale blue-green systems are also implemented per sub-catchment. Thus, F_{BG} (extent of implementation) reflects the percentage of total drainage area in the sub-catchment (A_{SC}) that is converted to the mesoscale blue-green system (A_{BG}), according to Eq. 9.

$$F_{BG} = \frac{A_{BG}}{A_{SC}} \quad \text{Eq. 9}$$

Consequently, Eq. 8 can be expanded as follows:

$$\begin{aligned} Q_{TR} &= Q_{BG} + Q_{MU} \\ Q_{TR} &= Q_{BG} + Q_{FRC} \cdot (1 - F_{BG}) + Q_{SRC} + Q_{WW} \end{aligned} \quad \text{Eq. 10}$$

Subsequently, Q_{TR} is applied to the hydrodynamic model in MIKE Urban through which network simulations are run. The result from the hydrodynamic simulations includes hydraulic head (H) in the nodes (manholes) of the network and the flow dynamics (Q) in the links (pipes), as shown in Figure 14. Based on the simulated hydraulic heads, the number and location of the flooded manholes can be determined and used as a cost function parameter to optimize the placement and size of mesoscale blue-green stormwater systems throughout the city.

4 From meso- to macroscale: Upscaling and optimization

Blue-green stormwater systems can be placed in urban spaces, based on various criteria. Availability of space, willingness of the landowner, and the morphological properties of urban spaces are several factors that dictate the implementation point for blue-green stormwater systems (Bach *et al.*, 2013; Romnée *et al.*, 2015). However, with regard to piped drainage, the hydraulic interaction between blue-green retrofits and conventional sewer systems is a key parameter in the occurrence of pluvial floods. The effect of blue-green stormwater systems in relieving the pressure of a network is assumed to be a function of the size and location of the blue-green retrofit.

In this perspective, the upscaling of blue-green stormwater systems from mesoscale to macroscale concerns optimization. The placement of single (microscale) blue-green stormwater measures in cities has been optimized primarily with respect to biophysical characteristics and urban form, rather than socioeconomic considerations (Kuller *et al.*, 2018). There is significant published material that has addressed the optimization of blue-green measures (and even detention/storage units) with respect to flood mitigation, peak flow reduction, and mitigation of the first flush effect (Damodaram *et al.*, 2013; Baek *et al.*, 2015; Cunha *et al.*, 2016; Duan *et al.*, 2016; Wang *et al.*, 2017; Zischg *et al.*, 2018). However, these studies have focused on the optimal size and spatial distribution of *microscale* blue-green stormwater measures, rather than *mesoscale* systems, and do not explicitly address the interactions between pipe networks and blue-green systems in terms of the hydraulic performance of the network.

There are also studies that have argued that the implementation of blue-green measures must be accompanied by increased pipe capacity in the sewer network to obtain a robust and resilient drainage system (Zhou *et al.*, 2018; Bakhshipour *et al.*, 2019). For increased simplicity, Zhou *et al.* (2018) have modeled the impact of blue-green stormwater measures as altered imperviousness in the target catchments and thus fail to address the discharge dynamics from a blue-green system or how locating the blue-green measures affects drainage performance.

In this section, the upscaling of blue-green stormwater systems from meso- to macroscale is proposed by replication of mesoscale blue-green stormwater systems at the city level. This replication is characterized through multivariate optimization, in which a cost-effective scheme for the placement and size of blue-green stormwater systems throughout the city can be achieved. The goal is to optimize mesoscale blue-green systems such that the total cost of the optimized scenario—comprising implementation and maintenance costs of blue-green systems and flood cost—is less than that of the no-action scenario. This tool can be used to perform an initial citywide screen of catchments to identify the potential regions and areas in which it is hydraulically and economically efficient to implement mesoscale blue-green stormwater systems.

4.1 Hydroeconomic optimization

At this stage, the toolchain that was presented in the previous chapter in Figure 14 is supplemented with an additional module for automated optimization and input characterization (Figure 15). The joint model delivers hydraulic head in the network nodes (manholes), which can be used to determine whether a manhole is flooded—i.e., for each node, a critical threshold is defined such that if the hydraulic head in that node (H_{max}) exceeds the threshold, the node is marked as *flooded*. The introduced flood threshold for the manholes can be basement-level (in a combined sewer network) or ground-level (in a separate sewer network). In this thesis, the threshold is set as the basement level of buildings, which is assumed to be approximately 1.3 m below ground level for each manhole (**Paper IV**). Thus, the total number of the flooded nodes (n_{fn}) can be acquired from the model.

Moreover, a damage cost must be estimated for each flooded node (c_{fn}), constituting the total flood cost (C_{flood}). Within the framework of this thesis, each flooded node was estimated according to the compensation records that were available for the extensive flooding in Malmö on August 31, 2014, as described in **Paper IV**.

In addition, cost of action (C_{act}) needs to be determined. Cost of action is defined as the sum of investment - per hectare retrofitted area (C_{BG}) - and maintenance costs of a blue-green stormwater system.

The scalarized multiobjective incorporates the two crucial cost sources that are associated with urban drainage—namely, C_{act} , including the construction and maintenance costs for blue-green stormwater systems, and C_{flood} , including compensation by insurance companies and the local water utility company. For C_{act} , equivalent uniform annual worth of investment is calculated per Eq. 11 using the capital recovery factor.

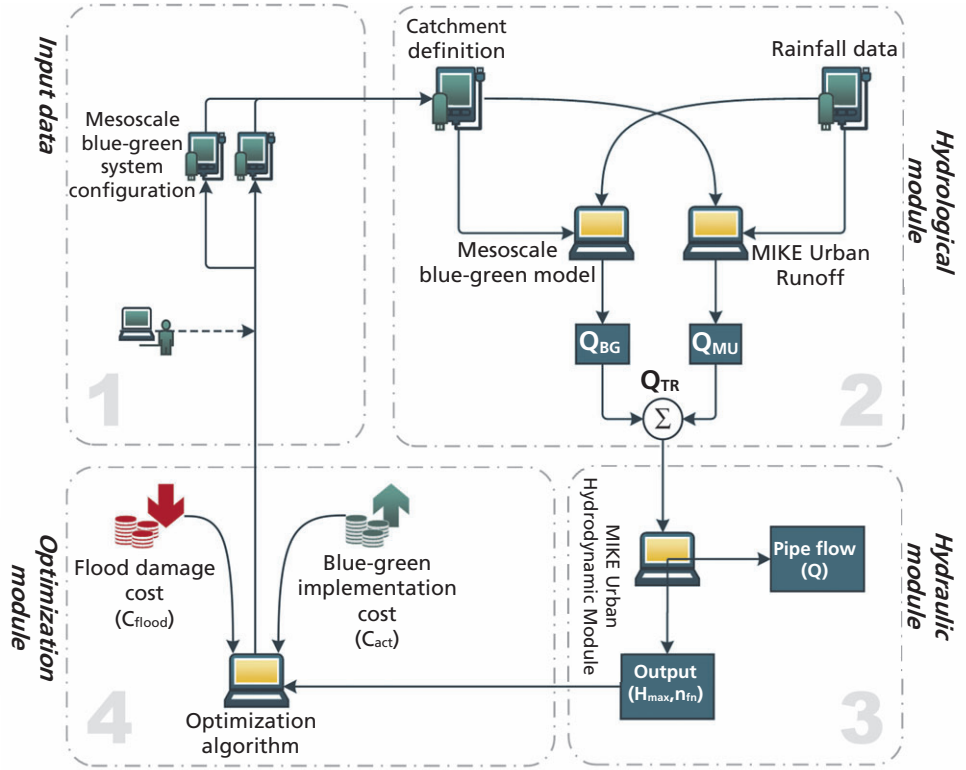


Figure 15.

Enhanced software architecture with the addition of an optimization module with respect to C_{flood} and C_{act} , with an automated input characterization module.

$$C_{act} = (C_{BG} \cdot \sum A_{BG}) \underbrace{\left[\frac{i(1+i)^L}{(1+i)^L - 1} \right]}_{\text{Capital Recovery Factor}} + \sum A_{BG} \cdot \frac{M}{L} \sum_{l=0}^{L-1} (1 + \alpha)^l \quad \text{Eq. 11}$$

in which $(C_{BG} \cdot \sum A_{BG})$ is the investment value at Year 0, i is the interest rate ($\cong 3\%$), M is the annual maintenance cost per hectare blue-green retrofit, α is the annual average pay raise ($\cong 2\%$), and L is the capital distribution period, assumed to be equal to the technical lifespan of the constructed structure ($\cong 50$ years). C_{flood} is the uniform annual series, using the sinking fund factor, equivalent to the future amount of damage costs—i.e., $(c_{fn} \cdot n_{fn})$ —and is calculated according to Eq. 12.

$$C_{flood} = (c_{fn} \cdot n_{fn}(u)) \underbrace{\left[\frac{i}{(1+i)^T - 1} \right]}_{\text{Sinking Fund Factor}} \quad \text{Eq. 12}$$

in which $(c_{fn} \cdot n_{fn})$ is the total damage cost at the end of the T^{th} period, i is the interest rate ($\cong 3\%$), and T is the total number of periods (in this case, years), assumed to be equal to the recurrence interval of the design storm ($\cong 10$ years in this study). The economic calculations in Eq. 11 and Eq. 12 are adapted from Blank and Tarquin (2012).

The reason why C_{act} is annualized for the period of the system's life span and C_{flood} is annualized for a period that is equal to the recurrence interval of the optimization rainfall is so that the long-term financial effects of multiple recurrences of the rainfall event can be incorporated into the optimization. Assuming, through common engineering practice, that the rainfall events are uniformly distributed, based on their respective recurrence frequency, it can be deduced that 5 rainfall events with a recurrence interval of 10 years is likely to occur during the operational life span of the built systems—i.e., 50 years. This approach intrinsically implements the long-term financial effects of multiple rainfall recurrences throughout the developed toolchain. However, the probability of occurrence of the scenario above (i.e., exactly 5 rainfalls with a recurrence interval of 10 years in 50 years) is low, at 17.6%.

With the uniform annual cost of flood damage and the cost of action for flood mitigation (implementation and maintenance of blue-green systems), a total cost function can be determined per Eq. 13.

$$\Phi(u) = C_{act}(u) + C_{flood}(u) \quad \text{Eq. 13}$$

The objective of optimization is to minimize the performance indicator, PI, defined as the relative change in $\Phi(u)$ for various situations of u compared with the total cost of the reference scenario, $\Phi(0)$ —i.e., no blue-green retrofits. Note that u reflects the distribution and size of mesoscale blue-green stormwater systems in the modeled sub-catchments (SC_i). PI is also considered a multiobjective, because the cost components (C_{act} and C_{flood}) are assumed to be competing:

$$\begin{aligned} \min \quad & PI = \frac{\Phi(u) - \Phi(0)}{\Phi(0)} \\ \text{w. r. t.} \quad & u \in \begin{bmatrix} SC_1 & SC_2 & SC_3 & \dots & SC_i \\ F_{BG,1} & F_{BG,2} & F_{BG,3} & \dots & F_{BG,i} \end{bmatrix} \\ \text{s. t.} \quad & F_{BG,i} \in [0,1] \end{aligned}$$

Subsequently, the optimization was performed using the constrained optimization by linear approximation (COBYLA) method, which is a derivative-free optimization algorithm (Powell, 1994; Conn *et al.*, 1997). The COBYLA method was implemented in Python™, in communication with the MIKE Operations platform that was discussed in the previous chapter, Section 3.3.

4.2 Implementation of the toolchain

The software that was developed in the previous chapter, in conjunction with the optimization algorithm, returns an optimized solution for any network model, depending on the initial values of the decision variables. However, the result is not a unique solution or necessarily the most optimal solution. Given the number of catchments that are to be assigned an extent of implementation—i.e., the number of decision variables in the optimization (e.g., 30 catchments in the case study in **Paper IV**)—the target optimization space becomes high-dimensional (e.g., 30 dimensional for 30 catchments), comprising many local optima. There are algorithms that can help identify the set of initial values for the decision variables that lead the optimization toward the ultimately best solution—the global optimum—in such complex high-dimensionality. However, these algorithms are time-consuming and computationally demanding for citywide hydraulic applications. An obvious follow-up of this study would thus be to use other optimization techniques and decision variable selection algorithms to address the challenge of the high-dimensionality that is associated with city-scale catchment studies.

Based on the optimization results for the combined sewer network in the city of Malmö, with a total catchment area of over 950 ha, only two catchments (of 30) were found to be hydroeconomically appropriate for the implementation of mesoscale blue-green stormwater systems under a 10-year CDS rain (**Paper IV**). Notably, one of these catchments lay close to the outlet, whereas the second was distant. The extent of the suggested retrofit areas constituted approximately 2% of the total modeled catchment area (**Paper IV**). Considering the classification per Eckart *et al.* (2018) for blue-green adoption rates (equivalent to F_{BG} in this thesis), $F_{BG} = 2\%$ is considered a *low retrofit* scenario.

The peak flow reduction in the optimized scenario was approximately 1.5%, which is on the same order of magnitude as in Eckart *et al.* (2018), as reported for a low retrofit scenario (i.e., approximately 1.2% to 1.3%). However, as described in the literature, the efficiency of the optimized scenario in peak flow reduction is strongly affected by the extent of implementation of blue-green retrofits and the rainfall characteristics under which the scenario is evaluated (Eckart *et al.*, 2018; Huang *et al.*, 2018).

According to the optimized scenario in **Paper IV**, the total cost (the sum of implementation and maintenance costs for the recommended blue-green stormwater systems and the cost for the resulting flooding) is estimated to be approximately 3% lower (PI=-0.03) than the reference scenario—i.e., the flooding cost when no blue-green stormwater system is implemented. Although these savings are modest, the

total number of flooded nodes decreased by 8.5% (65 nodes) in the optimized scenario compared with the reference case (779 nodes).

The modest overall savings in the optimal scenario is consistent with Eckart *et al.* (2017) and Li *et al.* (2019), who noted that budget is a major limiting factor in stormwater management projects. However, the PI is highly sensitive to cost estimates (**Paper IV**), which could substantially affect the outcome of the optimization. Also, blue-green stormwater systems are associated with several added values, such as mitigation of urban heat islands, promotion of biodiversity, improvement of discharged water quality, decrease in combined sewer overflow (CSO) occurrences, amenity effects, and lower loading and thus increased treatment capacity at wastewater treatment plants. Monetizing these valuable contributions would most likely affect the cost-benefit optimization considerably, although it is not always easy to monetize all effects. Thus, it will be invaluable to develop methods to adapt and incorporate available cost-benefit tools, such as Benefits of SuDS Tool (BeST) (Ashley *et al.*, 2016, 2018), in the economic cost estimation for hydroeconomic optimization of blue-green stormwater systems. Further, cost assessment studies should be conducted contextually according to the prevailing local circumstances.

One out of 325 iterations in the optimization in **Paper IV** led to more flooded manholes compared with the reference scenario—i.e., there was a scenario in which, despite the introduction of blue-green retrofits, the extent of flooding was worse than in the reference scenario. This finding is an indication that unoptimized random blue-green retrofits do not necessarily improve the hydraulic performance of sewer networks. One explanation is that because the overflow from the mesoscale blue-green retrofit is still connected to the original sewer network, the retained and detained discharge will coincide with high pipe flows, thus causing flooding of the network.

This interpretation dovetails with the tentative conclusion in **Paper I**, which recommends that the implementation of blue-green retrofits be prioritized primarily in the upstream areas of the city catchment to avoid such peak-flow coincidences. Such coincidences between detained and delayed discharges from blue-green stormwater systems and flows in the sewer network are more likely to occur in city-scale networks, which have high complexity. Thus, it is important to determine the sensitivity of the optimization to not only cost assessments and interest rates but also other factors, such as rain characteristics (hyetograph) and catchment parameters, which can alter the discharge hydrograph from the blue-green retrofit and the dynamics of the flow in the pipe system.

In addition to optimization method, adopted cost function, and the specific hydrological parameters of the study catchments, there are three factors that might be important in the interpretation of the study results.

High network complexity on a city scale, especially when the discharge from the blue-green retrofit remains connected to the sewer network, could cause unprecedented coincidences of peak flows. These coincidences (due to different rain patterns or changes in catchment characteristics) could still lead to flooding. Depending on the coincident flow values, the flooding could be as bad as the reference scenario or even worse.

Combined sewer systems, as is the case in this thesis, are more demanding due to the lower critical levels—i.e., *basement level* rather than *ground level*—that are used to estimate inundation costs for surface flooding. In practice, this leads to tougher optimization constraints or other conditions that must be satisfied; thus, the mitigation of basement floods might not be economically justified by the implementation of blue-green stormwater retrofits. However, how blue-green retrofits perform in the context of separate sewer systems in which ground levels are critical for flooding must also be studied and assessed.

Mesoscale retrofits through which an entire neighborhood is transformed into a blue-green stormwater system are likely to be more costly to implement versus single, discrete blue-green measures. Such steps would increase action costs when the target catchment area is large. Note that the study area in the optimization context of this thesis (approximately 950 ha) is roughly 7 times larger than that in Huang *et al.* (2018) (approximately 140 ha), denoted as a megacity. This considerably larger study area in **Paper IV** has strong impacts on computational expenses, thus influencing the choice of optimization algorithm.

5 Conclusions

This thesis has examined a specific setup of blue-green stormwater systems, termed the *mesoscale blue-green stormwater system*. These systems, comprising several interconnected blue-green measures for the retention and detention of runoff, have an invaluable role in the transformation of neighborhoods into large blue-green retention cells. Based on the results and discussion in this thesis, the following conclusions are made:

- Through a case study, mesoscale blue-green systems are effective in the control and confinement of surface floods at the local level. The influence of mesoscale blue-green systems is not limited to local boundaries, also affecting the surrounding pipe-bound catchments. Thus, blue-green retrofits in cities should be designed with regard to larger urban drainage rather than merely local circumstances.
- The case study revealed that the outflow hydrograph from the mesoscale blue-green stormwater system under a 100-year rainfall was equivalent to that of a 6.5-year rainfall from the conventional pipe-bound catchment.
- The performance of a mesoscale blue-green stormwater system in terms of the final discharged flow dynamics (hydrographical characteristics) is a function of the spatial distribution of its constituent blue-green measures, considering their retention capacity.
- More stringent demands for flood mitigation in combined sewer networks and the large areas of city-scale catchments (leading to high dimensionality and high complexity) render the optimization of mesoscale blue-green stormwater systems over the entire city a challenging issue.
- The method of and approach to the cost-benefit assessment of citywide blue-green scenarios with respect to financial consequences and monetized value and damage have a decisive role in the outcome of the optimization.
- In the case that blue-green retrofits are drained into the original sewer network, there might be blue-green retrofit scenarios in which the overall flood performance of the sewer network deteriorates in terms of the number of flooded manholes compared with the reference scenario. This correlation is tentatively associated with the high complexity of networks on the city

scale through which even retained and detained blue-green discharges could coincide with peak flows that pass in the pipe network, giving rise to the hydraulic head and, thus, flooding. Consequently, this thesis recommends that the discharge from mesoscale blue-green retrofits should not be connected to the original network if the economy and local circumstances allow—i.e., it is hydraulically safe and beneficial, with regard to the underlying sewer network perspective, to eliminate the impact of the catchment versus discharging detained and delayed flow.

6 Future research

The findings of this thesis suggest that hydraulically unoptimized implementation of blue-green stormwater retrofits has unprecedented consequences in terms of deteriorated flood situations and limited economic gain. However, these observations were based solely on the study of a combined sewer network. Thus, the implementation and optimization of blue-green retrofits in the framework of separate sewer networks should also be examined.

Moreover, it is also important to study how a group of scattered microscale blue-green measures functions hydraulically compared with an equivalent mesoscale setup with a similar total retention volume. Such a study would provide valuable insights into how blue-green measures with various scales and configurations affect drainage. This endeavor is also important, practically speaking, because differences in scale and configuration might have considerable effects on the implementation cost of the retrofits.

As discussed in Section 2.2.1, there are uncertainties that are associated with rain measurements due to point data being extracted from tipping bucket gauges. To minimize the error from local point measurements of rain data, it is preferable to use distributed rain data using X-band weather radars. Today, there are two X-band weather radars that have been newly installed in the region, and a third is to be established soon. Using high-resolution precipitation data from weather radars, although it requires substantial revisions in the modeling procedures, would open a new front in rainfall-runoff studies that hopefully leads to a better understanding of urban hydrology.

The modeling platform and software that were developed in this thesis can be expanded in various aspects. The mathematical model that was introduced and discussed in Section 3.2 is currently based on one nonlinear reservoir model that is implemented in a virtual reservoir that is discharged into the system outlet, whereas the flow detention effect is not applied to upstream physical components. Thus, a natural continuation of the development of the model would be to facilitate all model components with nonlinear reservoir models to simulate the detention effect at various points in the mesoscale blue-green stormwater system (not solely at the discharge point). This step will lead to a complicated calibration procedure due to the numerous nonlinear reservoir routing parameters—i.e., two for each component.

However, it might be possible to theoretically relate the nonlinear reservoir routing parameters for a particular blue-green stormwater measure to certain physical characteristics of the measure, which could reduce the number of coefficient values that need to be estimated, yielding a more reliable and easier-to-use model. Yet, the calibration and validation of the enhanced model would require thoroughly monitoring different types of blue-green measures regarding their construction—such as bed soil properties, geometrical shape, and dimensions—and careful records of rainfalls, water levels in the measures, and the corresponding discharges.

In addition to the hydrodynamic runoff model for mesoscale blue-green stormwater systems, the optimization procedure can be developed. The adopted optimization algorithm, COBYLA, like all optimization algorithms, delivers optimization results, depending on the initial values of the decision variables. These results are thus highly local and do not necessarily reflect the most optimal solution of the extremely high-dimensional optimization space. To overcome this problem, appropriate scouting methods must be applied and evaluated to estimate the initial values of decision variables, which would most likely lead the optimization to the global optimum. Methods, such as Latin Hypercube Sampling (LHS) and Subset Selection Algorithm (SSA), might be valuable in adapting and testing for enhanced optimization.

This thesis has demonstrated that from a hydraulic perspective, blue-green stormwater measures can be represented by static volumes. These volumes can be introduced onto the catchments, regardless of their type, shape, and construction material. Thus, even concrete basins and ponds could reproduce similar hydraulic effects as those that are expected from blue-green measures. However, there is a substantial aesthetic and social aspect concerning the function of blue and green elements in urban landscapes. Compelling future research could study and map the effects of blue-green spaces—as integrated infrastructural elements in an urban environment—on human well-being.

With regard to cost-benefit calculations, a comprehensive study must be performed in advance to be introduced into the optimization process. This step will require the development of methods to monetize the social and ecological benefits of blue-green spaces, in addition to construction and maintenance costs, with regard to local circumstances. The sensitivity of the adopted optimization algorithm to perturbations in economic and financial assessments, interest rates, and hydrological and hyetographical characteristics should also be examined.

7 References

- Albrecht, J.C., 1974. Alterations in the Hydrologic Cycle Induced by Urbanization in Northern New Castle County, Delaware: Magnitudes and Projections. University of Delaware, Delaware, USA.
- Alley, W.M., Veenhuis, J.E., 1983. *Effective impervious area in urban runoff modelling*. J. Hydraul. Eng 109, 313–319.
- Ashley, R., Digman, C., Horton, B., Gersonius, B., Smith, B., Baylis, A., 2016. *Using the multiple benefits of SuDS tool (BeST) to deliver long-term benefits*, in: The 9th International Conference on Planning and Technologies for Sustainable Management of Water in the City, 28 June-1 July 2016. NOVATECH, Lyon, France.
- Ashley, R.M., Gersonius, B., Digman, C., Horton, B., Bacchin, T., Smith, B., Shaffer, P., Baylis, A., 2018. *Demonstrating and Monetizing the Multiple Benefits from Using SuDS*. Journal of Sustainable Water in the Built Environment 4.
- Bach, P.M., McCarthy, D.T., Urich, C., Sitzenfrei, R., Kleidorfer, M., Rauch, W., Deletic, A., 2013. *A planning algorithm for quantifying decentralised water management opportunities in urban environments*. Water Science and Technology 68, 1857–1865.
- Back, S.-S., Choi, D.-H., Jung, J.-W., Lee, H.-J., Lee, H., Yoon, K.-S., Cho, K.H., 2015. *Optimizing low impact development (LID) for stormwater runoff treatment in urban area, Korea: Experimental and modeling approach*. Water Research 86, 122–131.
- Bakhshipour, A.E., Dittmer, U., Haghighi, A., Nowak, W., 2019. *Hybrid green-blue-gray decentralized urban drainage systems design, a simulation-optimization framework*. Journal of Environmental Management 249, 109364.
- Becker, P., 2018. *Enviro-organizational rift in Swedish flood risk governance*, in: Sociologidagarna. Lund, Sweden.
- Bengtsson, L., Grahn, L., Olsson, J., 2005. *Hydrological function of a thin extensive green roof in southern Sweden*. Hydrology Research 36, 259–268.

- Berndtsson, R., Becker, P., Persson, A., Aspegren, H., Haghighatafshar, S., Jönsson, K., Larsson, R., Mobini, S., Mottaghi, M., Nilsson, J., Nordström, J., Pilesjö, P., Scholz, M., Sternudd, C., Sörensen, J., Tussupova, K., 2019. *Drivers of changing urban flood risk: A framework for action*. Journal of Environmental Management 240, 47–56.
- Bernstad Saraiva Schott, A., Aspegren, H., Bissmont, M., la Cour Jansen, J., 2013. Modern Solid Waste Management in Practice: The City of Malmö Experience, SpringerBriefs in Applied Sciences and Technology. Springer London, UK.
- Blank, L., Tarquin, A., 2012. Engineering Economy, 7th ed. McGraw-Hill, New York, USA.
- Boyd, M.J., Bufill, M.C., Knee, R.M., 1993. *Pervious and impervious runoff in urban catchments*. Hydrological Sciences Journal 38, 463–478.
- Butler, D., Davies, J.W., 2011. Urban Drainage, 3rd ed. Spon Press (Taylor & Francis Group), Abingdon, UK.
- Carpenter, S.R., Folke, C., Scheffer, M., Westley, F., 2009. *Resilience: Accounting for the noncomputable*. Ecology and Society 14.
- Conn, A.R., Scheinberg, K., Toint, P., 1997. *On the Convergence of Derivative-Free Methods for Unconstrained Optimization*, in: Iserles, A., Buhmann, M. (Eds.), Approximation Theory and Optimization: Tributes to M. J. D. Powell. Cambridge University Press, Cambridge, UK, pp. 83–108.
- Cunha, M.C., Zeferino, J.A., Simões, N.E., Saldarriaga, J.G., 2016. *Optimal location and sizing of storage units in a drainage system*. Environmental Modelling & Software 83, 155–166.
- Damodaram, C., Zechman, E.M., Asce, M., 2013. *Simulation-Optimization Approach to Design Low Impact Development for Managing Peak Flow Alterations in Urbanizing Watersheds*. Journal of Water Resources Planning and Management 139, 290–298.
- DellaSala, D.A., Goldstein, M.I., 2017. Encyclopedia of the Anthropocene.
- DHI, 2019. MIKE OPERATIONS [WWW Document]. URL <https://www.mikepoweredbydhi.com/products/mike-operations> (accessed 3.19.19).
- Duan, H.-F., Li, F., Yan, H., 2016. *Multi-Objective Optimal Design of Detention Tanks in the Urban Stormwater Drainage System: LID Implementation and Analysis*. Water Resources Management 30, 4635–4648.
- Ebrahimian, A., Gulliver, J.S., Wilson, B.N., 2016. *Effective impervious area for runoff in urban watersheds*. Hydrological Processes 30, 3717–3729.

- Eckart, K., McPhee, Z., Bolisetti, T., 2018. *Multiobjective optimization of low impact development stormwater controls*. Journal of Hydrology 562, 564–576.
- Eckart, K., McPhee, Z., Bolisetti, T., 2017. *Performance and implementation of low impact development – A review*. Science of The Total Environment 607–608, 413–432.
- Fiener, P., Auerswald, K., 2009. *Spatial variability of rainfall on a sub-kilometre scale*. Earth Surface Processes and Landforms 34, 848–859.
- Fletcher, T.D., Andrieu, H., Hamel, P., 2013. *Understanding, management and modelling of urban hydrology and its consequences for receiving waters: A state of the art*. Advances in Water Resources 51.
- Fletcher, T.D., Shuster, W., Hunt, W.F., Ashley, R., Butler, D., Arthur, S., Trowsdale, S., Barraud, S., Semadeni-Davies, A., Bertrand-Krajewski, J.-L., Mikkelsen, P.S., Rivard, G., Uhl, M., Dagenais, D., Viklander, M., 2015. *SUDS, LID, BMPs, WSUD and more – The evolution and application of terminology surrounding urban drainage*. Urban Water Journal 12, 525–542.
- Hoegh-Guldberg, O., Jacob, D., Taylor, M., Bindi, M., Brown, S., Camilloni, I., Diedhiou, A., Djalante, R., Ebi, K., Engelbrecht, F., Guiot, J., Hijioka, Y., Mehrotra, S., Payne, A., Seneviratne, S.I., Thomas, A., Warren, R., G., Z., 2018. *Impacts of 1.5 °C of Global Warming on Natural and Human Systems*, in: Global Warming of 1.5 °C. An IPCC Special Report on the impacts of global warming of 1.5°C above pre-industrial levels and related global greenhouse gas emission pathways, in the context of strengthening the global response to the threat of climate change, sustainable development, and efforts to eradicate poverty [Masson-Delmotte, V., P. Zhai, H.-O. Pörtner, D. Roberts, J. Skea, P.R. Shukla, A. Pirani, W. Moufouma-Okia, C. Péan, R. Pidcock, S. Connors, J.B.R. Matthews, Y. Chen, X. Zhou, M.I. Gomis, E. Lonnoy, T. Maycock, M. Tignor, and T. Waterfield (eds.)]. In Press.
- Holling, C.S., 1996. *Engineering Resilience versus Ecological Resilience*. Engineering Within Ecological Constraints.
- Huang, C.L., Hsu, N.S., Liu, H.J., Huang, Y.H., 2018. *Optimization of low impact development layout designs for megacity flood mitigation*. Journal of Hydrology 564, 542–558.
- IPCC, 2014. Climate Change 2014: Synthesis Report. Contribution of Working Groups I, II and III to the Fifth Assessment Report of the Intergovernmental Panel on Climate Change [Core Writing Team, R.K. Pachauri and L.A. Meyer (eds.)], IPCC. The Intergovernmental Panel on Climate Change, Geneva, Switzerland.

- Keifer, C.J., Chu, H.H., 1957. *Synthetic Storm Pattern for Drainage Design*. Journal of the Hydraulics Division 83, 1–25.
- Kibirige, D., Tan, X., 2013. Evaluation of Open Stormwater Solutions in Augustenborg, Sweden. Master thesis at Water and Environmental Engineering, Department of Chemical Engineering, Lund University, Lund, Sweden.
- Kuller, M., Bach, P.M., Ramirez-Lovering, D., Deletic, A., 2018. *What drives the location choice for water sensitive infrastructure in Melbourne, Australia?* Landscape and Urban Planning 175, 92–101.
- Lerer, S.M., 2019. Tools and Methods to inform Planning and Design of Nature Based Stormwater Control Measures. Doctoral thesis at DTU Environment, Technical University of Denmark, Copenhagen, Denmark.
- Li, C., Peng, C., Chiang, P.C., Cai, Y., Wang, X., Yang, Z., 2019. *Mechanisms and applications of green infrastructure practices for stormwater control: A review*. Journal of Hydrology.
- Lloyd-Davies, D.E., 1906. *The elimination of storm-water from sewerage systems*. Minutes of the Proceedings of the Institution of Civil Engineers 164, 41–67.
- Locatelli, L., Gabriel, S., Mark, O., Mikkelsen, P.S., Arnbjerg-Nielsen, K., Taylor, H., Bockhorn, B., Larsen, H., Kjølby, M.J., Blicher, A.S., Binning, P.J., 2015. *Modelling the impact of retention–detention units on sewer surcharge and peak and annual runoff reduction*. Water Science and Technology 71, 898–903.
- Mainstream™, 2017. Data Sheet for Mainstream™ Portable AV-Flowmeters.
- Malmö stad, 2017. Ekostaden Augustenborg [WWW Document]. URL <https://malmo.se/Bo-bygga--miljo/Miljoarbetet-i-Malmo/Malmo-stads-miljoarbete/Hallbar-stadsutveckling/Ekostaden-Augustenborg.html> (accessed 3.12.19).
- Melanen, M., Laukkanen, R., 1980. *Analysis of rainfall-runoff relationships in Finnish urban test basins*, in: Proceedings of the Helsinki Symposium. IAHS-AISH Publications.
- Milly, P.C.D., Betancourt, J., Falkenmark, M., Hirsch, R.M., Kundzewicz, Z.W., Lettenmaier, D.P., Stouffer, R.J., 2008. *Climate Change. Stationarity is dead: whither water management?* Science (New York, N.Y.) 319, 573–4.
- Nash, J.E., 1957. *The form of the instantaneous unit hydrograph*. International Association of Science Hydrology Publication 45, 114–121.
- Powell, M.J.D., 1994. *A Direct Search Optimization Method That Models the Objective and Constraint Functions by Linear Interpolation*, in: Advances in

- Optimization and Numerical Analysis. Springer Netherlands, Dordrecht, pp. 51–67.
- Python, 2019. About Python™ | Python.org [WWW Document]. URL <https://www.python.org/about/> (accessed 3.19.19).
- Rauch, W., Bertrand-Krajewski, J.-L., Krebs, P., Mark, O., Schilling, W., Schütze, M., Vanrolleghem, P.A., 2001. *Mathematical modelling of integrated urban drainage systems*. (Preprint) 1–16.
- Rauch, W., Schilling, W., Bertrand-Krajewski, J.-L., Vanrolleghem, P.A., Schütze, M., Mark, O., Krebs, P., 2002. *Deterministic modelling of integrated urban drainage systems*. Water Science and Technology 45, 81–94.
- Romnée, A., Evrard, A., Trachte, S., 2015. *Methodology for a stormwater sensitive urban watershed design*. Journal of Hydrology 530, 87–102.
- Sahoo, S.N., Pekkatt, S., 2018. *Detention Ponds for Managing Flood Risk due to Increased Imperviousness: Case Study in an Urbanizing Catchment of India*. Natural Hazards Review 19.
- Schwab, K., Brende, B., 2018. The Global Risks Report 2018 - Insight Report, 13th ed. World Economic Forum, Geneva, Switzerland.
- Shukri, A., 2010. Hydraulic Modeling of Open Stormwater System in Augustenborg, Sweden. Master thesis at Water and Environmental Engineering, Department of Chemical Engineering, Lund University, Lund, Sweden.
- Singh, V.P., 1997. *Effect of spatial and temporal variability in rainfall and watershed characteristics on stream flow hydrograph*. Hydrological Processes 11, 1649–1669.
- Stahre, P., 2008. Blue-green fingerprints in the city of Malmö, Sweden: Malmö's way towards a sustainable urban drainage.
- Stahre, P., 2006. Sustainability in urban storm drainage - planning and examples, 1st ed. Svenskt Vatten, Stockholm, Sweden.
- Thomas, C.D., Cameron, A., Green, R.E., Bakkenes, M., Beaumont, L.J., Collingham, Y.C., Erasmus, B.F.N., de Siqueira, M.F., Grainger, A., Hannah, L., Hughes, L., Huntley, B., van Jaarsveld, A.S., Midgley, G.F., Miles, L., Ortega-Huerta, M.A., Townsend Peterson, A., Phillips, O.L., Williams, S.E., 2004. *Extinction risk from climate change*. Nature 427, 145–148.
- UN, 2018. World Urbanization Prospects: The 2018 Revision.
- UNDRR, 2018. Disaster Statistics - United Nations Office for Disaster Risk Reduction (UNDRR) [WWW Document]. URL

- <https://www.unisdr.org/we/inform/disaster-statistics> (accessed 10.12.18).
- VA SYD, 2008. The Eco-city Augustenborg - A walk along the path of storm water. Malmö.
- van de Ven, F.H.M., Snep, R.P.H., Koole, S., Brolsma, R., van der Brugge, R., Spijker, J., Vergroesen, T., 2016. *Adaptation Planning Support Toolbox: Measurable performance information based tools for co-creation of resilient, ecosystem-based urban plans with urban designers, decision-makers and stakeholders*. Environmental Science & Policy 66, 427–436.
- Villarreal, E.L., 2007. *Runoff detention effect of a sedum green-roof*. Nordic Hydrology 38, 99–105.
- Villarreal, E.L., Bengtsson, L., 2005. *Response of a Sedum green-roof to individual rain events*. Ecological Engineering 25, 1–7.
- Villarreal, E.L., Semadeni-Davies, A., Bengtsson, L., 2004. *Inner city stormwater control using a combination of best management practices*. Ecological Engineering 22, 279–298.
- Walmsley, A., 1995. *Greenways and the making of urban form*. Landscape and Urban Planning 33, 81–127.
- Wang, M., Sun, Y., Sweetapple, C., 2017. *Optimization of storage tank locations in an urban stormwater drainage system using a two-stage approach*. Journal of Environmental Management 204, 31–38.
- Wihlborg, M., Sörensen, J., Alkan Olsson, J., 2019. *Assessment of barriers and drivers for implementation of blue-green solutions in Swedish municipalities*. Journal of Environmental Management 233, 706–718.
- Zhou, Q., Lai, Z., Blohm, A., 2018. *Optimising the combination strategies for pipe and infiltration-based low impact development measures using a multiobjective evolution approach*. Journal of Flood Risk Management 12.
- Zischg, J., Zeisl, P., Winkler, D., Rauch, W., Sitzenfrie, R., 2018. *On the sensitivity of geospatial low impact development locations to the centralized sewer network*. Water Science and Technology 77, 1851–1860.

Paper I

Efficiency of blue-green stormwater retrofits for flood mitigation – Conclusions drawn from a case study in Malmö, Sweden

Salar Haghighatafshar^{a*}

Beatrice Nordlöf^b

Maria Roldin^c

Lars-Göran Gustafsson^c

Jes la Cour Jansen^a

Karin Jönsson^a

Journal of Environmental Management, 207, 60–69.
(2018)

^a Water and Environmental Engineering, Department of Chemical Engineering,
Lund University, P.O. Box 124 SE-22100, Lund, Sweden

^b Ramböll Sweden, Skeppsgatan 5, SE-21111 Malmö, Sweden

^c DHI Sweden, Södra Tullgatan 3, SE-21140 Malmö, Sweden

* Corresponding author



Research article

Efficiency of blue-green stormwater retrofits for flood mitigation – Conclusions drawn from a case study in Malmö, Sweden



Salar Haghighatafshar^{a,*}, Beatrice Nordlöf^b, Maria Roldin^c, Lars-Göran Gustafsson^c, Jes la Cour Jansen^a, Karin Jönsson^a

^a Water and Environmental Engineering, Department of Chemical Engineering, Lund University, P.O. Box 124, SE-221 00 Lund, Sweden

^b Ramböll Sweden, Skeppsgatan 5, SE-211 11 Malmö, Sweden

^c DHI Sweden, Södra Tullgatan 3, SE-211 40 Malmö, Sweden

ARTICLE INFO

Article history:

Received 28 June 2017

Received in revised form

2 October 2017

Accepted 7 November 2017

Keywords:

Blue-green

Cloudburst

Urban drainage

Flood mitigation

Retrofit

Stormwater

ABSTRACT

Coupled one-dimensional (1D) sewer and two-dimensional (2D) overland flow hydrodynamic models were constructed to evaluate the flood mitigation efficiency of a renowned blue-green stormwater retrofit, i.e. Augustenborg, in Malmö, Sweden. Simulation results showed that the blue-green stormwater systems were effective in controlling local surface flooding in inner-city catchments, having reduced the total flooded surfaces by about 70%. However, basement flooding could still be a potential problem depending on the magnitude of the inflows through combined sewer from upstream areas. Moreover, interactions between blue-green retrofits and the surrounding pipe-system were studied. It was observed that the blue-green retrofits reduced the peak flows by approximately 80% and levelled out the runoff. This is a substantial advantage for downstream pipe-bound catchments, as they do not receive a cloudburst-equivalent runoff from the retrofitted catchment, but a reduced flow corresponding to a much milder rainfall. Blue-green retrofits are more effective if primarily implemented in the upstream areas of a pipe-bound catchment since the resulting reduced runoff and levelled out discharge would benefit the entire network lying downstream. Implementing blue-green retrofits from upstream towards downstream can be considered as a sustainable approach.

© 2017 Elsevier Ltd. All rights reserved.

1. Introduction

1.1. Background

According to the 5th assessment report published by the *Intergovernmental Panel on Climate Change* (IPCC) in 2013, climate change causes more intense and frequent rainfalls over some parts of the world, including northern Europe and Scandinavia (Collins et al., 2013). The current status of the climate in the member states of the European Union (EU), for instance, shows that devastating storms and cloudbursts are already occurring more frequently and have resulted in economic losses (Jongman et al., 2014). According to the definition provided by the Swedish Meteorological and Hydrological Institute (SMHI), a cloudburst is a rainfall with the minimum depth of 50 mm in 1 h or 1 mm per minute for shorter durations (SMHI, 2011).

The runoff generated from cloudbursts is too large to be handled by conventional pipe-bound sewerage networks (either separate or combined) which have traditionally been adopted by most European cities. These networks are usually designed to manage rainfalls of a certain magnitude. In Sweden, for instance, the existing drainage systems in the core of cities were designed for rainfalls of 10-year recurrence interval (RI), (SWWA, 2004), which corresponds to about 26 mm in 1 h. This means that the city planners statistically accepted the risk for one possible flooding in ten years. However, with climate change, this criterion becomes inadequate since rainstorms occur more frequently. From a design point of view, the inadequacy in the traditional design criteria is now recommended to be compensated by application of a climate factor along with increased design RIs (SWWA, 2016).

Both separate and combined sewer networks are considered as pipe-bound networks in general, and even if separate sewer networks overcome the problem of basement flooding, they would still be overloaded and would consequently flood onto the urban surfaces during cloudbursts. Flooding of urban surfaces might in

* Corresponding author.

E-mail address: Salar.Haghighatafshar@chemeng.lth.se (S. Haghighatafshar).

fact be more detrimental than basement flooding since it could paralyze urban emergency services by affecting their mobility and responsiveness. There is thus an ongoing debate regarding the available alternative solutions for handling cloudbursts and mitigation of pluvial flooding in pipe-bound drainage networks. These alternatives can mainly be categorized as i) buffer-based solutions adding to the hydraulic capacity of the underground drainage "system", such as detention basins, stormwater tunnels and pumps (e.g. Yazdi et al., 2015); and ii) surface-based measures reducing the volume and intensity of the generated runoff also known as blue-green stormwater solutions (e.g. Young et al., 2011). In contrast to pipe-bound solutions where there is an apparent boundary between the system and the catchment, the definitions of system and catchment are tightly integrated and inseparable within the framework of blue-green systems (Haghighatafshar et al., 2017). However, in the context of pipe-bound sewer networks, catchments with blue-green stormwater systems would rather be considered as surfaces/catchments with longer lag times.

Despite reports demonstrating the benefits of the blue-green stormwater systems in flood mitigation at cloudbursts (Liu et al., 2014; Sørensen, 2016), it seems that there is still some hesitance in the planning profession and decision makers with respect to the functionality of such systems. The existing uncertainty in the upper levels of decision and policy making leads to lack of strong political commitment within the context of integrated urban water management, IUWM (Mitchell, 2006; Rauch et al., 2005). This can be one of the reasons that keeps authorities from making concrete decisions as well as allocating clear responsibilities and resources (Tingsanchali, 2012). As a result, it negatively influences fundamental steps towards establishment of a well thought-out legal and regulative framework for systematic implementation of blue-green practices, especially in the core of the cities (Sørensen et al., 2016). One potential reason for the hesitance can be the lack of sufficient research and of established catchment-scale blue-green systems. It is therefore of high priority to provide city planners and decision makers with studies and discussions which can help them conceive a clearer picture of the functions and consequences of blue-green alternatives (Viavattene and Ellis, 2013).

1.2. Blue-green stormwater systems

Stormwater control measures (SCM), as components of blue-green stormwater systems, have been discussed in the literature with regards to both runoff management and flood mitigation. It is important to consider that these measures may pursue different purposes in an urban environment and may function differently depending on the scale of implementation (Demuzere et al., 2014). Accordingly, the following classification is suggested:

- 1) *Microscale*, at which a single SCM, e.g. green roof, soakaway, swale, porous asphalt, is investigated under site-specific conditions.
- 2) *Mesoscale*, i.e. a group of several SCMs implemented at a catchment/neighbourhood scale.
- 3) *Macroscale*, through which catchments with blue-green stormwater systems are put into a broader context and are studied in an infrastructural perspective with city-wide consequences.

It should also be noted that the definition of blue-green stormwater systems within the framework of this paper is limited to implementations on the catchment surface. Thus, underground measures such as wastewater detention basins are not defined as blue-green solutions. In this context, blue-green stormwater systems are seen as preventive measures against further overloading of the existing pipe network whereas underground detention

basins in the pipe-bound sewer network could be considered as a remedial action in order to relieve existing capacity constraints of the network.

Single scattered SCMs (i.e. microscale local implementations) with limited detention capacity (e.g. green roofs) are assumed not to be specifically effective in confronting cloudbursts. In contrast, blue-green stormwater systems, i.e. combinations of several SCMs in an urban catchment (mesoscale), have been shown to be beneficial for flood mitigation (Ahiablame and Shakya, 2016; Jato-Espino et al., 2016; Liu et al., 2014).

In this perspective, blue-green systems might function differently depending on where they are implemented (Biesbroek et al., 2010; Heidrich et al., 2013; Jato-Espino et al., 2016). New developments, which are usually located in suburban areas, could easily utilize these systems along with dedicated (separate) wastewater networks. In such cases, the applied blue-green systems would be at the most upstream point of the catchment, conveying the storm runoff to the closest possible receiving water. The circumstances are much tougher when retrofitting blue-green systems into the tighter districts of the inner city. In these cases, the implemented systems are forced to interact with the existing sewer network since there is not necessarily always an accessible receiving water in the city core. Understanding the interactions between different constituents of urban infrastructure is key to a sustainable climate adaptation plan (Mottaghi et al., 2016). There is therefore a need to elevate the discussions to a higher level at which blue-green stormwater systems are assessed in an infrastructural perspective.

1.3. Aim of the study

The number of studies on the efficiency of individual SCMs, i.e. microscale evaluations, is abundant. However, less attention has been directed towards understanding the collective effect of SCMs in a blue-green stormwater system and their interactions with the existing sewerage network of the city. It is important to notice that the process of retrofitting blue-green stormwater systems in mesoscale has two distinct consequences. Firstly, the retrofit conducts the local runoff in an open system through the implemented SCMs and secondly, the retrofit isolates/disconnects the catchment from the upstream sewer network catchments. Therefore, this study aims to suggest strategies for sustainable implementation of blue-green stormwater systems and provide a deeper insight into functions and effects of the systems via:

- Evaluation of an existing blue-green stormwater retrofit with respect to local flood mitigation (mesoscale: handling local runoff).
- Analysis of the flooding processes and studying the interactions at the interface between the retrofit and the surrounding pipe-bound sewerage system (mesoscale: catchment isolation).

2. Methodology

The study adopts an infrastructural perspective including different parts of the storm- and wastewater collection system, i.e. blue-green implementations in the target catchment, sewerage network upstream and downstream, as well as their possible interactions. The adopted approach is a model-based case study in the famous large-scale blue-green retrofit, Augustenborg in Malmö, Sweden (Fig. 1).

2.1. Case-study area

In the aftermath of frequent basement floodings, the

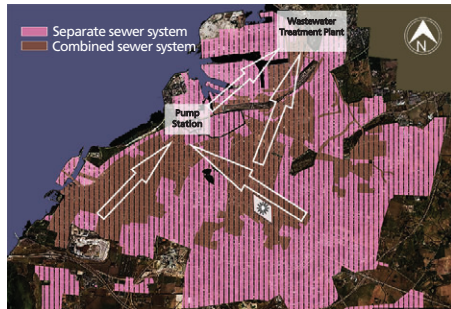


Fig. 1. Location of the Eco-city of Augustenborg (marked with a star) with respect to the sewerage infrastructure of Malmö. Arrows represent the general flow direction in the combined sewer network. The background map is courtesy of the municipality of Malmö (Malmö stad).

stormwater system in Augustenborg was rebuilt in the late 1990s by which the runoff from the area was disconnected from the combined sewer network and was instead handled locally on the surface through implementations of blue-green stormwater systems. In the process of retrofitting, the majority of the implemented SCMs were constructed at elevations lower than the critical flood elevation of the buildings. Moreover, public spaces such as playgrounds and yards/lawns were also lowered in elevation. In this way, not only the residential buildings were secured against possible flooding, but also a larger retention volume was introduced to the neighbourhood.

The existing underground pipe system is still part of the municipal sewer network that in the post-retrofit case receives *a*) domestic wastewater from the households in Augustenborg and *b*) combined stormwater and domestic wastewater from the upstream areas of the combined sewer catchment. The connected upstream catchments are also developed areas and have a total effective impervious area of approximately 33 ha.

Fig. 2 shows the different sub-catchments and their corresponding systems in the area of Augustenborg. The study area consists of two major sub-catchments with blue-green retrofits (Northern and Southern retrofits with areas of 6.3 and 9.5 ha, respectively) along with a smaller part (3.5 ha) which is drained via a separate stormwater pipe system. All three systems are ultimately connected to the municipal sewerage network of Malmö via the illustrated connection points (CP) in Fig. 2. More details of the sub-catchments in Augustenborg are described in Nordlöf (2016).

2.2. Model concept

The model concept used in this study is based on a coupled 1D/2D model, in which the 1D model (MIKE URBAN) is used to describe the pipe network and the 2D model (MIKE21) is used to describe the overland flow. The integrated software that couples MIKE URBAN and MIKE21 is named MIKE FLOOD (DHI, 2017). MIKE FLOOD models were constructed for Augustenborg, simulating the existing blue-green stormwater system and the situation before the reconstruction, respectively. Comparison of these two cases made it possible to achieve a mesoscale evaluation of the implemented blue-green retrofits in a drainage infrastructure perspective.

2.2.1. Post-retrofit model of Augustenborg

The post-retrofit model of Augustenborg describes the

stormwater system in the area in its current state. The model describes the separate pipe network, the ponds and canals of the blue-green stormwater systems, and the terrain of the area (according to Fig. 3).

2.2.1.1. Distribution of model components in 1D and 2D. The hydraulic model consists of two dynamically coupled sub-models, a 1D (MIKE URBAN) model of the stormwater network, and a 2D (MIKE21) model of the catchment surface. Different modelling approaches are applied for the rainfall-runoff modelling in different parts of the catchment, similar to the method adopted by Chang et al. (2015). Fig. 3 shows how the surfaces and model components are distributed between the 1D and the 2D models. On directly connected impervious areas (DCIA) such as roofs and pavements, rainfall is applied directly to the 1D-model. Runoff from these surfaces is calculated using a time-area method with a constant runoff coefficient as well as a mean surface velocity from which the time of concentration is derived. On pervious surfaces, such as parks, and impervious surfaces drained by the open stormwater system, all rainfall is applied directly onto the 2D model. The surface runoff is calculated using the 2D shallow water equations. The 1D model is used to simulate the hydraulics of the pipe-networks as well as the canals in the blue-green systems.

Infiltration is modelled as a sink in the 2D model. Water is removed from the surface with an infiltration rate depending on a given maximum infiltration capacity and the available surface water volume in each time step, which in turn is also affected by the surface water velocity. Once the maximum infiltration capacity has been reached and the soil is saturated, water will be removed from the surface at a slower rate, corresponding to the hydraulic conductivity of the soil. In this way, it is possible to simulate the situation in which the pervious surfaces are saturated and start to contribute to the runoff.

The MIKE21 model is dynamically coupled to the MIKE URBAN model, enabling simultaneous modelling of overland flow and flow in the hydraulic network. With this approach, the model can simulate overland flow draining to the hydraulic network as well as manhole surcharge. The exchange flow between the 1D and 2D domain is described by a weir equation.

2.2.1.2. MIKE URBAN model setup. The MIKE URBAN model describing the pipes and open canals of the Augustenborg system has been set up based on an existing pipe network database and field visits to the area. The initial model setup was constructed by Shukri (2010).

2.2.1.3. MIKE21 model setup. The MIKE21 model has a spatial resolution of 2×2 m. The model consists of a Digital Elevation Model (DEM), parameters describing the infiltration layer, and parameters describing the friction resistance of the surface. Infiltration and friction parameters are spatially distributed. Initial parameter values were determined based on land use, and adjusted iteratively during the calibration process.

2.2.1.4. Model parameters. Table 1 shows the adjusted values of the fundamental parameters used in the 1D and 2D models. The input parameters such as infiltration rates, depth of infiltration layer, porosity and friction values (Manning's n) were adjusted by simulating three rainfall events with depths of 13.6, 15.6 and 22.8 mm (captured by a tipping bucket rain gauge with 0.2 mm tip, Casella™) for which corresponding runoffs from the sub-catchments were monitored using Mainstream™ Area-Velocity Flowmeters. More information about the process of the parameter estimation is described in Nordlöf (2016).

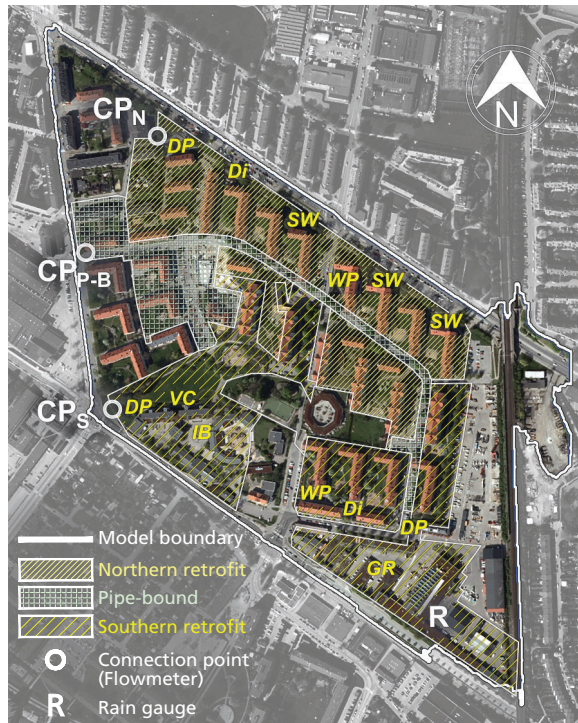


Fig. 2. Pipe-bound system, Northern and Southern blue-green retrofits in Augustenborg and their connection points to the municipal sewer network. Connection points marked as CP_N , CP_{P-B} and CP_S are the discharge points for the Northern retrofit, the pipe-bound catchment and the Southern retrofit, respectively. Note that the flow is in the Northwest direction, i.e. towards the connection points. Different types of SCMs are shown in the figure as follows: **DP**: dry pond; **DI**: stormwater ditch; **SW**: swale; **WP**: wet pond; **VC**: vegetated channel; **IB**: infiltration basin; **GR**: green roof. Background picture: GSD-Orthophoto, courtesy of The Swedish Mapping, Cadastral and Land Registration Authority, ©Lantmäteriet (2015). (For interpretation of the references to colour in this figure legend, the reader is referred to the web version of this article.)

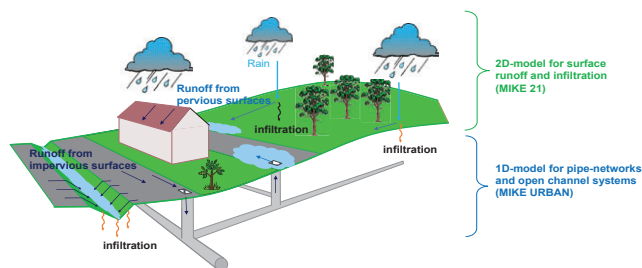


Fig. 3. Distribution of model components in 1D (MIKE URBAN) and 2D (MIKE21) models.

2.2.1.5. Model boundary and boundary conditions. The boundary for the 2D model is delineated based on the topographic characteristics

of the area (shown in Fig. 2). The same model boundary was also used for the 1D model for which boundary conditions were

Table 1
Input parameters for the MIKE FLOOD runoff model.

| Land use | 2D model parameters | | | | 1D model parameters | | |
|-----------------|-----------------------------------|--------------------------|---|-----------------------|-------------------------------|------------------------|--|
| | Manning's n^* ($s/(m^{1/3})$) | Infiltration rate (mm/h) | Storage volume in infiltration layer (mm) | Leakage rate** (mm/h) | Surface runoff velocity (m/s) | Runoff coefficient (-) | |
| Grass | 0.67 | 10 | 15 | 0.036 | n/a | 0 | |
| Sand and gravel | 0.50 | 30 | 25 | 0.036 | n/a | 0 | |
| Paved areas | 0.025 | 0 | 0 | 0 | 0.1 | 1 | |
| Green roofs | 0.67 | 120 | 45 | 0 | n/a | 0 | |

*Initial values for Manning's n for overland flow were adopted from Gustafsson and Mårtensson (2014).

**Leakage rate is the rate at which the infiltrated water is drained into the groundwater/deeper soil layers, and thus is removed from the model.

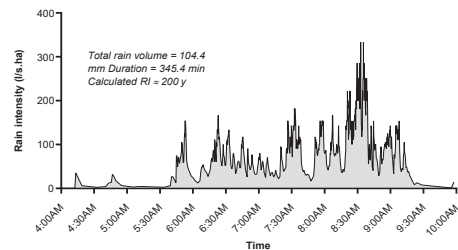


Fig. 4. The simulated extreme rainfall (cloudburst) on Augustenborg. The cloudburst was monitored and logged by a tipping bucket rain gauge within the area of Augustenborg.

introduced at the interface of the model boundary with the surrounding pipe network. The water levels and flows at the interfaces were collected from a larger 1D model for the entire pipe network of the Malmö city, provided by the local water utility company.

2.2.1.6. Error sources and uncertainties. Since the process of parameter estimation was based on the observed rainfall-runoff data that corresponded to milder rain events, some uncertainty is probably introduced to the simulation results of extreme rain events/cloudbursts. On the other hand, there are uncertainties associated with measuring instruments as well. For example, data from a single tipping bucket rain gauge was used in the simulations, assuming that the same rain depth/intensity was valid for the entire catchment. All these assumptions and error sources introduce uncertainties to the modelling process. However, it is important to notice that this work does not employ modelling for an in-depth quantitative evaluation, but rather it uses the models as tools for understanding general processes and interactions within the drainage area from a management point of view.

2.2.2. Pre-retrofit model of Augustenborg

The pre-retrofit model describes the hydraulic drainage network prior to the reconstruction when the area was drained by a combined sewer network connected to upstream parts of the city of Malmö. The model had in principle the same setup as the post-retrofit model (described above) except that it included the DEM representing the terrain prior to reconstruction and the impervious areas such as streets, rooftops, etc. were connected to the combined sewer network. Based on ocular comparison of aerial photos of the area before and after reconstruction, the total impervious area in both cases was assessed to be identical.

2.3. Applied rainfalls

For the mesoscale evaluation with respect to handling local runoff, the cloudburst which fell on the 31st of August 2014 in Malmö (Fig. 4) was applied to both pre- and post-retrofit MIKE FLOOD models of the area. During the cloudburst, about 100 mm of rain fell in less than 4 h including an extreme peak of about 22 mm over 20 min (between 8:20 a.m.–8:40 a.m.). The cloudburst is estimated to have a RI of about 200–300 years based on an extrapolation using Dahlström formula (Dahlström, 2010). More insights into the cloudburst are presented in Table 2.

For evaluating the effects of catchment isolation, a Chicago Design Storm (CDS) of 100 years RI (see Table 2 for more details) was applied to the post-retrofit MIKE FLOOD model to investigate

Table 2

Characteristics of the applied rainfalls for the approaches to mesoscale evaluation.

| Duration (min) | 31 st of August 2014 Cloudburst (Subsection 3.1.) | | CDS ($r = 0.37^*$) (Subsection 3.2.) | |
|----------------|--|------------|--|------------|
| | Rainfall depth (mm) | RI (years) | Rainfall depth (mm) | RI (years) |
| 30 | 27 | 22 | 45 | 100 |
| 60 | 42 | 45 | 55 | 100 |
| 120 | 68 | 115 | 65 | 100 |
| 220 | 100 | 240 | 75 | 100 |

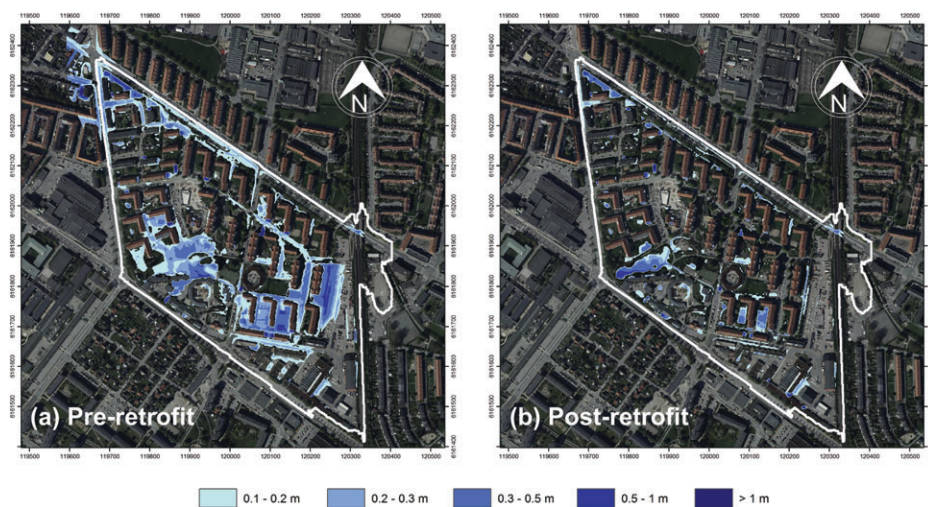


Fig. 5. Flood map (maximum flood depth) of the Augustenborg area based on simulations of the cloudburst on 31st of August 2014 for both (a) pre-retrofit and (b) post-retrofit cases. Background picture: GSD-Orthophoto, courtesy of The Swedish Mapping, Cadastral and Land Registration Authority, ©Lantmäteriet (2015). (For interpretation of the references to colour in this figure legend, the reader is referred to the web version of this article.)

the effect of the levelled-out runoff from the Southern retrofit in Augustenborg (CP₅). Levelled out runoff from the Southern retrofit was then translated into an equivalent rainfall over the pipe-bound catchment resulting in a similar runoff pattern. All RI calculations were carried out using Dahlström formula (Dahlström, 2010).

3. Results and discussions

In the following subsections, the results and findings are presented and discussed at mesoscale with regards to handling capacity of local runoff and effects from catchment isolation, respectively, reflecting the two main objectives of the study.

3.1. Mesoscale: handling local runoff

Fig. 5a and b shows the simulation results for terrain flooding in Augustenborg for cases before and after reconstruction, respectively. The figures illustrate the maximum flood depth in both cases, i.e. the maximum depth of flood at a given point regardless of time. In other words, the calculated water depths at different points do not necessarily occur simultaneously. As seen in Fig. 5a, in the case concerning the situation before the implementation of the blue-green system (pre-retrofit case), flood covers about 8.7 ha and is

uncontrolled and widely spread towards nearby buildings and would probably cause significant damage.

In the post-retrofit case (Fig. 5b), the implementation of a blue-green stormwater system has resulted in more controlled and concentrated flooding. Controlled flooding means that excessive amounts of water lie on the surfaces which are designed and designated to be flooded. It is also observed that the area covered by flood (2.8 ha) is reduced by approximately 70% compared to pre-retrofit case.

A quantitative representation of controlled and uncontrolled flooding can be seen in Fig. 6 in which a mass balance over the stormwater systems before and after implementation of the retrofits is illustrated. It is important to notice that the mass balances reflect the situation only in the stormwater systems in both cases. In other words, the domestic wastewater system in the Augustenborg (which also receives combined wastewater and stormwater flows from upstream catchments) is not represented in the mass balances. The mass balances represent the situation at the end of the simulated cloudburst, i.e. 10:00 a.m. (see Fig. 4). The boxes in the centre of the mass balance diagrams show the volume of the water that is still within the model boundaries (see Fig. 2). From the total volume of about 22 300 m³ remaining in the area in case of pre-retrofit, about 21 600 m³ is on the surface while only 700 m³ is

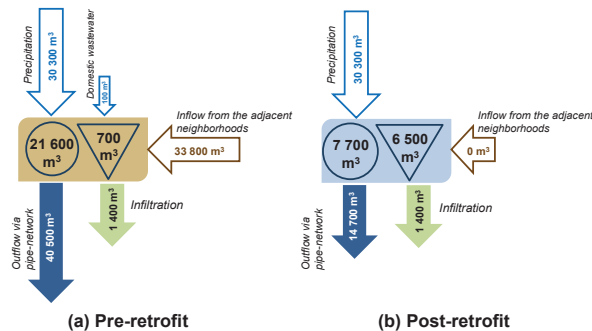


Fig. 6. Mass balances (a) over combined sewer network in pre-retrofit case and (b) over the stormwater management system in post-retrofit case within the framework of this study. Note that in the post-retrofit case, there is a separate flow line for the wastewater from Augustenborg and the combined sewer inflows from the adjacent neighbourhoods, which is not presented here. The mass balances were calculated at the time by which the rainfall (cloudburst) ended; that was about 6 h after the rain started and about 1 h and 40 min after the rain peak struck. The box in the centre of each mass-balance chart shows the total volume of water within the system boundaries. The number in the circle represents the volume lying on the terrain, whereas the number in the triangle is the water volume in the structural components of the stormwater systems.

accommodated in the structural components (i.e. combined sewer pipes).

The situation for the post-retrofit case is considerably different regarding the distribution of the remaining water. In this case, about 7700 m³ water lies mostly on the designated surfaces while an almost similar amount (about 6500 m³) is in the blue-green stormwater structures such as ponds, canals, swales, etc. These numbers do not include the volume of water which was already present in the system (mainly in wet ponds) at the very beginning of the simulation (=2400 m³). It is important to underline that not only the distribution, but also the volume of the water to be handled in the presented cases are extremely different. The combined sewer system in the pre-retrofit case receives more than twice as much water as the post-retrofit case. This is due to the integrative behaviour of pipe-bound systems which is reflected in the amount of combined wastewater and stormwater inflow from the adjacent neighbourhoods (33 800 m³).

In presence of blue-green stormwater solutions, more water is expected to infiltrate due to the enhanced infiltration capacity of the catchment. However, the results show that the total volume of infiltrated water in the pre-retrofit case is approximately as high as in the post-retrofit case. This observation can probably be explained by the broader areas unintentionally flooded in the pre-retrofit case (compare flooded areas in Fig. 5a and b).

Moreover, it can be claimed that the location of the introduced retrofit with respect to the entire urban infrastructure plays an important role in the overall functionality of blue-green stormwater systems. This is found to be mainly due to the external flow loads from the neighbouring areas. As shown in Fig. 6, there is a substantial difference in total volume of water that needs to be handled in the pre- and post-retrofit cases. In the pre-retrofit case (Fig. 6a), a considerable volume of water (= 33 800 m³ of combined wastewater and stormwater) has entered into Augustenborg's combined sewer network from the adjacent neighbourhoods while this amount is completely omitted in the post-retrofit case (Fig. 6b) since the blue-green retrofit is basically responsible only for management of local rainfall which falls over the area. This omitted volume of water in the post-retrofit case is in fact handled by the existing sewer (pipe) network in Augustenborg. Please note that the sewer pipe network in Augustenborg, although locally disconnected from stormwater inflows, is still part of the combined sewer

network that serves the upstream catchments. In other words, the total amount of water in both pre- and post-retrofit cases is the same, but in the latter case, this volume is handled by two separate systems. Simulation results of the existing combined sewer network in Augustenborg show that some nodes/manholes in the model are still flooded mainly due to large inflow from the neighbouring areas. This type of flooding could directly be associated with basement flooding in the context of combined sewer systems. It should also be noted that Augustenborg is located relatively upstream with respect to the entire sewerage system of Malmö (Fig. 1), and this might be the reason why it reportedly managed the cloudburst on 31st of August 2014 relatively better than the rest of the city (Sørensen, 2016). If Augustenborg was located further downstream in the network, the volume of combined sewer inflow from the adjacent areas would actually be much larger and hence a greater risk for basement flooding would exist. In case of a more intensive rain event, there is also a risk that the large volume of combined sewer flow entering through the system boundaries from the neighbouring upstream areas could possibly cause flooding in downstream catchments or even in the target catchment despite blue-green retrofits implemented. Conclusively, the efficiency of blue-green stormwater systems in flood mitigation can considerably be limited if implemented in an area with a hydraulically overloaded pipe-network. Due to the possible overpressure in the downstream sections of a pipe-bound sewerage catchment, it is suggested that implementation of blue-green stormwater retrofits be considered suitable for the upstream areas of a catchment. In that case, the resulting lag time and reduced runoff would benefit the entire network downstream.

Another important point in the context of urban flooding is that the processes of accumulation of water on the surfaces in the studied cases are different. In the pre-retrofit case (Fig. 5a), the generated flood depth is the result of the overloaded combined sewer pipe-network, i.e. flooded manholes, while in the post-retrofit case (Fig. 5b), the runoff is intentionally kept on the surface before entering the sewerage network. Consequently, it can also be reasonably assumed that the water quality may be different. The flood in the pre-retrofit case is in fact the mixed domestic wastewater and stormwater accumulated on the surfaces, which is likely to be contaminated and contains pathogenic microorganisms (De Man et al., 2014; Ten Veldhuis et al., 2010) whereas the flood in

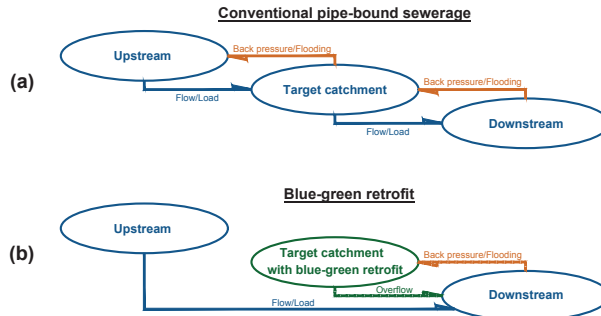


Fig. 7. Comparison of conventional pipe-bound systems with blue-green retrofits with respect to flow interactions with upstream and downstream systems for stormwater management. Flows illustrated with dashed lines represent possible interactions that might occur depending on the constructional circumstances of the system. For instance, an overflow from the retrofit initiates as soon as the volumetric threshold of the blue-green system is saturated (i.e. detention capacity), while the backflow flooding would occur in the target catchment only if the drainage gradient of surfaces and elevations dictates so. (For interpretation of the references to colour in this figure legend, the reader is referred to the web version of this article.)

post-retrofit case is considered as local stormwater runoff and is expected to be less contaminated than combined wastewater and stormwater.

It is therefore crucial to consider the quality and health-risk aspects of urban floods in the design process. Implementing blue-green stormwater systems as temporary detention structures for combined sewer surcharges shall be avoided since these systems must be kept relatively hygienic due to their multi-purpose role in the urban landscape. This is another reason why blue-green stormwater retrofits shall be implemented as upstream as possible while severe flooding issues downstream shall be counteracted by adding extra buffer to the network, for example via introduction of detention basins.

3.2. Mesoscale: catchment isolation (downstream effects)

Fig. 7 is based on the pre- and post-retrofit cases in Augustenborg and illustrates the systematic differences in the flow interactions that pipe-bound and blue-green systems have with the upstream and downstream catchments. Contrary to pipe-bound systems, blue-green retrofits disintegrate the catchment and manage the runoff in a decentralized manner. In other words, the blue-green retrofit is hydraulically isolated from its upstream. Moreover, since only the overflow (surplus runoff from the blue-green systems) reaches the downstream pipe-system, it can be interpreted as the blue-green catchment relieves pressure downstream by holding back the runoff volume/flow. Consequently, not only the total volume of the runoff within the catchment boundaries will be smaller and limited to the local circumstances (due to elimination of inflows from upstream), the discharge from the retrofitted catchment will also be smaller and levelled out.

In order to evaluate the effect of the levelled out discharge, the post-retrofit 1D/2D model was used to simulate the Chicago Design Storm (CDS) of 100 year RI with 6 h duration. Fig. 8a shows the simulated hydrographs for the pipe-bound system (at CP_{P-B}) as well as the blue-green retrofit in the southern part of Augustenborg (CP_S) during the 100 year RI CDS. Both hydrographs are normalized against the total area of the sub-catchments. It is seen that the generated hydrograph for the pipe-bound sewerage correlates strongly with the cloudburst intensity while the outflow from the

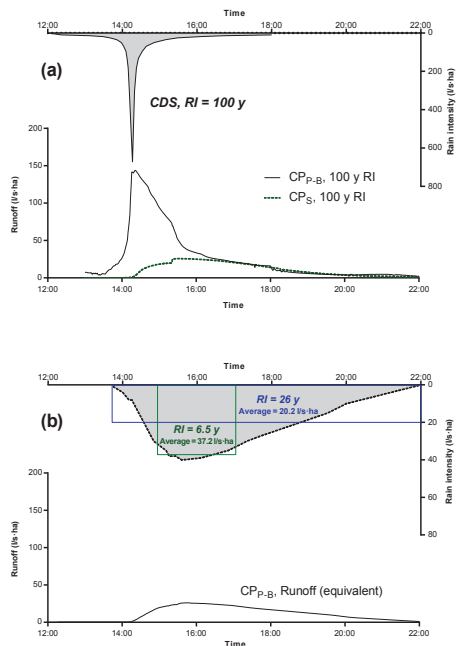


Fig. 8. (a) Simulated hydrographs for a CDS with 100 years RI on the pipe-bound system (at CP_{P-B}) and the Southern retrofit (at CP_S) in Augustenborg. (b) The equivalent rainfall which would generate a levelled-out runoff for the pipe-bound system similar to the runoff from the Southern retrofit under a 100 year storm. Note the difference of scale on y-axis for the hydrographs in (a) and (b).

blue-green retrofit is relatively levelled out and does not contain any severe peaks. The simulation results show that the peak flow from the pipe system is approximately 5–6 times larger than the peak flow from the blue-green retrofit. This levelled out hydrograph from the blue-green retrofit during a 100 year rainstorm can in principle be generated by an equivalent rainfall on the catchment with the conventional pipe-bound system. Based on this hypothesis, a 1D hydrodynamic rainfall-runoff model was used in order to estimate the equivalent rainfall which would result in the same hydrograph from the pipe-bound system in Augustenborg.

However, the equivalent hyetograph can be approximated by a series of block rains with different durations and average intensities. Two examples of such approximations (with 2-h and 8-h durations) as well as the equivalent runoff in the pipe-bound system are shown in Fig. 8b. As seen in Fig. 8b, the runoff in the pipe-bound system ($CP_{p,b}$) is in strong agreement with the levelled-out runoff from CP_S shown in Fig. 8a. Furthermore, the 2-h period during the peak intensity of the equivalent rainfall corresponds to a block rain with 6.5 year RI while the entire duration with average intensity of 20.2 l/s-ha corresponds to a block rain with 26 year RI. It is worth mentioning that urban catchments are often associated with shorter times of concentration and hence shorter rain durations are taken into considerations in the design process. Therefore, in this specific case, the 2-h rain with 6.5 RI would be the decisive rain to consider. This is an indication that the receiving pipe-bound sewerage system of the city, which is designed for rain events of up to a certain RI, would be considerably relieved if blue-green stormwater retrofits are implemented. However, more research has to be carried out in order to find out if extensive implementation of retrofits could completely alleviate the urban flood issue.

The illustrated levelled out runoff and longer lag time would relieve the hydraulic pressure in the downstream areas of a pipe-bound sewerage system. Within the context of a combined sewer network, this can also be directly associated with 1) fewer combined sewer overflow (CSO) occurrences, especially during first foul flush (Kim et al., 2009) and 2) the reduced hydraulic loading at the receiving wastewater treatment plant. Thus, blue-green stormwater solutions do potentially improve the hygiene and public health quality even in the downstream areas of a combined sewerage network.

4. Conclusions

This study concludes that blue-green stormwater systems can be very efficient in controlling local pluvial floods through larger retention capacity built in the system as well as flood-oriented elevation adjustments on the terrain. It is also found that blue-green retrofits in the core of the cities, where catchments constantly interact with different drainage systems with different upstream-downstream conditions, do not necessarily solve the flooding problem. This is due to overloaded pipe network caused by the inflows from neighbouring upstream areas. Retrofitting blue-green systems in downstream catchments of a combined sewer network would also trigger the risk of them receiving contaminated combined sewer floods, which poses high risks for public health and hygiene. Therefore, it might be more beneficial – from a sustainability point of view – to start the implementation process of blue-green stormwater retrofits at the most upstream areas in the network and then move towards downstream areas.

It is also found that blue-green stormwater systems disintegrate catchments and manage runoff locally. The detention capacity of the blue-green systems along with the observed levelled-out outflow, make the downstream parts of the pipe-bound network receive flows equivalent to much milder rain events rather than a cloudburst. This interaction between the existing pipe system of

the city and blue-green stormwater retrofits could possibly sustain the functionality of the urban drainage infrastructure during the changed climate era.

Acknowledgements

This work was financially supported by Sweden Water Research, J. Gustaf Richert Foundation at SWECO (grant number 2015-00181) and the Swedish Water and Wastewater Association (SWWA) (grant number 15-108) via VA-teknik Södra. The authors express their gratitude to the Municipality of Malmö [Malmö stad] (for providing DEM and sewer network map), VA SYD (for providing the sewerage network data) as well as the Swedish Mapping, Cadastral and Land Registration Authority [©Lantmäteriet] (for orthophotos and historical maps of the area).

Appendix A. Supplementary data

Supplementary data related to this article can be found at <https://doi.org/10.1016/j.jenvman.2017.11.018>.

References

- Ahiablame, L., Shakya, R., 2016. Modeling flood reduction effects of low impact development at a watershed scale. *J. Environ. Manag.* 171, 81–91. <https://doi.org/10.1016/j.jenvman.2016.01.036>.
- Biesbroek, G.R., Swart, R.J., Carter, T.R., Cowan, C., Henrichs, T., Mela, H., Morecroft, M.D., Rey, D., 2010. Europe adapts to climate change: comparing national adaptation strategies. *Global Environ. Change* 20, 440–450. <https://doi.org/10.1016/j.gloenvcha.2010.03.005>.
- Chang, T.-J., Wang, C.-H., Chen, A.S., 2015. A novel approach to model dynamic flow interactions between storm sewer system and overland surface for different land covers in urban areas. *J. Hydrol.* 524, 662–679. <https://doi.org/10.1016/j.jhydrol.2015.03.014>.
- Collins, M., Knutti, R., Arblaster, J., Dufrense, J.-L., Fichet, T., Friedlingstein, P., Gao, X., Gutowski Jr., W.J., Johns, T., Krinner, G., Shongwe, M., Tebaldi, C., Weaver, A.J., Wehner, M., 2013. Long-term climate change: projections, commitments and irreversibility. Intergovernmental Panel on Climate Change. In: *Climate Change 2013-The Physical Science Basis*. Cambridge University Press, Cambridge, pp. 1029–1136. <https://doi.org/10.1017/CBO9781107415324.024>.
- Dahlström, B., 2010. Regintensitet – en molnfysikalisk betraktelse (in Swedish) (Rain intensity – a cloud-physical contemplation). Stockholm.
- De Man, H., Van Den Berg, H.H.J.L., Leenen, E.J.T.M., Schijven, J.F., Schets, F.M., Van Der Vliet, J.C., Van Knapen, F., De, A.M., Husman, R., 2014. Quantitative assessment of infection risk from exposure to waterborne pathogens in urban floodwater. *Water Res.* 48, 90–99. <https://doi.org/10.1016/j.watres.2013.09.022>.
- Demuzere, M., Orru, K., Heidrich, O., Olazabal, E., Genelletti, D., Orru, H., Bhawe, A.G., Mittal, N., Feliu, E., Faehne, M., 2014. Mitigating and adapting to climate change: multi-functional and multi-scale assessment of green urban infrastructure. *J. Environ. Manag.* 146. <https://doi.org/10.1016/j.jenvman.2014.07.025>.
- DHI, 2017. MIKE FLOOD. <https://www.mikepoweredbydhi.com/products/mike-flood>. (Accessed 23 March 2017).
- Gustafsson, L.-G., Mårtensson, E., 2014. Kartläggning Av Skyfalls Påverkan På Samhällets Viktiga Verksamheter: Framtagande Av Metodik För Utredning På Kommunal Nivå [Mapping the Impact of Cloudbursts on the Vital Societal Functions and Critical Infrastructure].
- Haghighatafshar, S., la Cour Jansen, J., Aspegren, H., Jönsson, K., 2017. Introduction of a novel conceptual model for sustainable drainage systems based on observed rainfall-runoff patterns – a case study. In: *In The Digital Proceedings of the 14th IWA/IAHR International Conference on Urban Drainage (ICUD)*, pp. 991–998. Prague, Czech Republic.
- Heidrich, O., Dawson, R.J., Reckien, D., Walsh, C.L., Heidrich, O., Dawson, R.J., Walsh, C.L., Reckien, D., 2013. Assessment of the climate preparedness of 30 urban areas in the UK. *Clim. Change* 120, 771–784. <https://doi.org/10.1007/s10584-013-0846-9>.
- Jato-Espino, D., Charlesworth, S., Bayon, J., Warwick, F., 2016. Rainfall-runoff simulations to assess the potential of SuDS for mitigating flooding in highly urbanized catchments. *Int. J. Environ. Res. Publ. Health* 13, 149. <https://doi.org/10.3390/ijerph13010149>.
- Jongman, B., Hochrainer-Stigler, S., Feyen, L., Aerts, J., Mechler, R., Botzen, W.J.W., Bouwer, L.M., Pfliug, G., Rojas, R., Ward, P.J., 2014. Increasing stress on disaster-risk finance due to large floods. *Nat. Clim. Change* 4, 264–268.
- Kim, W.J., Managaki, S., Furumai, H., Nakajima, F., 2009. Diurnal fluctuation of indicator microorganisms and intestinal viruses in combined sewer system. *Water Sci. Technol.* 60, 2791. <https://doi.org/10.2166/wst.2009.732>.
- Liu, W., Chen, W., Peng, C., 2014. Assessing the effectiveness of green infrastructures on urban flooding reduction: a community scale study. *Ecol. Modell.* 291, 6–14. <https://doi.org/10.1016/j.ecolmodel.2014.07.012>.

- Mitchell, V.G., 2006. Applying integrated urban water management concepts: a review of Australian experience. *Environ. Manage.* 37, 589–605. <https://doi.org/10.1007/s00267-004-0252-1>.
- Mottaghi, M., Aspegren, H., Jönsson, K., 2016. Integrated urban design and open storm drainage in our urban environments: merging drainage techniques into our city's urban spaces. *Water Pract. Technol.* 11.
- Nordlöf, B., 2016. 1D/2D Modeling of the Open Stormwater System of Augustenborg Using MIKE FLOOD by DHI. Project report available at Water and Environmental Engineering at the Department of Chemical Engineering, Lund University, Lund, Sweden.
- Rauch, W., Seggelke, K., Brown, R., Krebs, P., 2005. Integrated approaches in urban storm drainage: where do we stand? *Environ. Manage.* 35, 396–409. <https://doi.org/10.1007/s00267-003-0114-2>.
- Shukri, A., 2010. Hydraulic Modeling of Open Stormwater System in Augustenborg, Sweden. Master thesis at Water and Environmental Engineering, Department of Chemical Engineering, Lund University, Lund, Sweden.
- SMHI, 2011. Heavy Rainfalls and Cloudbursts [Rotblöta Och Skyfall] | SMHI. <https://www.smhi.se/kunskapsbanken/rotblota-1.17339>. (Accessed 26 June 2017).
- SWWA, 2016. Drainage of Runoff and Wastewater - Functional Requirements, Hydraulic Dimensioning and Design of Public Sewer Systems (In Swedish). Publication P110, Swedish Water and Wastewater Association (Svenskt Vatten), Bromma, Sweden.
- SWWA, 2004. Dimensioning of Public Sewer Systems (In Swedish). Publication P90, Swedish Water and Wastewater Association (Svenskt Vatten), Stockholm, Sweden.
- Sörensen, J., 2016. Open LID stormwater system tested during severe flood event. In: 2016 International Low Impact Development Conference, pp. 1–4. Beijing, China.
- Sörensen, J., Persson, A., Sternudd, C., Aspegren, H., Nilsson, J., Nordström, J., Jönsson, K., Mottaghi, M., Becker, P., Pilesjö, P., Larsson, R., Berndtsson, R., Mobini, S., 2016. Re-thinking urban flood management - time for a regime shift. *Water* 8. <https://doi.org/10.3390/w8080332>.
- Ten Veldhuis, J.A.E., Clemens, F.H.L.R., Sterk, G., Berends, B.R., 2010. Microbial risks associated with exposure to pathogens in contaminated urban flood water. *Water Res.* 44, 2910–2918. <https://doi.org/10.1016/j.watres.2010.02.009>.
- Tingsanchali, T., 2012. Urban flood disaster management. *Process Eng.* 32, 25–37.
- Viavattene, C., Ellis, J.B., 2013. The management of urban surface water flood risks: SUDS performance in flood reduction from extreme events. *Water Sci. Technol.* 67. <https://doi.org/10.2166/wst.2012.537>.
- Yazdi, J., Lee, E.H., Kim, J.H., 2015. Stochastic multiobjective optimization model for urban drainage network rehabilitation. *J. Water Resour. Plann. Manag.* 141, 4014091. [https://doi.org/10.1061/\(ASCE\)WR.1943-5452.0000491](https://doi.org/10.1061/(ASCE)WR.1943-5452.0000491).
- Young, K.D., Dymond, R.L., Kibler, D.F., 2011. Development of an improved approach for selecting storm-water best management practices. *J. Water Resour. Plann. Manag.* 137, 268–275. [https://doi.org/10.1061/\(ASCE\)WR.1943-5452.0000110](https://doi.org/10.1061/(ASCE)WR.1943-5452.0000110).

Paper II



Conceptualization and schematization of mesoscale sustainable drainage systems: a full-scale study

Salar Haghighatafshar ^{a*}

Jes la Cour Jansen ^a

Henrik Aspegren ^{a,b}

Karin Jönsson ^a

Water, 10(8), 1041
(2018)

^a Water and Environmental Engineering, Department of Chemical Engineering,
Lund University, P.O. Box 124 SE-22100, Lund, Sweden

^b VA SYD, P.O. Box 191, SE-201 21 Malmö, Sweden

* Corresponding author

Conceptualization and Schematization of Mesoscale Sustainable Drainage Systems: A Full-Scale Study

Salar Haghighatafshar ^{1,*} , Jes la Cour Jansen ¹, Henrik Aspegren ^{1,2}  and Karin Jönsson ¹

¹ Water and Environmental Engineering, Department of Chemical Engineering, Lund University, P.O. Box 124, SE-221 00 Lund, Sweden; jes.la_cour_jansen@chemeng.lth.se (J.L.C.J.); henrik.aspegren@chemeng.lth.se (H.A.); karin.jonsson@chemeng.lth.se (K.J.)

² VA SYD, P.O. Box 191, SE-201 21 Malmö, Sweden

* Correspondence: salar.haghighatafshar@chemeng.lth.se; Tel.: +46-46-222-8998

Received: 18 June 2018; Accepted: 3 August 2018; Published: 6 August 2018



Abstract: Sustainable Drainage Systems (SuDS) can be considered the joint product of water engineering and urban planning and design since these systems must comply with hydraulic, hydrologic, and social-ecological functions. To enhance this joint collaboration, a conceptual model of mesoscale SuDS is introduced based on the observed rainfall-runoff responses from two catchments with SuDS and a pipe-bound catchment. The model shows that in contrast to pipe systems, SuDS disaggregates the catchment into a group of discrete mini catchments that have no instant connection to the outlet. These mini catchments start to connect to each other (and perhaps to the outlet) as the rainfall depth increases. It is shown that the sequence of stormwater control measures (SCMs as individual components of SuDS) affects the system's overall performance depending on the volumetric magnitude of the rainfall. The concept is useful in the design and implementation of mesoscale SuDS retrofits, which include several SCMs with different retention and detention capacities within a system.

Keywords: rainfall-runoff; storm water control measure; SuDS; urban drainage; urban landscape; urban planning

1. Introduction

Sustainable Drainage Systems (SuDS) within the context of green infrastructure are becoming more accepted and popular in urban landscapes. Numerous studies indicate that these systems, besides delivering multiple ecosystem services and promoting public health [1–3], have large retention capacities for the management of rainfall events up to the design magnitude [4]. It has also been pointed out that SuDS have positive effects on flood mitigation [5,6]. Therefore, SuDS are occupying more space in urban landscapes either as an alternative solution or as a complement to the existing combined or separate wastewater collecting infrastructure. The large retention capacity associated with SuDS is achieved by introducing extended pervious areas, which allows increased infiltration along with larger retention and retention volumes as well as slow transport of runoff towards the outlet point [7]. In other words, the management of storm water with SuDS utilizes urban spaces and, therefore, affects their functionality. This means that the urban surfaces occupied by SuDS have to comply with social-ecological qualities besides fulfilling their hydraulic role in an urban drainage perspective. Therefore, the planning and designing of SuDS has to be brought about collaboratively by water engineers and urban planners [8–10].

SuDS in urban areas can be implemented at three different levels, i.e., microscale, mesoscale, and macroscale, which was proposed by Haghighatafshar et al. [11]. A graphical illustration of these three levels is presented in Figure 1. A microscale implementation of SuDS (Figure 1a) consists

of scattered individual stormwater control measures (SCMs) from which the excess discharge is directly connected to the urban drainage pipe-network (either separated or combined sewer networks). The procedure for designing an individual SCM is already established and widely practiced based on applying existing methods such as the Rational Method or the Time-Area Method. Details of the design process for individual SCMs can be found in e.g., Water Sensitive Urban Design [12].

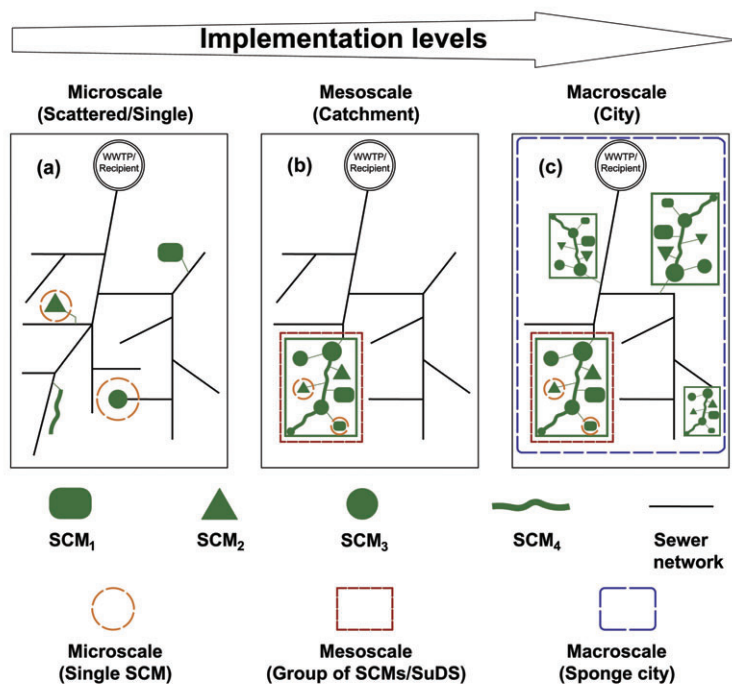


Figure 1. Different levels of implementation for SuDS/SCMs, (a) Microscale, (b) Mesoscale, and (c) Macroscale.

Mesoscale SuDS (Figure 1b) is implemented at the catchment level. This means that a group of interconnected SCMs are integrated in an urban catchment. In this type of implementation, SCMs are connected to each other so that the collected stormwater could flow from an upstream SCM to a downstream SCM. Mesoscale, in this context, has been referred to as “SuDS management train” by [13]. The extensive implementation of SuDS over the entire city catchments could be considered a macroscale approach (Figure 1c) through which the city could be transformed to a sponge city [14]. In contrast to microscale, studies regarding the hydraulic performance of SuDS at meso-scales and macroscales, as the train of several individual SCMs, are comparatively rare in the literature, e.g., [13,15,16].

In order to facilitate the implementation of SuDS, it is necessary to provide tools and models to enhance the communication between the urban water engineers and urban planners [8]. This can be done by characterizing SCMs as well as understanding their cumulated affect in a larger system, which is reported to be challenging and empirically less attended [17].

One of the early standard frameworks for implementation of SCMs was introduced by Stahre [7] in Sweden in the city of Malmö. Peter Stahre developed administrative procedures where it was outlined how different SCMs could be implemented on private and public land, respectively. As a result, several SCMs were introduced in the late 1990s in Malmö as part of the drainage system. A list of the implemented SCMs/SuDS in Malmö was presented by Haghighatafshar et al. [18]. The most

prominent of these implementations is the neighborhood Augustenborg in Malmö, which in contrast to others, is located in the densely constructed and populated part of the city. The implemented SuDS were, to some extent, demonstration facilities showing the potential and the benefits of a new game-changing type of planning process where aesthetically designed open drainage systems were part of the urban landscape in accordance with the motto “make space for the water”. While some potentially suitable measures were tentatively suggested at each level from upstream to downstream, the hydraulic and hydrologic performance of the suggested SCMs and of the entire system were not addressed. With the more intense rainfall events that have been experienced in many parts of the world as well as an elevated densification of our cities, the interest in SCMs especially in already built areas has grown [6,11].

The aim of this study is to introduce a new conceptual function-oriented description of the SuDS at a mesoscale level. The suggested model is based on observed rainfall-runoff data from the perspective of connectedness of surfaces and, to what extent, they contribute to the observed runoff. Consequently, the concept is applied to schematize the existing SuDS in Augustenborg as a demonstration. This approach aims to bridge an engineering design to urban planning and design by providing a simple hydraulic scheme for mesoscale SuDS.

2. Methodology

This study is based on rainfall-runoff measurements in an urban catchment of about 20 ha in which the runoff from most surfaces is managed through combinations of SCMs. All the implemented SCMs in the study area are surface-based (open) stormwater solutions. The study area known as Augustenborg was originally drained through the underground pipe-system of the city. For two years, flow measurements were carried out at the most downstream of catchments where the excess runoff is diverted into the major wastewater collecting system of the city. The following subsections present the adopted parametrical assessment method, a brief description of the study area, and the employed measurement instrument.

2.1. The Study Area—Augustenborg

Augustenborg is located in the inner city of Malmö, Sweden and is one of the most renowned SuDS retrofits. The area is often regarded as a unique example of an integrated collaboration of urban planners and urban water engineers. In this scenario, an area about 20 ha, which was originally drained with a combined sewer network, is managed via interconnected combinations of SCMs (i.e., mesoscale). The area was retrofitted in the late 1990s and has been in operation for about 20 years now. Augustenborg has been associated with many tentatively positive effects over the years such as, among other benefits, mitigation of basement flooding [19]. However, the effect and the in-depth understanding of the function of the SCMs have never been described in detail and the ideas have not been reproduced elsewhere despite the very positive verdict. One prerequisite for the reproduction is understanding the functionality so that the results, rather than the layout, can be transferred to other places. There is, therefore, a need to develop concepts that discuss SuDS and their functionality in a city-wide perspective to help urban planners and water engineers systematically design and reshape the urban landscapes through a shared perspective. An enhanced communication between engineers and planners can help alleviate some of the institutional shortcomings [20] for the widespread adoption of SCMs.

The Augustenborg area, which is shown in Figure 2, handles the storm water runoff through three different systems with each serving its unique catchment; i.e., the pipe-system (3.5 ha), the Northern SuDS (6.3 ha), and the Southern SuDS (9.5 ha). Figure 2 also shows the location of the flow and rainfall monitoring points as well as the systems' connection points to the municipal wastewater collection network of Malmö.

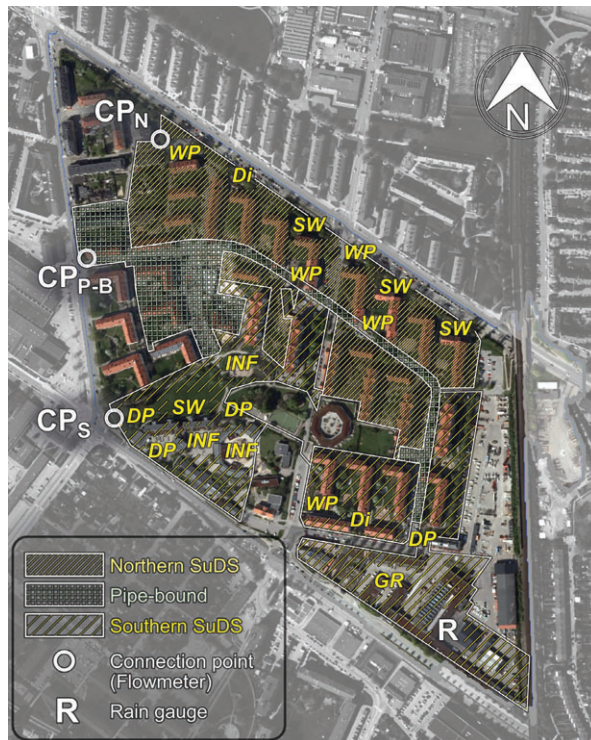


Figure 2. The locations of rainfall and runoff monitoring points as well as the catchment delineation in Augustenborg. The unmarked areas within the borders of the Augustenborg area are directly drained into the existing municipal pipe-bound combined sewer network. Connection points marked as CP_N , CP_{P-B} , and CP_S are the discharge points for the Northern retrofit, the pipe-bound catchment, and the Southern retrofit, respectively. Note that the flow is in the north-west direction, i.e., towards the connection points [21]. For SCM types, see Figure A1. Background picture: GSD-Orthophoto, courtesy of The Swedish Mapping, Cadastral and Land Registration Authority, ©Lantmäteriet (2015). [This figure—slightly modified—is adopted from Haghighatafshar et al. [11] with permission].

Catchments in all three stormwater subsystems consist of various types of surfaces such as tile roofs, green roofs, asphalt surfaces, concrete surfaces, grass, and sand covered areas. A Geographical Information System (GIS) analysis of different land uses in each of the subsystems in Augustenborg, using orthophotos of the area, shows that about 50% of the catchment in both Northern and Southern SuDS is occupied by surfaces assumed to be impervious from an engineering point of view (i.e., tile roofs, asphalt, and concrete) while the corresponding value in the pipe-bound catchment is above 70%. Green roofs make up a considerable part in the Southern SuDS (about 11%) while it is almost negligible in the pipe-bound catchment as well as the Northern SuDS. A schematic representation of different land uses in the area are presented in Table 1. The numbers are based on a GIS-analysis of the land use and the digital elevation model (DEM) of Augustenborg by Nordlöf [21].

Table 1. Distribution of different types of surfaces in the catchments in Augustenborg extracted from Reference [21].

| Surface Type | Pipe-Bound | | Northern SuDS | | Southern SuDS | |
|------------------|------------|-----|---------------|-----|---------------|-----|
| | ha | % | ha | % | ha | % |
| Tile roof | 0.5 | 15 | 1.7 | 27 | 1.7 | 17 |
| Asphalt/Concrete | 2.0 | 56 | 1.5 | 24 | 3.0 | 32 |
| Grass area | 1.0 | 28 | 2.9 | 46 | 3.0 | 31 |
| Green roof | 0.0 | 0 | 0.0 | 0 | 1.0 | 11 |
| Sand | 0.0 | 1 | 0.1 | 1 | 0.8 | 8 |
| Gravel | 0.0 | 0 | 0.1 | 2 | 0.1 | 1 |
| Total | 3.5 | 100 | 6.3 | 100 | 9.5 | 100 |

Different types of the implemented SCMs in the Northern and Southern SuDS are shown in Figure 2. The Northern SuDS consists of a major flow-path of swales and a stormwater ditch to which some stormwater ponds are also connected. Outflow from the Northern systems occurs in the form of overflow from the final pond (Figure 2 (CP_N)). In contrast, the Southern SuDS includes several relatively large retention ponds (with larger areas/freeboards) with a considerable area of green roofs at the most upstream parts of the catchment (Figure 2 (GR)). Outflow from the Southern SuDS is the result of overflow from the final pond in the system (Figure 2 (CP_S)). Some photos of the SCMs in Augustenborg are presented in Appendix A.

2.2. On-Site Measurements

Discharges from the sub-catchments were monitored and logged at connection points (marked as CP in Figure 2). The flow was measured using Mainstream Portable AV-Flowmeters with velocity and level sensors. Flow-monitoring was carried out for a period of over two years, which is shown in Figure 3. A total of 10 rainfall events (denoted A–J) with reliable corresponding flow measurements were selected. The selected rainfalls were all volumetrically considered, which means that they led to a discharge from at least one of the SuDS in Augustenborg. As seen in Figure 3, all selected rainfalls belong to the period of May–August during which most intense rainfalls were observed. Details of the selected rainfall events are shown in Table 2. The rainfall was monitored and logged by a Casella CEL tipping bucket rain gauge with 0.2 mm resolution, which was installed at the south-east part of the area.

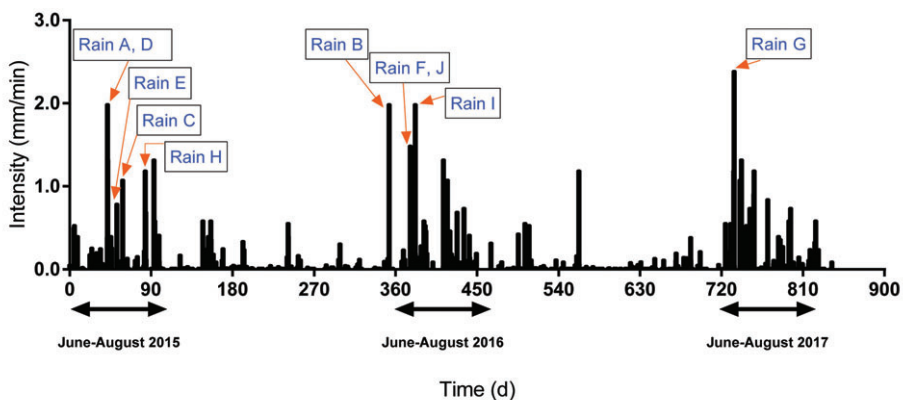
**Figure 3.** Hyetograph over the period of the study.

Table 2. Calculated REIAs and their corresponding contribution coefficients for 10 rain events.

| Rainfall Event ID | Rainfall Depth (mm) | Rainfall Duration (h) | V_{out} (m ³) | | | Contribution Coefficient—Equation (2) (-) | | |
|-------------------|---------------------|-----------------------|-----------------------------|------------------------|------------------------|---|------------------------|------------------------|
| | | | Pipe-System (3.5 ha) | Northern SuDS (6.3 ha) | Southern SuDS (9.5 ha) | Pipe-System (3.5 ha) | Northern SuDS (6.3 ha) | Southern SuDS (9.5 ha) |
| A | 7.8 | 0.45 | 107.47 | 24.28 | 0.00 | 0.55 | 0.10 | 0 |
| B | 10.6 | 3.37 | 129.56 | n/a | 5.40 | 0.49 | n/a | 0.01 |
| C | 13.4 | 2.18 | 189.55 | 107.78 | 14.00 | 0.57 | 0.25 | 0.02 |
| D | 13.8 | 9.25 | 197.15 | 86.22 | 12.76 | 0.57 | 0.19 | 0.02 |
| E | 15.6 | 4.78 | 174.31 | 96.43 | 11.14 | 0.45 | 0.19 | 0.02 |
| F | 17.4 | 3.90 | 165.17 | 142.27 | 132.66 | 0.38 | 0.25 | 0.16 |
| G | 17.8 | 15.5 | 154.73 | 117.23 | 101.4 | 0.35 | 0.20 | 0.12 |
| H | 19.0 | 22.7 | 268.9 | 164.49 | 93.75 | 0.57 | 0.27 | 0.11 |
| I | 22.6 | 4.15 | 273.23 | 258.04 | 215.89 | 0.48 | 0.35 | 0.20 |
| J | 28.4 | 9.14 | 352.19 | 288.53 | 293.02 | 0.50 | 0.32 | 0.22 |

2.3. Runoff-Equivalent Impervious Area

The parts of the impervious surfaces in a catchment that are hydraulically connected to the drainage network within the context of pipe-systems are known as directly connected to an impervious area (DCIA) [22]. DCIA is often regarded as an effective impervious area (EIA) in an interchangeable manner [22–24], which implies that the effectiveness of the surfaces from a runoff contribution point of view is reflected in DCIA. DCIA has widely been employed to understand the rainfall-runoff patterns in urban basins. Lee and Heaney [25] report that connectedness of the impervious area has the most noticeable effect on urban hydrology. It has also been shown that mild changes of imperviousness are reflected as amplified runoff responses. For instance, grass areas contribute to runoff as soon as rain intensity exceeds the infiltration rate [22]. It is also important to consider that the routed runoff from ineffective impervious areas onto the pervious surfaces would lead to rapid consumption of percolation capacity, which makes the previous surface react as impervious [26]. The generated runoff under such scenarios is then not only contributed by DCIA, but also other types of impervious and pervious surfaces start to contribute.

Using the same indicators for functionality of various types of stormwater handling systems makes it easy to compare and understand the role of these systems in urban runoff management. While DCIA can be quantified through GIS maps of high spatial resolution as well as intensive in-situ assessment of the catchment connected to the pipe network [27], it is not convenient to apply the same method to SuDS since the boundaries between the “catchment” and the “system” cannot be clearly drawn in case of SuDS. Therefore, a lumped parameter representing the *runoff-equivalent impervious area* (REIA) is introduced in this paper to explain the activeness of the surfaces. This parameter, REIA, is the equivalent surface area with 100% contribution to runoff, which is calculated based on the observed accumulated outflow from systems. It should be noted that REIA and DCIA could be identical parameters in case of pipe-bound conventional drainage systems. The difference between these two parameters lies in their conceptual definitions through which REIA could be used for evaluating the efficiency of SuDS as alternative solutions for urban runoff management and is estimated using Equation (1).

$$REIA = \frac{V_{out}}{R} \quad (1)$$

in which $REIA$ is expressed in m², V_{out} is the total volume of the observed runoff outflow at the most downstream point (m³), and R is the rainfall depth (m). Total runoff volume was measured until the discharge was either zero or reached a minimum before the subsequent rainfall. The ratio between the observed $REIA$ and the GIS-based quantified total impervious area (TIA) is then considered as the contribution coefficient of the system (Equation (2)).

$$Contribution\ coefficient = \frac{REIA}{TIA} \quad (2)$$

3. Results and Discussion

3.1. Development of the Conceptual Model

All 10 rainfall-runoff datasets (hyetographs and hydrographs) included in this study are provided as supplementary material. Figure 4 shows two examples of the observed rainfall-runoff events. Rainfall I (Figure 4(I)) is the most intensive rainfall event with a recurrence interval of about two years according to Dahlström (2010) [28]. It has one peak with a large depth that leads to discharges from both the Northern and the Southern SuDS. Rainfall D (Figure 4(D)), however, consists of two peaks while the discharge occurs only from the Northern SuDS and only in connection to the second peak.

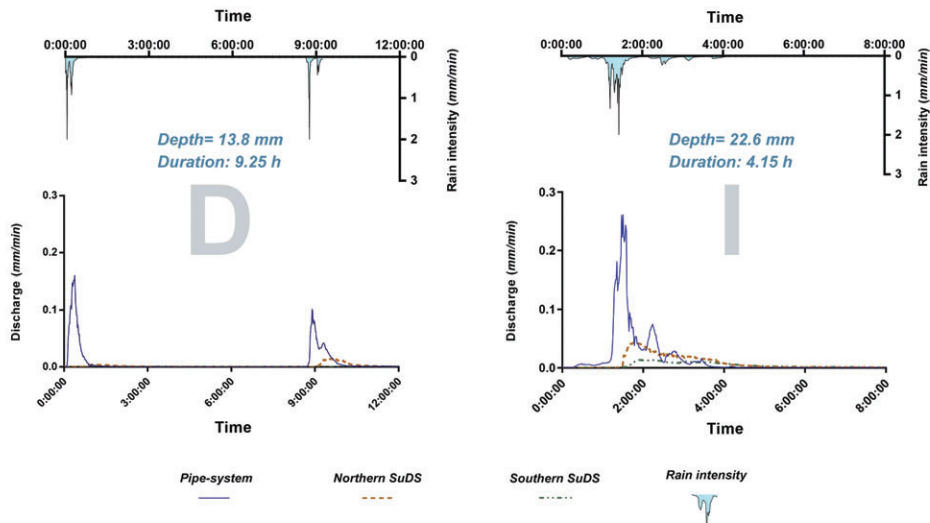


Figure 4. Two examples from the monitored hyetographs and hydrographs during this study. See rainfalls D and I in Table 2. The details of all rainfall-runoff observations are provided as supplementary material (available online).

Analysis of the hydrographs, which are the normalized outflows against the total catchment area, shows that the pipe system is very sensitive to rain peaks even in smaller magnitudes. In other words, there is always an observed peak in the hydrograph, which corresponds to a certain peak monitored in the rain pattern (see Figure 4(D) and Figure 4(I)). The correlation between the rain intensity and the outflow from the pipe-system indicates that pipe-systems are flow oriented and should be designed in accordance with flow capacity. In contrast to the pipe-system, the outflow from SuDS is observed to be a function of the rainfall depth rather than rainfall intensity. For instance, as seen in Figure 4(D), outflow from the Northern SuDS occurs in connection with the second peak observed at about 8 h 45 min after the start of the event while there is no outflow from the system at the first peak in the rain (at about 30 min after the start of the event). This means that the first part of the rainfall (60 min from the start, depth = 8 mm) is retained in the SuDS and to some extent fills the existing capacity while the second peak, although lower (depth = 6 mm), exceeds the threshold and initiates an outflow from the Northern SuDS.

The monitored hydrographs indicate an almost negligible delay in the flow initiation in the pipe network followed by relatively shorter lag times, i.e., 5–20 min depending on the rainfall pattern. The observed lag time for Northern SuDS and Southern SuDS was found to be about 20–100 min and 90–190 min, respectively.

The observed range of accumulated rainfall required for the initiation of runoff in the pipe system is found to be 0.8 mm to 2.2 mm, which aligns with findings of Albrecht [29] who reported a runoff initiation threshold of 0.8 mm to 2.3 mm for cool and hot weather, respectively. The almost immediate initiation of flow in the pipe system can be an indication that the major part of the flow is contributed by the DCIA, which lies close to the measurement point. In contrast to the pipe system, the small contribution coefficient in the catchments with SuDS (see Table 2) agrees well with the observed long periods of delay in the flow initiation, which is an indication of larger retention capacity of the SuDS catchments.

The larger retention capacity in the SuDS can be accredited to storage, evapotranspiration, and direct and indirect infiltration. The term indirect infiltration is assigned to the infiltration that takes place when the runoff from impervious surfaces is diverted to pervious surfaces for infiltration. In contrast, direct infiltration is when the rain falls on a pervious surface and is infiltrated directly.

Table 2 summarizes the total discharge volumes (V_{out}) and their corresponding contribution coefficients for the catchments in Augustenborg for 10 rainfall events were monitored for two years. Figure 5 presents the graphical illustration of the calculated REIA values for the subsystems in Augustenborg. As observed in Table 2, the contribution coefficient for the catchment with pipe-system is about 50% (i.e., $0.48 \pm 0.08\%$) of the TIA. This is in agreement with the published literature in which the proportion of contributing surfaces (also regarded as EIA) is reported to vary from 14% to 60% depending on the physical characteristics of the catchment such as slopes, gutters, curbs, and more [30–33].

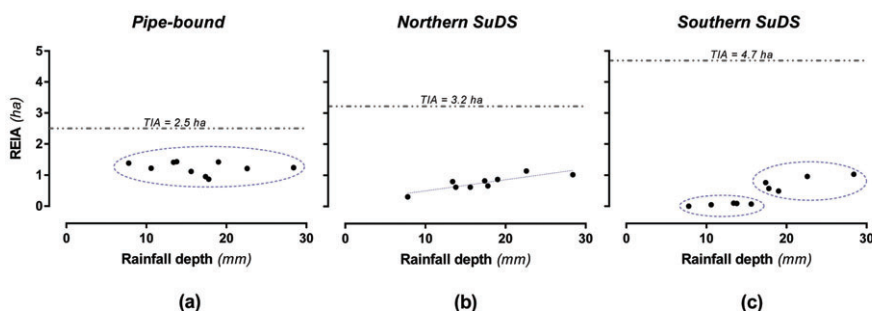


Figure 5. Calculated REIA in case of the observed rainfalls for all three catchments in Augustenborg compared to the TIA (based on field surveys and GIS maps as given in Nordlöf [21]): (a) Pipe-bound; (b) Northern SuDS; (c) Southern SuDS.

The contribution coefficient is considerably lower in the catchments with SuDS implementations (varying values) but note that the two SuDS (Northern and Southern) differ with respect to how they react under different rain depths. The REIA in the Northern SuDS tends to increase gradually when the rainfall depth increases (Figure 5b) while, in the Southern SuDS, the REIA is generated first when the rainfall depth exceeds a larger threshold of about 17 mm (Figure 5c). It was also observed that the outflow from the SuDS in Augustenborg is not only levelled out and flat (no intensive peaks as seen in Figure 4) but is also much smaller in accumulative volume when compared to the pipe system (compare the contribution coefficients given in Table 2). This implies that the retention capacity including surface storage, infiltration and evapotranspiration in catchments with SuDS in Augustenborg is higher than the pipe-bound catchment.

The observed gradual increase in the REIA for the Northern SuDS (REIA from 0.3 ha to 1.1 ha corresponds to rainfall depths of 8 mm to 23 mm, which is shown in Figure 5b) means that the contributing proportion of the catchment grows as the rainfall depth increases. The corresponding projection of this observation in the field could be considered if the system is constituted of a network

of several small disaggregated (discrete) individual mini catchments with each having a certain retention volume. These discrete mini catchments are filled gradually as the rainfall depth grows. Eventually, when their threshold is exceeded, overflow to the corresponding immediate downstream mini catchment. Accordingly, if the rainfall depth is large enough, the number of connected mini catchments increases and the accumulated overflows might finally contribute to the final discharge from the system.

The same conceptual model is also valid for the REIA trend observed for the Southern SuDS. As seen in Figure 5c and Table 2, the calculated REIA is almost negligible for rainfall depths up to about 16 mm while a dramatic increase is observed in the case of 17 mm of rainfall. The same concept presented above (discrete mini catchments) explains the observed phenomenon. A possible explanation for this very abrupt alteration in behavior (sudden jump in REIA from 16 mm to 17 mm of rainfall) could be associated with the relatively large retention volume at the most downstream part of the Southern SuDS (see Figure A1(DP 4)). Another possible explanation could be that some other mini catchments further upstream join the rest of the system when a threshold is exceeded. Both hypotheses could generate a relatively large outflow volume considering the possible connectedness of the catchment at that stage after the initial 16 mm has filled up the capacity up to the system's threshold. However, application of the concept to the systems in Augustenborg could possibly reveal what hypothesis is a valid explanation for the observed phenomenon.

A schematic illustration of the conceptual model is presented in Figure 6. In this illustration, five retention cells (SCMs) with each having a connected mini catchment area = A are presented. The constant connected area, A , for each SCM is assumed to promote the comprehensibility of the conceptual model. Each of these SCMs has a certain retention capacity as different multiples of an assumed unit capacity (i.e., V [mm]). The retention capacity of each SCM is reflected in the size of the schematic circles in Figure 6. As evident in Figure 6, both illustrated models have identical total retention capacity ($=25 \times V$), but the circumstances under which a discharge is initiated from the systems depend on the spatial distribution of the mini catchments with respect to their retention capacity. It is important to note that retention capacity, V , in this context is considered the sum of surface storage, retention, and losses in the form of infiltration and evapotranspiration.

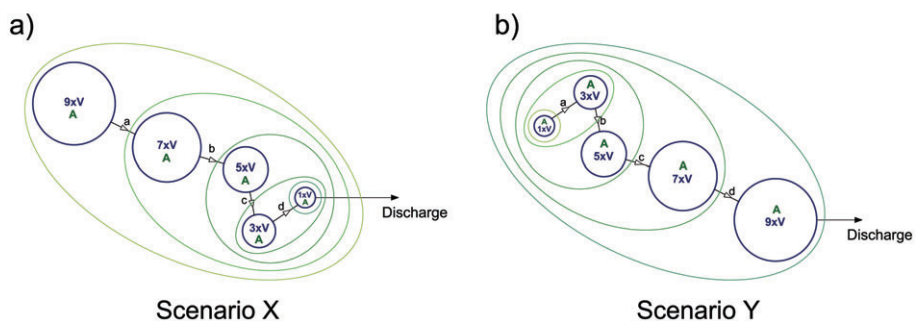


Figure 6. Conceptual illustration of two extreme setups for construction of SuDS with different components. Please note that all the shown mini catchments have the same area, i.e., A , while the size of the circles represents the retention capacity of SCMs: (a) Scenario X; (b) Scenario Y.

Figure 6a (Scenario X) is comparable to Northern SuDS in Augustenborg. The mini catchments with smaller retention capacities are placed close to the discharge point. A consequence of this configuration is that a discharge from the system will be observed as soon as the most downstream mini catchment ($1 \times V$) is saturated in capacity, which is when the rain depth exceeds $1 \times V$. As the rainfall depth continues to increase, more mini catchments are connected to each other and contribute

more to the final discharge. The growth direction of the contributing catchments in this case is downstream-to-upstream, i.e., links are activated from **d** towards **a** (Table 3).

Table 3. Response matrix of the conceptual model in the case of scenarios X and Y (see Figure 6).

| Rain Depth (mm) | Scenario X | | | Scenario Y | | |
|-----------------|--------------|----------------|-------------------|--------------|----------------|-------------------|
| | Active Links | Discharge (mm) | Contributing Area | Active Links | Discharge (mm) | Contributing Area |
| $<1 \times V$ | - | - | - | - | - | - |
| $2 \times V$ | - | $1 \times V$ | A | a | - | - |
| $3 \times V$ | - | $2 \times V$ | A | a, b | - | - |
| $4 \times V$ | d | $4 \times V$ | $2 \times A$ | a, b, c | - | - |
| $5 \times V$ | d | $6 \times V$ | $2 \times A$ | a, b, c, d | - | - |
| $6 \times V$ | d, c | $9 \times V$ | $3 \times A$ | a, b, c, d | $5 \times V$ | $5 \times A$ |
| $9 \times V$ | d, c, b | $20 \times V$ | $4 \times A$ | a, b, c, d | $20 \times V$ | $5 \times A$ |
| $10 \times V$ | d, c, b, a | $25 \times V$ | $5 \times A$ | a, b, c, d | $25 \times V$ | $5 \times A$ |

In Figure 6b (Scenario Y), comparable to the situation in Southern SuDS, the final discharge would not flow out unless a certain rain depth is obtained. In the specific example, the outflow from the model presented as Scenario Y is initiated when a rainfall larger than $5 \times V$ mm is applied on the system while all rainfalls up to $5 \times V$ mm would result in higher connectedness of the system without any downstream discharges. In this type of setup, the connectedness of the system propagates from the upstream towards the downstream, i.e., links are activated from **a** towards **d** (Table 3).

In the presented conceptual model, if a longer lag time is desired for the system, it is more beneficial that the SCMs with higher retention or retention capacity are placed downstream.

Additionally, relatively smaller volumes of discharge can also be expected for rainfalls up to a certain magnitude (see the data for rainfall $6 \times V$ in Table 3). These advantages become especially important and effective when the final recipient for the SuDS is the municipal sewer system, which is the case in Augustenborg. In the municipal sewer system, the bought time in terms of longer lag times may be enough for the receiving pipe-bound stormwater network to maintain some pressure relief.

Figure 6 along with Table 3 illustrate the basic concept behind the functionality and behavior of SuDS in a full-scale urban catchment by demonstrating two straightforward examples under simplified circumstances in which connectedness grows along a single pathway. Basically, the SCMs can be visualized as a flow train of interconnected bowls with physical properties that, at least from theoretical point of view, should be quantifiable. Once the properties have been determined, the functionality of the flow train is set.

However, in contrast with the unique setups of the concept (Figure 6), each SCM in a real implementation of mesoscale SuDS is assigned to a specific mini catchment varying in area and characteristics. In addition to the local retention depth available (= storage depth in the freeboard, S_{fb}^i + storage depth in the infiltration layer, S_{inf}^i) in the SCM, the area of the connected catchment is also important in the overall retention performance of the SCM. It is also assumed that the effect of evapotranspiration is negligible in case of short term individual rainfall events. Therefore, it is excluded from the model. Consequently, in order to be able to compare the retention capacity of each SCM, the effective retention of each SCM is calculated, according to Equation (3).

$$R_e^i = \frac{(S_{fb}^i + S_{inf}^i) \times A_{SCM}^i}{DCIA^i} \quad (3)$$

in which R_e^i is the effective retention capacity of the SCM i (mm), S_{fb}^i is the storage depth in the freeboard of the SCM (mm), S_{inf}^i is the storage depth in the infiltration layer, A_{SCM}^i is the area occupied by the SCM (m²), and $DCIA^i$ is the directly connected impervious area to the SCM (m²). Please notice that DCIA (mainly tile roofs and some asphalt in the Northern SuDS [21]) is used to simplify the model

since it is anticipated that DCIA is the dominant parameter for runoff volume, which is reported by Shuster et al. [19].

3.2. Remarks on the Schematized Augustenborg

The developed conceptual model is used to characterize the processes in the Northern and Southern SuDS in Augustenborg. Figure 7 shows the conceptualized representations of Northern (top) and Southern (bottom) SuDS in Augustenborg based on the effective retention depth (Equation (3)) of SCMs.

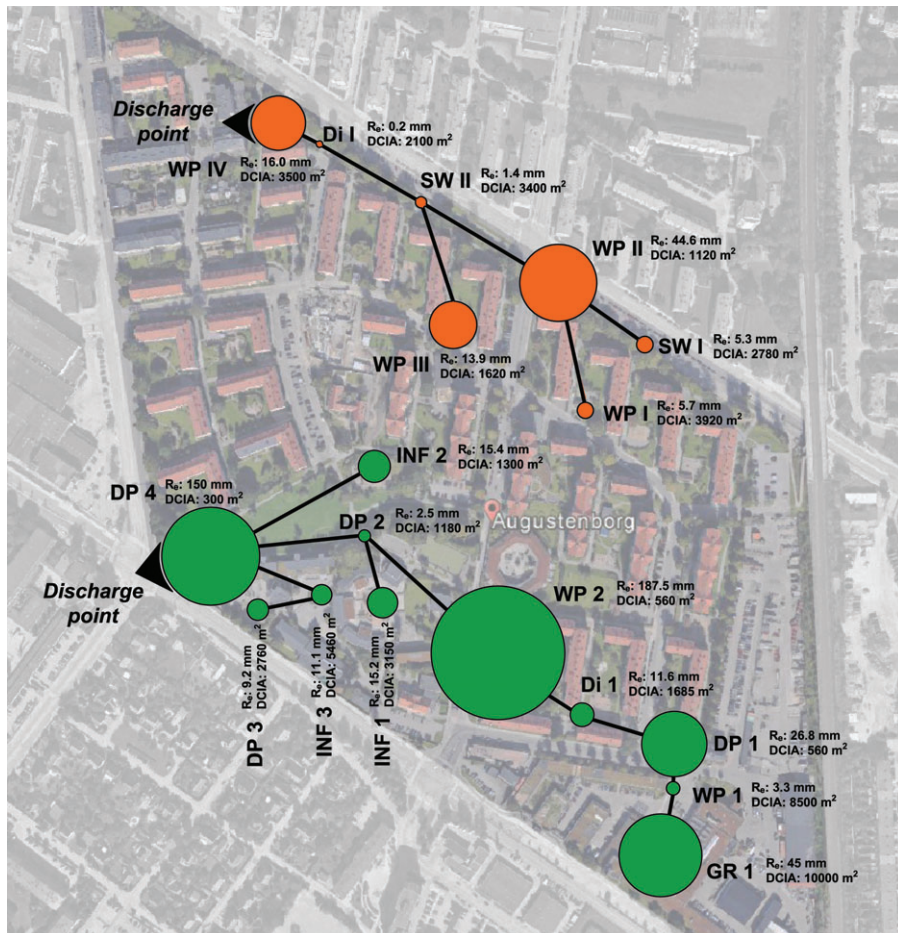


Figure 7. Conceptual illustration of Northern SuDS (top) and Southern SuDS (bottom) in Augustenborg. Each SCM is represented as a circle. The size of the circle corresponds to the effective retention capacity of the SCM, i.e., R_e^i . Please notice that the SCMs belonging to the Northern SuDS are indexed with Roman numerals while SCMs in the Southern SuDS are numbered with Arabic numerals. The size of the circle representing SCM is an indicator of its effective detention depth (sizes are not proportionally correct). The background picture is acquired from Google Earth.

In Table 4, all the different SCMs have been systematically assigned names and properties accordingly. The details of the characterized SCMs shown in Figure 7 are also presented in Table 4. Equation (3) and Equation (4) were subsequently employed to build a model to estimate the discharges from the SCMs along all the flow paths in the Northern and Southern SuDS. The model was built in an Excel spreadsheet.

Table 4. Characteristics of the SCMs in the Northern and the Southern SuDS in Augustenborg. The sequence of the SCMs with respect to flow path (upstream-downstream) is illustrated in Figure 7.

| System | SCM ID | Storage, S_{fb}^i (mm) | Infiltration S_{inf}^i (mm) | SCM Area, A_{SCM} (m ²) | DCIA (m ²) | Effective Retention, R_e^i (mm) |
|---------------|--------|-----------------------------|----------------------------------|--|------------------------|--------------------------------------|
| Northern SuDS | SW I | 5 | 15 | 740 | 2780 | 5.3 |
| | WP I | 250 | 0 | 90 | 3920 | 5.7 |
| | WP II | 250 | 0 | 200 | 1120 | 44.6 |
| | WP III | 250 | 0 | 90 | 1620 | 13.9 |
| | SW II | 5 | 15 | 240 | 3400 | 1.4 |
| | Di I | 5 | 0 | 80 | 2100 | 0.2 |
| | WP IV | 350 | 0 | 160 | 3500 | 16.0 |
| Southern SuDS | GR 1 | 0 | 45 | 10,000 | 10,000 | 45 |
| | WP 1 | 200 | 0 | 140 | 8500 | 3.3 |
| | DP 1 | 105 | 45 | 100 | 560 | 26.8 |
| | Di 1 | 200 | 0 | 98 | 1685 | 11.6 |
| | WP 2 | 150 | 0 | 700 | 560 | 187.5 |
| | INE. 1 | 35 | 25 | 800 | 3150 | 15.2 |
| | DP 3 | 105 | 45 | 170 | 2760 | 9.2 |
| | INE. 2 | 0 | 25 | 800 | 1300 | 15.4 |
| | DP 2 | 0 | 15 | 200 | 1180 | 2.5 |
| | INE. 3 | 500 | 25 | 115 | 5460 | 11.1 |
| | DP 4 | 25 | 25 | 900 | 300 | 150.0 |

More information about the type of the implemented SCMs are shown in Figure 2 (also in Appendix A). The information regarding the characteristics of the SCMs (S_{inf}^i , S_{fb}^i , and A_{SCM}^i) as well as their corresponding mini catchment ($DCIA^i$) is collected from the hydrodynamic model of the area, which was developed by Haghghatafshar et al. [11], the on-site measurements, and the GIS maps. These parameters are relatively easy to estimate and can be measured on site.

As seen in Table 4, it is obvious that water ponds, (Dry Ponds and Wet Ponds) are the backbone of the systems regarding effective retention, which account for a total effective retention depth of 80 mm and 380 mm in the Northern and Southern SuDS, respectively. The second most important feature in terms of effective retention are the infiltration areas that contribute with approximately 42 mm of effective retention in the Southern SuDS. In case of infiltration areas, effective retention capacity in most cases has two components, which include a storage volume that can be determined from the geometrical properties of the basin and measured on site, and the infiltration capacity (i.e., the function of the underlying soil properties).

The ditches and the swales, however, have a limited storage volume since they add up to 7 mm and 12 mm of effective retention depth to the Northern and Southern SuDS, respectively. For the observed rain events, these components act as connection nodes between the different ponds and also provide a connected and diverse blue-green landscape. Despite relatively large retention at the most downstream pond in the Northern SuDS (WP IV), a discharge is initiated as soon as rainfall depth reaches around 7 mm. This rapid fill-up of retention capacity is due to the two upstream SCMs, i.e., Di I and SW II, from which the discharged volume overrides the remaining free capacity in WP IV and leads to a discharge. By comparing the conceptual approach with the onsite SCMs in the Northern SuDS, it can be claimed that using swales with large DCIA as the backbone of SuDS for the conveyance of runoff from upstream SCMs to downstream SCMs without introducing substantial retention structures on the flow path leads to decreased overall effectiveness of SuDS in runoff reduction. This aligns with findings of Qin et al. [34] who found that the retention capacity of swales is very limited and, therefore,

is saturated quickly. Generally, ponds and infiltration basins with an overflow threshold (freeboard) have a pronounced role in the overall runoff retention when compared to other SCMs.

At this point, it is important to make clear that, although different SCMs can relatively easily be translated to effective retention volumes, the concept of SuDS needs to be studied through a combination of SCMs to be understood and adopted by the city planners as well as the individual house-owners. This is the key to the success of this technique. In order to better understand the response pattern of the different combinations of SCMs, it is beneficial to expand our knowledge on how SuDS as the flow train of different SCMs can be introduced in the best way.

At this stage, the conceptual model provides a better understanding of hydraulics that prevail in mesoscale SuDS implementations, which can promote the required dialogue between different actors at the planning phase. However, in the prospect of future studies, the concept can be further developed to estimate the discharge hydrographs from mesoscale SuDS. A mathematically simple representation of the hydraulics in mesoscale SuDS could result in computationally faster models. Such fast models can then be used for large-scale simulations as an alternative to the computationally costly and time-consuming 2-dimensional distributed hydrodynamic models. Fast and cheap models are needed to study the upscaling effects of SuDS on the city-level.

4. Conclusions

Extensive rainfall-runoff measurements at two urban catchments with SuDS along with one pipe-bound catchment were used to investigate the systems' responses at different rainfalls. Runoff measurements at the most downstream point of each catchment showed that, in contrast with the SuDS, the flow from the pipe-system was directly affected by the rainfall intensity. However, the total runoff volume was still a function of the total rain depth. In order to describe this transformation that takes place in a SuDS, a conceptual model was introduced from the viewpoint of catchments' runoff-equivalent impervious area. In the model, implementation of SuDS disintegrates the catchment area into a group of discrete and disaggregated mini catchments. These mini catchments establish connections with each other depending on the volume of the rain event. The dynamics of the conceptual model demonstrated that the order and placement of different stormwater control measures within the framework of SuDS with different retention capacities affects the overall performance of the system. The conceptualization of SuDS establishes a new platform for further evaluation and discussion of these systems at mesoscale. The model promotes the communication between urban planners and water engineers. This, in turn, can lead to the design of SuDS in which hydraulic performance alongside aesthetical and architectural quality is taken into consideration.

Supplementary Materials: The following are available online at <http://www.mdpi.com/2073-4441/10/8/1041/s1>, Figure S1: Rainfall A, Figure S2: Rainfall B, Figure S3: Rainfall C, Figure S4: Rainfall D, Figure S5: Rainfall E, Figure S6: Rainfall F, Figure S7: Rainfall G, Figure S8: Rainfall H, Figure S9: Rainfall I, and Figure S10: Rainfall J.

Author Contributions: Conceptualization, J.J., H.A. and S.H. Methodology, S.H., K.J., and J.J. Investigation, J.J. and H.A. Resources, K.J., J.J., and H.A. Data Curation, S.H. and H.A. Writing-Original Draft Preparation, S.H. Writing-Review & Editing, S.H., J.J., H.A., and K.J. Supervision, K.J., J.J., and H.A. Visualization, S.H. Project Administration, S.H. Funding Acquisition, K.J., J.J., and H.A.

Funding: This research was financially supported by VA SYD, Sweden Water Research, J. Gustaf Richert Foundation (grant number 2015-00181) at SWECO as well as the Swedish Water and Wastewater Association (*Svenskt Vatten*) via VA-teknik Södra (grant number 15-108).

Acknowledgments: The authors thank the personnel at VA SYD for their practical support in the installation of flowmeters and the collection of data. Tomas Wolf and John Hägg, VA SYD, are especially acknowledged for their invaluable contribution to the setup and the maintenance of the measurement system. Professor Magnus Larson, Division of Water Resources Engineering at the Department of Building and Environmental Technology, Lund University is also sincerely acknowledged for his thoughtful input to the final manuscript.

Conflicts of Interest: The authors declare no conflict of interest.

Appendix A



Figure A1. The photos of some of the implemented SCMs in Augustenborg. Different types of SCMs are shown in the figure as follows: (DP 4) dry pond, (Di I & 1) stormwater ditch, (SW I & II) swale, (WP 2, II & IV) wet pond, (INF 3) infiltration basin, (GR) green roof. The major runoff directions in the Northern and Southern systems are SW I → WP IV and GR → DP 4, respectively. Pictures for INF 3, WP 2, Di 1, and SW I & II are taken by Henrik Thorén (Rambøll). Background picture: GSD-Orthophoto, courtesy of The Swedish Mapping, Cadastral and Land Registration Authority, ©Lantmäteriet (2015).

References

1. Meerow, S.; Newell, J.P. Spatial planning for multifunctional green infrastructure: Growing resilience in Detroit. *Landsc. Urban Plan.* **2017**, *159*, 62–75. [[CrossRef](#)]
2. Tzoulas, K.; Korpela, K.; Venn, S.; Yli-Pelkonen, V.; Kaźmierczak, A.; Niemela, J.; James, P. Promoting ecosystem and human health in urban areas using Green Infrastructure: A literature review. *Landsc. Urban Plan.* **2007**, *81*, 167–178. [[CrossRef](#)]

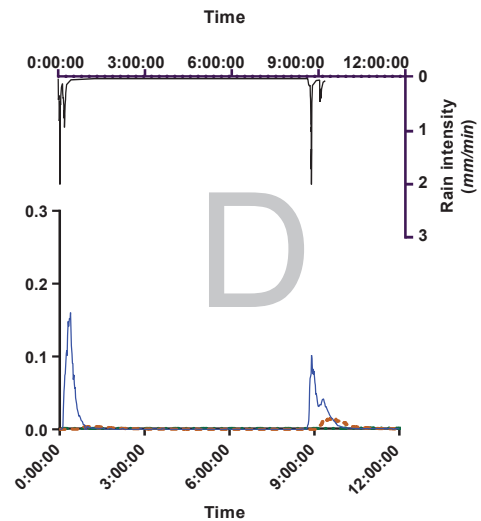
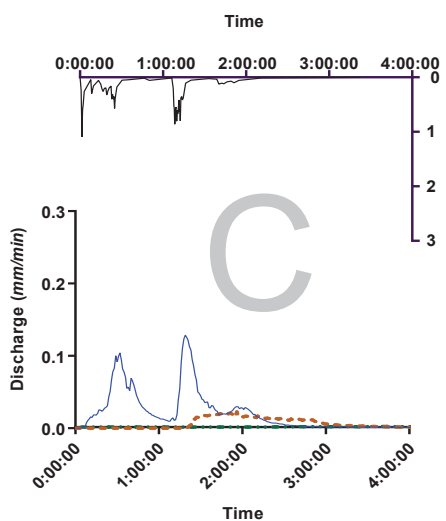
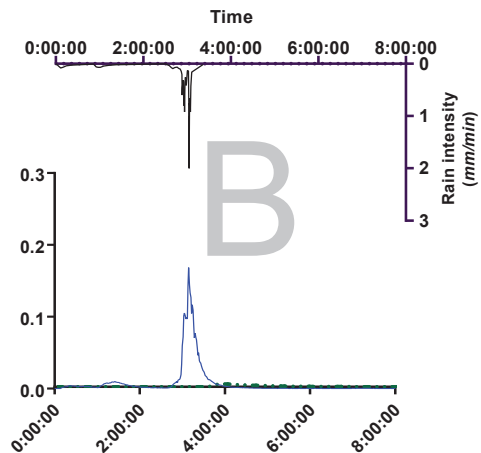
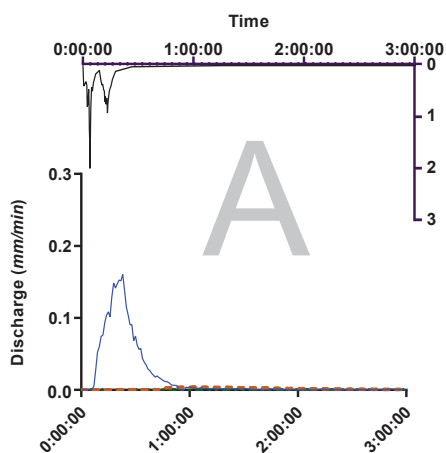
3. Wolch, J.R.; Byrne, J.; Newell, J.P. Urban green space, public health, and environmental justice: The challenge of making cities ‘just green enough. *Landsc. Urban Plan.* **2014**, *125*, 234–244. [[CrossRef](#)]
4. Palla, A.; Gnecco, I. Hydrologic modeling of Low Impact Development systems at the urban catchment scale. *J. Hydrol.* **2015**, *528*, 361–368. [[CrossRef](#)]
5. Ahiablame, L.; Shakya, R. Modeling flood reduction effects of low impact development at a watershed scale. *J. Environ. Manag.* **2016**, *171*, 81–91. [[CrossRef](#)] [[PubMed](#)]
6. Jato-Espino, D.; Charlesworth, S.; Bayon, J.; Warwick, F. Rainfall–Runoff Simulations to Assess the Potential of SuDS for Mitigating Flooding in Highly Urbanized Catchments. *Int. J. Environ. Res. Public Health* **2016**, *13*, 149. [[CrossRef](#)] [[PubMed](#)]
7. Stahre, P. *Sustainability in Urban Storm Drainage—Planning and Examples*, 1st ed.; Svenskt Vatten: Malmö, Sweden, 2006.
8. Sörensen, J.; Persson, A.; Sternudd, C.; Aspegren, H.; Nilsson, J.; Nordström, J.; Jönsson, K.; Mottaghi, M.; Becker, P.; Pilesjö, P.; et al. Re-Thinking Urban Flood Management—Time for a Regime Shift. *Water* **2016**, *8*, 332. [[CrossRef](#)]
9. Mottaghi, M.; Aspegren, H.; Jönsson, K. Integrated urban design and open storm drainage in our urban environments: Merging drainage techniques into our city’s urban spaces. *Water Pract. Technol.* **2016**, *11*, 118–126. [[CrossRef](#)]
10. Fletcher, T.D.; Shuster, W.; Hunt, W.F.; Ashley, R.; Butler, D.; Arthur, S.; Trowsdale, S.; Barraud, S.; Semadeni-Davies, A.; Bertrand-Krajewski, J.-L.; et al. SUDS, LID, BMPs, WSUD and more—The evolution and application of terminology surrounding urban drainage. *Urban Water J.* **2015**, *12*, 525–542. [[CrossRef](#)]
11. Haghighatafshar, S.; Nordlöf, B.; Roldin, M.; Gustafsson, L.-G.; la Cour Jansen, J.; Jönsson, K. Efficiency of blue-green stormwater retrofits for flood mitigation—Conclusions drawn from a case study in Malmö, Sweden. *J. Environ. Manag.* **2018**, *207*, 60–69. [[CrossRef](#)] [[PubMed](#)]
12. Healthy Land and Water. *WSUD Water Sensitive Urban Design—Technical Design Guidelines for South East Queensland*; Healthy Land and Water: Brisbane, Australia, 2006.
13. Charlesworth, S.; Warwick, F.; Lashford, C. Decision-Making and Sustainable Drainage: Design and Scale. *Sustainability* **2016**, *8*, 782. [[CrossRef](#)]
14. Liu, H.; Jia, Y.; Niu, C. “Sponge city” concept helps solve China’s urban water problems. *Environ. Earth Sci.* **2017**, *76*, 473. [[CrossRef](#)]
15. Jarden, K.M.; Jefferson, A.J.; Grieser, J.M. Assessing the effects of catchment-scale urban green infrastructure retrofits on hydrograph characteristics. *Hydrol. Process.* **2016**, *30*, 1536–1550. [[CrossRef](#)]
16. Loperfido, J.V.; Noe, G.B.; Jarnagin, S.T.; Hogan, D.M. Effects of distributed and centralized stormwater best management practices and land cover on urban stream hydrology at the catchment scale. *J. Hydrol.* **2014**, *519*, 2584–2595. [[CrossRef](#)]
17. Jefferson, A.J.; Bhaskar, A.S.; Hopkins, K.G.; Fanelli, R.; Avellaneda, P.M.; McMillan, S.K. Stormwater management network effectiveness and implications for urban watershed function: A critical review. *Hydrol. Process.* **2017**, *31*, 4056–4080. [[CrossRef](#)]
18. Haghighatafshar, S.; la Cour Jansen, J.; Aspegren, H.; Lidström, V.; Mattsson, A.; Jönsson, K. Storm-water management in Malmö and Copenhagen with regard to Climate Change Scenarios. *J. Water Manag. Res.* **2014**, *70*, 159–168.
19. Sörensen, J.; Mobini, S. Pluvial, urban flood mechanisms and characteristics—Assessment based on insurance claims. *J. Hydrol.* **2017**, *555*, 51–67. [[CrossRef](#)]
20. Burns, M.J.; Fletcher, T.D.; Walsh, C.J.; Ladson, A.R.; Hatt, B.E. Hydrologic shortcomings of conventional urban stormwater management and opportunities for reform. *Landsc. Urban Plan.* **2012**, *105*, 230–240. [[CrossRef](#)]
21. Nordlöf, B. *1D/2D Modeling of the Open Stormwater System of Augustenborg Using MIKE FLOOD by DHI*; Project Report Available at Water and Environmental Engineering at the Department of Chemical Engineering; Lund University: Lund, Sweden, 2016.
22. Shuster, W.D.; Bonta, J.; Thurston, H.; Warnemuende, E.; Smith, D.R. Impacts of impervious surface on watershed hydrology: A review. *Urban Water J.* **2005**, *2*, 263–275. [[CrossRef](#)]
23. Yao, L.; Wei, W.; Chen, L. How does imperviousness impact the urban rainfall-runoff process under various storm cases? *Ecol. Indic.* **2016**, *60*, 893–905. [[CrossRef](#)]

24. Bell, C.D.; McMillan, S.K.; Clinton, S.M.; Jefferson, A.J. Hydrologic response to stormwater control measures in urban watersheds. *J. Hydrol.* **2016**, *541*, 1488–1500. [[CrossRef](#)]
25. Lee, J.G.; Heaney, J.P. Estimation of Urban Imperviousness and its Impacts on Storm Water Systems. *J. Water Resour. Plan. Manag.* **2003**, *129*, 419–426. [[CrossRef](#)]
26. Leopold, L.B. Lag times for small drainage basins. *CATENA* **1991**, *18*, 157–171. [[CrossRef](#)]
27. Ebrahimian, A.; Gulliver, J.S.; Wilson, B.N. Effective impervious area for runoff in urban watersheds. *Hydrol. Process.* **2016**, *30*, 3717–3729. [[CrossRef](#)]
28. Dahlström, B. *Regnintensitet—En Molnfysikalisk Beträktelse (in Swedish) [English: Rain Intensity—A Cloud-Physical Contemplation]*; Svenskt Vatten AB: Stockholm, Sweden, 2010.
29. Albrecht, J.C. *Alterations in the Hydrologic Cycle Induced by Urbanization in Northern New Castle County, Delaware: Magnitudes and Projections*; University of Delaware: Newark, DE, USA, 1974.
30. Arnell, V. Estimating Runoff Volumes from Urban Areas. *J. Am. Water Resour. Assoc.* **1982**, *18*, 1–21. [[CrossRef](#)]
31. Miller, R.A. *Characteristics of Four Urbanized Basins in South Florida*; Open-File Report 79–694; United States Geological Survey: Reston, VA, USA, 1979.
32. Dinicola, R.S. *Characterization and Simulation of Rainfall-Runoff Relations for Headwater Basins in Western King and Snohomish Counties, Washington*; Water-Resources Investigations Report 89–4052; United States Geological Survey: Reston, VA, USA, 1990.
33. Alley, W.M.; Veenhuis, J.E. Effective impervious area in urban runoff modelling. *J. Hydraul. Eng.* **1983**, *109*, 313–319. [[CrossRef](#)]
34. Qin, H.; Li, Z.; Fu, G. The effects of low impact development on urban flooding under different rainfall characteristics. *J. Environ. Manag.* **2013**, *129*, 577–585. [[CrossRef](#)] [[PubMed](#)]



© 2018 by the authors. Licensee MDPI, Basel, Switzerland. This article is an open access article distributed under the terms and conditions of the Creative Commons Attribution (CC BY) license (<http://creativecommons.org/licenses/by/4.0/>).

Supplementary material for **Paper II**

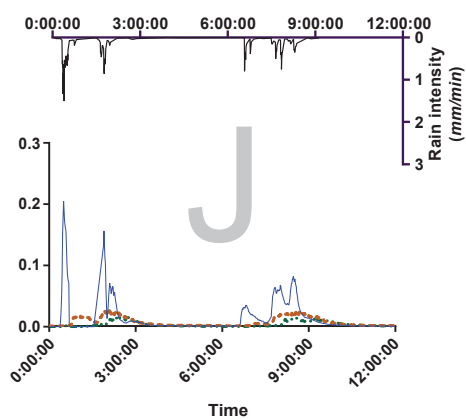
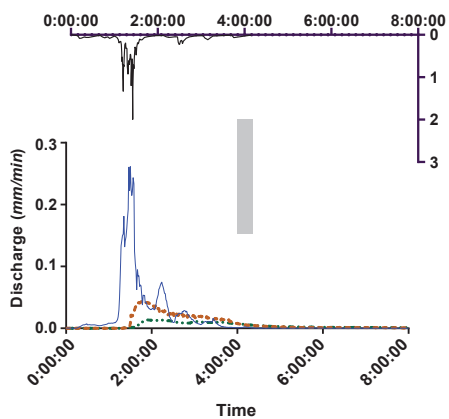
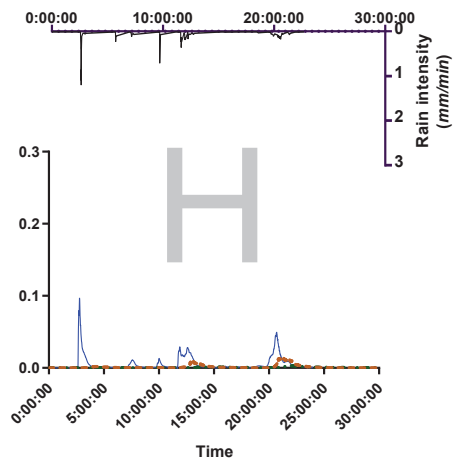
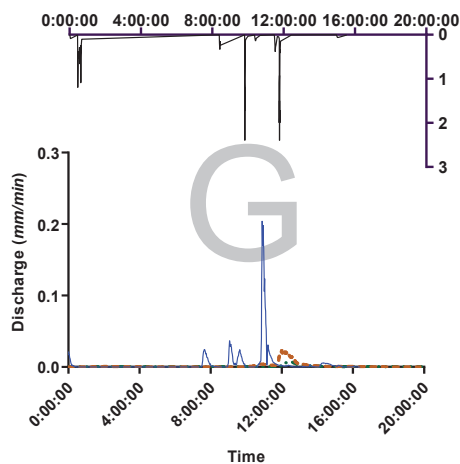
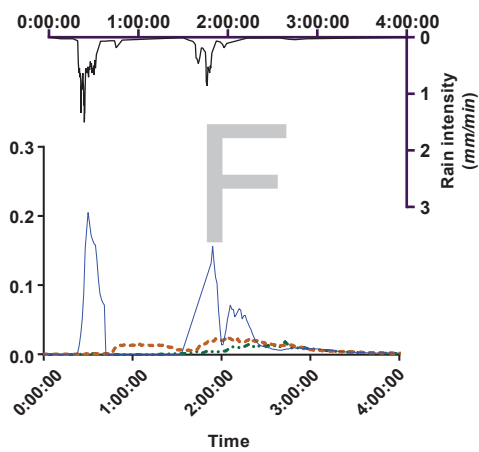
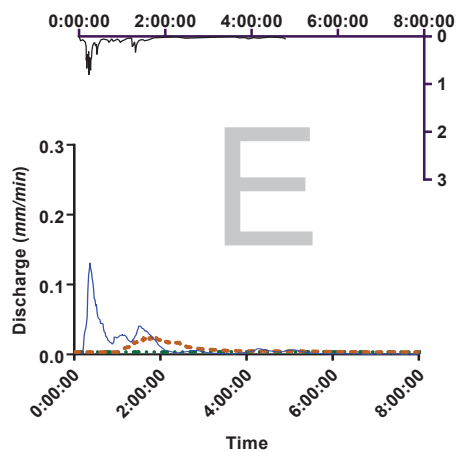


Rain intensity

Pipe system

Northern SuDS

Southern SuDS



Rain intensity

Pipe system

Northern SuDS

Southern SuDS

Paper III

A physically based model for mesoscale SuDS – an alternative to large-scale urban drainage simulations



Salar Haghighatafshar^{a*}

Mikael Yamanee-Nolin^b

Magnus Larson^c

Journal of Environmental Management, 240, 527-536
(2019)

^a Water and Environmental Engineering, Department of Chemical Engineering,
Lund University, P.O. Box 124 SE-22100, Lund, Sweden

^b Department of Chemical Engineering, Lund University,
P.O. Box 124, SE-22100 Lund, Sweden

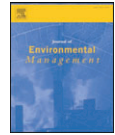
^c Department of Water Resources Engineering, Lund University,
P.O. Box 118, SE-221 00 Lund, Sweden

* Corresponding author



Contents lists available at ScienceDirect

Journal of Environmental Management

journal homepage: www.elsevier.com/locate/jenvman

Research article

A physically based model for mesoscale SuDS – an alternative to large-scale urban drainage simulations

Salar Haghighatafshar^{a,*}, Mikael Yamanee-Nolin^b, Magnus Larson^c^a Water and Environmental Engineering, Department of Chemical Engineering, Lund University, P.O. Box 124, SE-221 00 Lund, Sweden^b Department of Chemical Engineering, Lund University, P.O. Box 124, SE-221 00 Lund, Sweden^c Department of Water Resources Engineering, Lund University, P.O. Box 118, SE-221 00 Lund, Sweden

ARTICLE INFO

Keywords:

SuDS

SCM

Modelling

Hydraulics

Rainfall-runoff

Urban hydrology

ABSTRACT

This study presents a deterministic, lumped model to simulate mesoscale sustainable drainage systems (SuDS) based on a conceptualization of the stormwater control measures (SCMs) making up the system and their influence on the runoff process. The conceptualization mainly relies on parameters that are easily quantifiable based on the physical characteristics of the SCMs. Introducing a nonlinear reservoir model at the downstream end of the SuDS results in a fast model that can realistically describe the runoff process at low computational cost. Modelled hydrographs for the study area in Malmö, Sweden, matched data with regard to the overall shape of the hydrograph as well as the peak discharge and lag time. These output parameters are critical factors to be considered in the design of large systems consisting of mesoscale SuDS. The algebraic foundation of the developed model makes it suitable for large-scale applications (e.g., macroscale), where the simulation time is a decisive factor. In this respect, city-wide optimization studies for the most efficient location and implementation of SuDS are substantially accelerated due to fast and easy model setup. Moreover, the simplicity of the model facilitates more effective communication between all the actors engaged in the urban planning process, including political decision makers, urban planners, and urban water engineers.

1. Introduction

Sustainable drainage systems (SuDS) are considered as a viable alternative for urban drainage in a changed climate. SuDS as a concept has been around since the 1970s, but has gained increased attention in the research community during the recent decades due to full-scale implementations. So far, numerous research and investigations have focused on the effects and consequences of stormwater control measures (SCMs) at local scale, whereas a clear shortage has been identified regarding the knowledge on upscaling SCMs (Golden and Hoghooghi, 2018). Thus, determining the hydraulic behavior of SuDS is of great significance and different modelling approaches have been suggested for describing individual SCMs as constituents of SuDS (García-Serrana et al., 2017; Locatelli et al., 2014; Roldin et al., 2013). However, examples of models covering both the mesoscale (neighbourhood-scale) and macroscale (city-scale) processes are relatively rare. Two major factors are known to be the main reasons for the lack of appropriate modelling approaches at these scales: (1) scarce large-scale implementations of SuDS in cities (Loperfido et al., 2014; Zhang et al.,

2012) and (2) complexity of the existing modelling methodologies leading to extensive parameter estimation and calibration/validation procedures, as well as computationally costly models (Elliott et al., 2009; Freni et al., 2010; Haghighatafshar et al., 2018b; Jayasooriya and Ng, 2014; Krebs et al., 2014; Locatelli et al., 2014). Therefore, studies regarding upscaling of SuDS to a city-wide level, which demand numerous simulations of SuDS-drainage network interaction, are presently not feasible using the available distributed hydrodynamic models (e.g., MUSIC, SWMM, MIKE 21 and MIKE FLOOD). Even models based on artificial intelligence (AI), such as Artificial Neural Networks (ANN) using machine learning techniques that are widely used for rainfall-runoff simulations in regional scale watershed studies – with rare applications in exclusively urban studies – (Adamowski and Prasher, 2012; Hu et al., 2018; Mosavi et al., 2018), would not serve the urban drainage requirements with regard to upscaling of SuDS to city level. This is mainly because such black-box models do not provide substantial information on how the characteristics and the configuration of the system would affect the runoff outcome, ignoring any interaction between SuDS and the existing pipe-network. More importantly,

* Corresponding author.

E-mail addresses: Salar.Haghighatafshar@chemeng.lth.se (S. Haghighatafshar), Mikael.Yamanee-Nolin@chemeng.lth.se (M. Yamanee-Nolin), Magnus.Larson@tvrl.lth.se (M. Larson).<https://doi.org/10.1016/j.jenvman.2019.03.037>

Received 5 November 2018; Received in revised form 28 January 2019; Accepted 7 March 2019

0301-4797/ © 2019 Elsevier Ltd. All rights reserved.

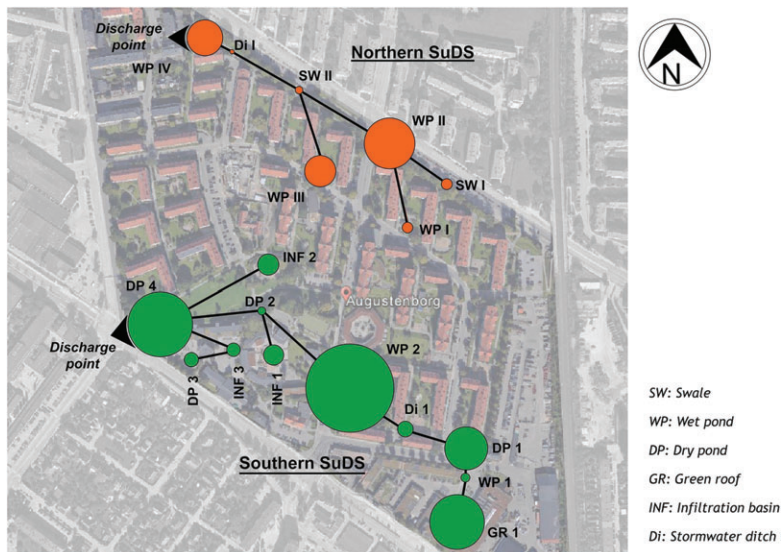


Fig. 1. The configuration the Northern and Southern SuDS, Augustenborg with different types and setups of SCMs, adopted from Haghighatafshar et al. (2018a).

enormous amount of monitored rainfall-runoff data with large diversity are required for training the model to deliver reliable results for any likely scenario (Géron, 2017; Halevy et al., 2009). Such datasets are rarely available within the field of urban drainage modelling.

In order to tackle the abovementioned challenges regarding large-scale simulations, new appropriate and efficient model concepts have to be developed for SuDS. Since urban drainage infrastructure performs as a dynamic and interconnected complex system of systems – i.e. reservoirs, SCMs, SuDS, pipe-networks, combined sewer overflows (CSO), wastewater treatment plants, receiving waters, etc. – the required simulation tool for SuDS should be capable of taking hydraulic interactions with the other elements of urban drainage network into consideration, in addition to being fast and reliable. The compromise would be to adopt simplified conceptual models for SuDS with focus on estimation of key parameters of the generated hydrographs, a catchment response time parameter and the peak discharge (Gericke and Smithers, 2018).

Thus, the aim of this study is to develop a fast, robust and flexible physically based model for inexpensive simulation of existing SuDS at meso- and macroscale with focus on estimation of lag time (as the selected catchment response time parameter) and peak discharge. The model has to be capable of being coupled with 1-dimensional sewer models for investigation of interactions between SuDS and sewer networks. This can be used in preliminary screening studies regarding the required retention capacity and the location of SuDS with respect to the entire sewer network (Zoppou, 2001), while in the later stages of the study, more complex models can be employed for detailed investigation of the selected locations.

2. Methodology

Haghighatafshar et al. (2018a) introduced a conceptual model for SuDS, developed using observed discharge patterns from a full-scale implementation of unique mesoscale SuDS in downtown Malmö,

Sweden. The model schematized mesoscale SuDS as a 1-dimensional series of interconnected retention basins (SCMs) of different sizes and types. It was shown that the order and placement of the constituent SCMs determine the overall performance of the SuDS. In the present study, the conceptual model is implemented mathematically to estimate the total discharge volumes using easily quantifiable physical parameters. Moreover, the model is further developed and enhanced to simulate the entire discharge hydrograph from mesoscale SuDS with the objective to predict the peak discharge and lag time, which are important parameters in the design of individual SCMs as well as meso- and macroscale SuDS. The algebraic formulation of the developed model makes it suitable for large-scale applications (e.g., macroscale), where the simulation time is a decisive factor. The development of the model is based upon studies made in Augustenborg in Malmö, Sweden. Flow measurements at the SuDS in Augustenborg were carried out during a 2-year period and were used for calibration and validation of the model. This section provides information about the case study area and the discharge measurements.

2.1. Augustenborg, Malmö

The Augustenborg area in the centre of Malmö, Sweden, contains unique examples of mesoscale SuDS. Augustenborg was originally drained via the municipal combined sewer network that was built during the 1950s. However, in the late 1990s, the runoff from the area was disconnected from the combined sewer system and it was led through the SuDS-retrofits constructed on the surface. The area consists of two separate SuDS-retrofits (denoted as the Northern and Southern SuDS), in total encompassing a drainage area of about 16 ha. The implementation of SuDS-retrofits in Augustenborg was done as part of a larger project for upgrading the social status of the neighbourhood. The Northern SuDS serves a catchment of about 6.3 ha and mainly consists of swales and open channel/ditch systems with a few wet ponds. The Southern SuDS receives runoff from an area of about 9.6 ha and is more

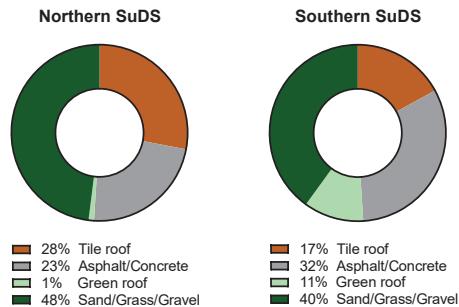


Fig. 2. The distribution of different types of surfaces in the Northern and Southern SuDS, Augustenborg.

diverse in terms of the employed SCMs. Green roofs, infiltration basins, wet/dry ponds, swales, and designated flood area are all present in the Southern SuDS.

The outflow from both systems is eventually discharged into the underground pipe network of the city, where the flowmeters were installed. The configuration and setup of the Northern and the Southern SuDS in Augustenborg are presented and discussed in detail in Haghighatafshar et al. (2018a). The layout of the implemented SCMs in each system and their connection order are presented in Fig. 1.

Fig. 2 shows the distribution of different types of surfaces in the Northern and Southern SuDS in Augustenborg. As seen, almost 50% of the surfaces in both the Northern and Southern SuDS consist of pervious surfaces of different kinds. Green roofs encompass a substantial share of the catchment for the Southern SuDS (approximately 11%), whereas the share of green roofs in the Northern SuDS is negligible (1%).

2.2. Rainfall-runoff measurements

The discharge from the Northern and the Southern SuDS in Augustenborg was measured at the most downstream points of the catchments where the overflow from the systems is diverted into the municipal pipe-network. The flow gauges used in this study were Mainstream Portable Area-Velocity (AV)-flowmeters. A single tipping bucket rain gauge with 0.2 mm resolution, Casella CEL, was installed in the area for monitoring the rainfall. The rainfall and runoff was monitored and logged for about 2 years recording 10 larger rainfall events that generated significant discharge from the systems; these events were selected for model calibration and validation in this study. Table 1 presents the characteristics of the recorded rainfall events denoted with the identifiers (IDs) A to J. The four recorded rainfall events with the

Table 1
The characteristics of the rainfall events used in this study.

| Status | Rainfall ID | Rainfall depth (mm) | Rainfall duration (h) | Rainfall peak (h) |
|-------------|----------------|---------------------|-----------------------|-------------------|
| Validation | A | 7.8 | 1.34 | 0.07 |
| Validation | B | 10.6 | 3.41 | 3.05 |
| Validation | C | 13.4 | 2.25 | 0.03 |
| Calibration | D | 13.8 | 9.34 | 8.75 |
| Calibration | E ^a | 15.6 | 4.84 | 0.23 |
| Calibration | F ^b | 17.4 | 3.92 | 0.07 |
| Calibration | G | 17.8 | 15.58 | 11.77 |
| Validation | H | 19.0 | 22.70 | 2.64 |
| Validation | I | 22.6 | 4.17 | 1.42 |
| Validation | J | 28.4 | 9.17 | 6.58 |

^a Rain E was only included in the calibration of the Northern SuDS.

^b Rain F was only included in the calibration of the Southern SuDS.

median depths (i.e. D, E, F and G) were selected to be used for the calibration, while the remaining six events (both smaller and larger than the calibration events) were kept for the validation.

Lag time in hydrological studies may have different definitions depending on the compared reference points on the hydrograph and the corresponding hydrograph (Gericke and Smithers, 2014; Schulz and Lopez, 1974). However, in the context of urban hydrology, lag time can also be calculated as the time interval between the rainfall peak and the peak discharge (Grayson et al., 2010; Mansell, 2003), which is also employed in this study. In case of rainfall events with double peaks, the later peak and its corresponding discharge are employed for the lag time calculations. The reason behind this specific criterion is the hypothesis that the first peak is possibly consumed for filling the retention capacity in the system, whereas the second peak has a direct connection to the peak discharge.

2.2.1. Possible error sources

It is important to note that the on-site measurements of flow and rainfall are subjected to some degree of uncertainty. The flowmeters tend to miss the low flows when the water depth in the pipe is less than the thickness of the sensor. The effect of this uncertainty on the total runoff volume depends on the characteristics of the hydrograph with respect to the distribution of volume against flow. Moreover, it is assumed that the rainfall recorded by the single tipping bucket rain gauge is homogeneously distributed and thus is representative for the entire study area. However, studies show that the spatial variation in the rainfall pattern (with respect to depth, intensity, and duration) can be substantial, even across sub-kilometer catchment scale (Fiener and Auerswald, 2009). It is also found that the spatial variability resulting from the rainfall dynamics, i.e., movement of rainfall over a catchment, affects the resulting hydrograph (Singh, 1997). For example, in case of Augustenborg, the Southern SuDS with a catchment area of 9.6 ha is more than 50% larger than the Northern SuDS and this could negatively affect the reliability of the runoff measurements in the Southern SuDS compared to the Northern SuDS.

3. Model development

3.1. Schematization of SCMs and mesoscale SuDS

In the specific schematization employed in this study, a single SCM – regardless of its type – is defined by three fundamental parameters, being the surface area of the SCM (A_{SCM}), retention depth in the freeboard (S_R) and rapid infiltration depth (S_{inf}) (Haghighatafshar et al., 2018a). Rapid infiltration depth in this context is the infiltration capacity primarily provided by the unsaturated zone of the filter medium. For simplicity, it is assumed that the infiltration process stops as soon as the available capacity in the unsaturated zone is consumed, i.e., no seepage of infiltrated water to the groundwater/deeper soil layers is considered. The values for the rapid infiltration depths are adopted from (Haghighatafshar et al., 2018b; Nordlöf, 2016).

Fig. 3 shows how these three parameters are defined to characterize the principal retention-based functions of a SCM.

The SCMs in Augustenborg are characterized based on the scheme presented in Fig. 3 and their characteristic values are presented in Table 2.

Mesoscale SuDS consist of multiple interconnected SCMs, as shown in Fig. 4, through which proportions of the rainfall are intercepted in upstream SCMs (effective retention, R_e^i), and the rest of the runoff flows to the immediate downstream SCM (i.e., V_{out}^i). Consequently, a discharge from the entire system is initiated when the retention capacity of the most downstream SCM is exceeded. Thus, the model operates by employing a volume transfer approach, where the storage volumes and the volume transfers are derived from the properties of the SCMs and the general characteristics of the catchment. The governing equations for effective retention and discharge volume from each SCM are given

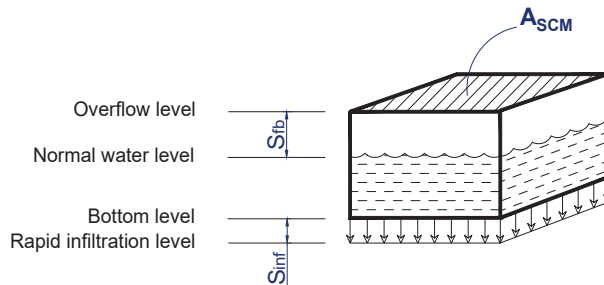


Fig. 3. The employed scheme for a single SCM within the framework of the developed model. A_{SCM} : surface area of the SCM, S_{fb} : retention depth in the freeboard and S_{inf} : rapid infiltration depth.

by equations (1) and (2).

$$R_e^i = \frac{(S_{fb}^i + S_{inf}^i) \times A_{SCM}^i}{DCLA^i} \quad (1)$$

$$V_{out}^i = \frac{(R - R_e^i) \times DCLA^i}{1000} + \sum_{j=1}^a V_{out}^{i-j} \quad (2)$$

In equations (1) and (2), R_e^i is the effective retention capacity of the SCM i (mm), S_{fb}^i is the storage depth in the freeboard of the SCM (mm), S_{inf}^i is the storage depth in the infiltration layer, A_{SCM}^i is the area occupied by the SCM (m^2), $DCLA^i$ is the directly connected impervious area to the SCM (m^2), V_{out}^i is the discharged volume from the SCM (m^3), R is the rainfall depth (mm), and $\sum_{j=1}^a V_{out}^{i-j}$ is the sum of the inflow to the SCM from the adjacent upstream SCM(s) (m^3), where a is the number of the immediate upstream SCMs connected to component i . Notice that if $V_{out}^i < 0$, it should be set equal to zero. Depending on the depth of rainfall with respect to the effective retention capacity ($R - R_e^i$), Eq. (2) represents different possible conditions with regard to the SCM. These conditions can be categorized as follows:

$R > R_e^i \rightarrow$ The local retention capacity of the SCM, i.e., $S_{fb}^i + S_{inf}^i$, is already exceeded and a discharge is initiated from the SCM. Any incoming volumes from the immediate upstream SCM(s), i.e., $\sum_{j=1}^a V_{out}^{i-j}$, will also pass through the system, without any retention.

$R = R_e^i \rightarrow$ The local retention capacity of the SCM, i.e., $S_{fb}^i + S_{inf}^i$, is already achieved so depending on whether there is an input from the

immediate upstream SCM(s), there might be a discharge from the system: $V_{out}^i = \sum_{j=1}^a V_{out}^{i-j}$.

$R < R_e^i \rightarrow$ The local retention capacity is partly used up. This means that the discharge from the system is initiated if and only if $\sum_{j=1}^a V_{out}^{i-j} > \frac{(R - R_e^i) \times DCLA^i}{1000}$, else $V_{out}^i = 0$.

In order to develop the volume-based equations (1) and (2) to describe flow from the SuDS, the rainfall data should be introduced as an *equally spaced accumulated rain depth time series*. In this study, the constant time-step is selected to be 5 min (i.e., $\Delta t = 5$ min). Thus, for any given time (t), equation (2) can be transformed to equation (3). No flow distribution is considered for the discharge from the components; the outflow from a component is obtained as an average flow for the entire time step.

$$q^{i,t} = \frac{V_{out}^{i,t} - V_{out}^{i,t-1}}{\Delta t} = \frac{(R^{acc,t} - R_e^i) \times DCLA^i}{\Delta t \times 1000} + \sum_{j=1}^a \frac{V_{out}^{i-j,t} - V_{out}^{i-j,t-1}}{\Delta t} = q^{i,t-1}, \quad \text{for } i = 1 \dots n \quad (3)$$

In which, $q^{i,t}$ is the discharge from component i at time t and $R^{acc,t}$ is the accumulated rainfall (mm) at time t . This equation is used to describe the discharge from components $i = 1 \dots n$. The flow characteristics of the discharge at the most downstream point in the SuDS (n) is especially important when simulating the influence of the entire urban drainage network on the runoff process. In the schematization used in this paper, the discharge from component (n) is assumed to be the inflow to a virtual component (Q_{in}), for which the discharge (Q_{out}) is simulated using a non-linear reservoir model. Fig. 4b shows how the final

Table 2
The characteristics of the implemented SCMs in the Augustenborg's SuDS, adopted from Haghighatafshar et al. (2018a,b).

| System | SCM ID | Storage, S_{fb} (mm) | Infiltration S_{inf} (mm) | SCM area, A_{SCM} (m^2) | DCLA (m^2) | Fed by |
|---------------|--------|------------------------|-----------------------------|-------------------------------|----------------|--------------------|
| Northern SuDS | SW I | 5 | 15 | 740 | 2780 | – |
| | WP I | 250 | 0 | 90 | 3920 | – |
| | WP II | 250 | 0 | 200 | 1120 | SW I, WP I |
| | WP III | 250 | 0 | 90 | 1620 | – |
| | SW II | 5 | 15 | 240 | 3400 | WP II, WP III |
| | Di I | 5 | 0 | 80 | 2100 | SW II |
| | WP IV | 350 | 0 | 160 | 3500 | Di I |
| | GR I | 0 | 45 | 10000 | 10000 | – |
| | WP I | 200 | 0 | 140 | 8500 | GR I |
| | DP I | 105 | 45 | 100 | 560 | WP I |
| Southern SuDS | Di I | 200 | 0 | 98 | 1685 | DP I |
| | WP 2 | 150 | 0 | 700 | 560 | Di I |
| | INF. 1 | 35 | 25 | 800 | 3150 | – |
| | DP 3 | 105 | 45 | 170 | 2760 | – |
| | INF. 2 | 0 | 25 | 800 | 1300 | – |
| | DP 2 | 0 | 15 | 200 | 1180 | WP 2, INF 1 |
| | INF. 3 | 500 | 25 | 115 | 5460 | DP 3 |
| | DP 4 | 25 | 25 | 900 | 300 | DP 2, INF 2, INF 3 |

SW: Swale, WP: Wet pond, DP: Dry pond, Di: Ditch (stormwater ditch), GR: Green roof, INF: Infiltration basin.

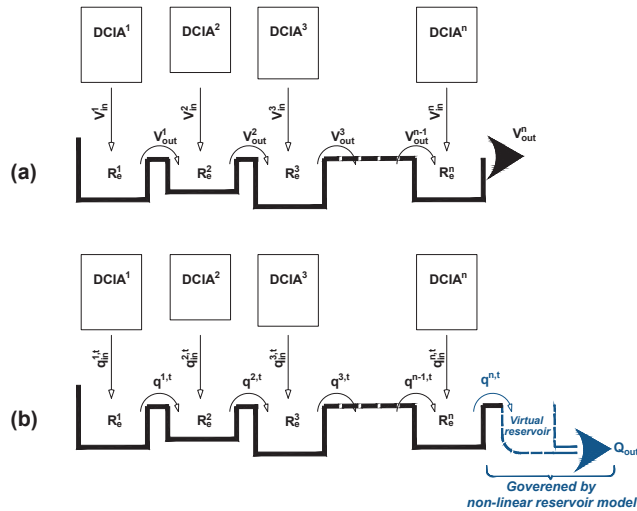


Fig. 4. (a) Schematization of mesoscale SuDS based on the conceptual model introduced by Haghighatafshar et al. (2018a). (b) Enhanced version of the volume-transfer model resulting in discharge (flow) simulation.

discharge is treated in the applied scheme, leading to the following equation:

$$\frac{dS}{dt} = Q_{in} - Q_{out} \quad Q_{out} = kS^m \Rightarrow \frac{dS}{dt} = Q_{in} - kS^m \quad (4)$$

where S (m^3) is the dynamic storage volume in the virtual reservoir, k (min^{-1}) and m (no units) are the reservoir coefficients.

As seen, the model utilizes very few (three) and consistent parameters to describe different types of SCMs, namely S_{in}^i , S_{in}^j , and A_{SCM}^i . This consistency and small number of parameters make the process of the parameter estimation relatively easy and straightforward compared to other models like SWMM, which requires approximately 12 parameters for simulation of green roofs or 7 parameters for pervious pavement structures (Jato-Espino et al., 2016).

The open-source programming language Python™ was employed for implementation of the model, as well as parameter estimation (calibration), validation, and sensitivity analysis. The Python-code generated for the model is able to communicate with Microsoft Excel in which an easy-to-use method is employed to describe the configuration of the mesoscale SuDS, similar to the setup presented in Table 2.

4. Results and discussion

4.1. Total flow volume

The ten rainfall events, monitored during the study, were simulated to estimate the total discharge volume using equations (1) and (2). Fig. 5 shows the observed discharge volume versus the results from the model. As seen, the model can reproduce the observed discharged volumes for the ten rainfall depths recorded during this study without a complex calibration process. In other words, only the physical description of the system, through equations (1) and (2), suffices to yield a satisfactory estimation of the total discharge volume. It is also shown that using DCIA as the sole contributor to the runoff can be an efficient alternative to simulate rainfalls of up to 2.5 mm/min with a maximum depth of about 30 mm.

4.2. Model calibration

Since not all of the registered rainfalls generated runoff/discharge, especially in the Southern SuDS, only three rainfall events with different volumes and durations (out of the total 10) were selected for calibrating the model for the Northern SuDS (rainfalls D, E, and G) and the Southern SuDS (rainfalls D, F, and G) as shown in Tables 2 and 3.

The Nash-Sutcliffe Efficiency Index (NSE) (Nash and Sutcliffe, 1970), was employed to objectively estimate the optimum k and m parameters for the nonlinear reservoir model, equation (4), and is presented in equation (5) below:

$$NSE = 1 - \frac{\sum_{i=1}^N (\hat{Q}_i - Q_i)^2}{\sum_{i=1}^N (Q_i - \bar{Q})^2}, \quad -\infty < NSE < 1.0 \quad (5)$$

where \hat{Q}_i and Q_i are the modelled and observed discharge values, respectively. \bar{Q} is the mean of the observed values and N is the number of data points in the sample (sample size).

The NSE has been widely employed in hydraulic and hydrological studies in order to assess the accuracy of the models (Brunetti et al., 2017; Palla and Gnecco, 2015; Rujner et al., 2018; Soulis et al., 2017). An NSE of 1 indicates perfect model fit with observations, whilst an NSE of 0 implies that the model is as good a predictor as the mean value of the observations (Jain and Sudheer, 2008).

The results of a preliminary investigation showed that the linear reservoir model showed as good agreement with observations as the nonlinear reservoir model (i.e. m -values for the Northern and Southern SuDS were about 1.05 and 1.10, respectively). Thus, the hydrographs behave according to a linear reservoir model. Consequently, to further simplify the model, a linear reservoir model was employed instead, i.e., $m = 1$. The model was then calibrated with respect to only the k parameter, which furthermore reduces the search space of the calibration problem, thereby decreasing the difficulty in the parameter estimation. In order to avoid negative and zero discharges, k is restricted to have positive/nonzero values during the calibration process. The final calibration procedure using the NSE was formulated as the

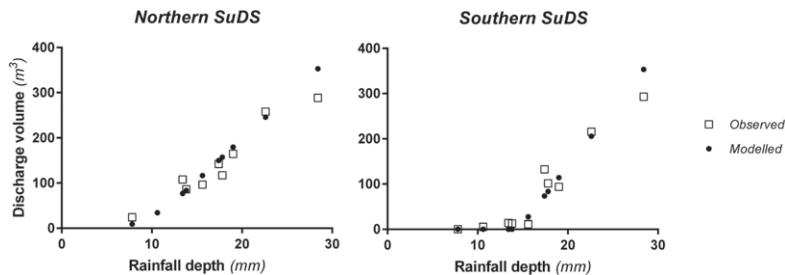


Fig. 5. Modelled and observed discharge volumes from the Northern and the Southern SuDS in Augustenborg for the studied rainfall events. Note that no flow measurement was available for Rainfall B (10.6 mm) in the Northern SuDS.

following optimization problem:

$$\begin{aligned} &\max \quad NSE \\ &\text{w.r.t. } k \\ &\text{s.t.} \quad \text{Equations (1) – (4)} \\ &\quad k > 0 \end{aligned}$$

The results of the calibration are presented in Table 3. With a constant value of 1.00 for m , the parameter k was calibrated to 0.017 min^{-1} and 0.014 min^{-1} for the Northern and Southern SuDS, respectively. The obtained maximized NSE values are also presented in Table 3. It is noted that the NSE values for the Northern SuDS are considerably larger than those of the Southern SuDS, implying that the selected calibration rainfall events deliver more reliable values for the calibration parameters in the former case. This can also be seen in the calibrated mean k where the corresponding standard deviation is smaller for the Northern SuDS (± 0.005) than that of the Southern SuDS (± 0.009). Generally, with respect to the achieved maximum NSE during the calibration process, most values are classified either *Satisfactory* ($0.50 < NSE < 0.65$), *Good* ($0.65 < NSE < 0.75$) or *Very good* ($NSE > 0.75$) based on a performance rating suggested by Moriasi et al. (2007).

4.3. Model validation

Fig. 6 shows examples of modelled versus observed hydrographs for the SuDS in Augustenborg. The model is able to satisfactorily predict the discharge rates from both the Northern and Southern SuDS for all events using similar parameter values, which indicate model reliability and robustness. NSE was also employed to evaluate the goodness of fit between measured and modelled values. NSE values, as shown in Fig. 6, are mostly high and close to 1.0 which is an indication for good agreement between observed and modelled discharge rates. The observed and modelled hydrographs for the Northern SuDS generally show a better agreement than those of the Southern SuDS. For Rainfall J in the Southern SuDS, NSE is found to be -0.18 . This is the only relatively low value among the NSEs found in this study, which can be due to in-built model characteristics that does not consider the reduction in

retention capacity due to antecedent rainfalls. As seen in Fig. 6f, the model underestimates the discharge rates during the first rainfall peak, while the discharges for the second peak in the rainfall are better estimated. This means that most probably, there has been an antecedent rainfall prior to the first peak, which has already filled up the SCMs. An already filled system, thereby, leads to higher discharge rates at the first peak in the rainfall, while the model assumes that the retention capacity of the system is vacant, generating smaller discharge rates. This effect decreases as the second rainfall peak strikes, leading to better modelled results.

Fig. 7 illustrates the performance of the model with regard to peak discharge for all rainfall-runoff events recorded in this study for the Northern and the Southern SuDS, respectively. The model produces comparable results for the Northern SuDS (Fig. 7a), whereas the simulations for the Southern SuDS show less good agreement with the observed data (Fig. 7b).

Fig. 8 shows how the modelled lag time deviates from the observed values after normalization with the rainfall duration. It is important to note that the accuracy of the estimated lag time shall be considered with regard to the duration of the rainfall. A longer rainfall duration implies that it is more likely to have a larger error between the modelled and the observed lag time. In order to compensate for the rainfall duration, the error between observed and modelled lag time is normalized with the rainfall duration. Results of the modelled lag times in the systems of Augustenborg also show that the Northern SuDS (Fig. 8a) is better simulated than the Southern SuDS (Fig. 8b). In addition to the error sources explained in section 2.2., the lower agreement between the observed and the modelled parameters in the Southern SuDS can partly be explained by the more complex discharge conditions and diverse types of SCMs that prevail in the Southern SuDS. Overall, the model is found to produce satisfactory results considering the simplifications made to achieve fast and easy simulations at low computational costs.

Such a fast and easily applicable model is essential for demanding simulations (e.g., city-wide modelling, application of long-term rainfall time series, Monte-Carlo techniques), but will also play an important

Table 3

The results of the calibration for m and k values as well as their corresponding NSE_{\max} obtained in Northern and Southern SuDS in Augustenborg.

| Rainfall ID | Northern SuDS | | | Rainfall ID | Southern SuDS | | |
|------------------|-----------------------|---------------------|---------------------|------------------|-----------------------|---------------------|---------------------|
| | k | m | NSE_{\max} | | k | m | NSE_{\max} |
| D | 0.011 | 1.00 | 0.70 | D | 0.006 | 1.00 | 0.12 |
| E | 0.023 | 1.00 | 0.78 | F | 0.026 | 1.00 | 0.70 |
| G | 0.017 | 1.00 | 0.85 | G | 0.010 | 1.00 | 0.59 |
| Mean (deviation) | 0.017 (± 0.005) | 1.00 (± 0.00) | 0.78 (± 0.06) | Mean (deviation) | 0.014 (± 0.009) | 1.00 (± 0.00) | 0.47 (± 0.25) |

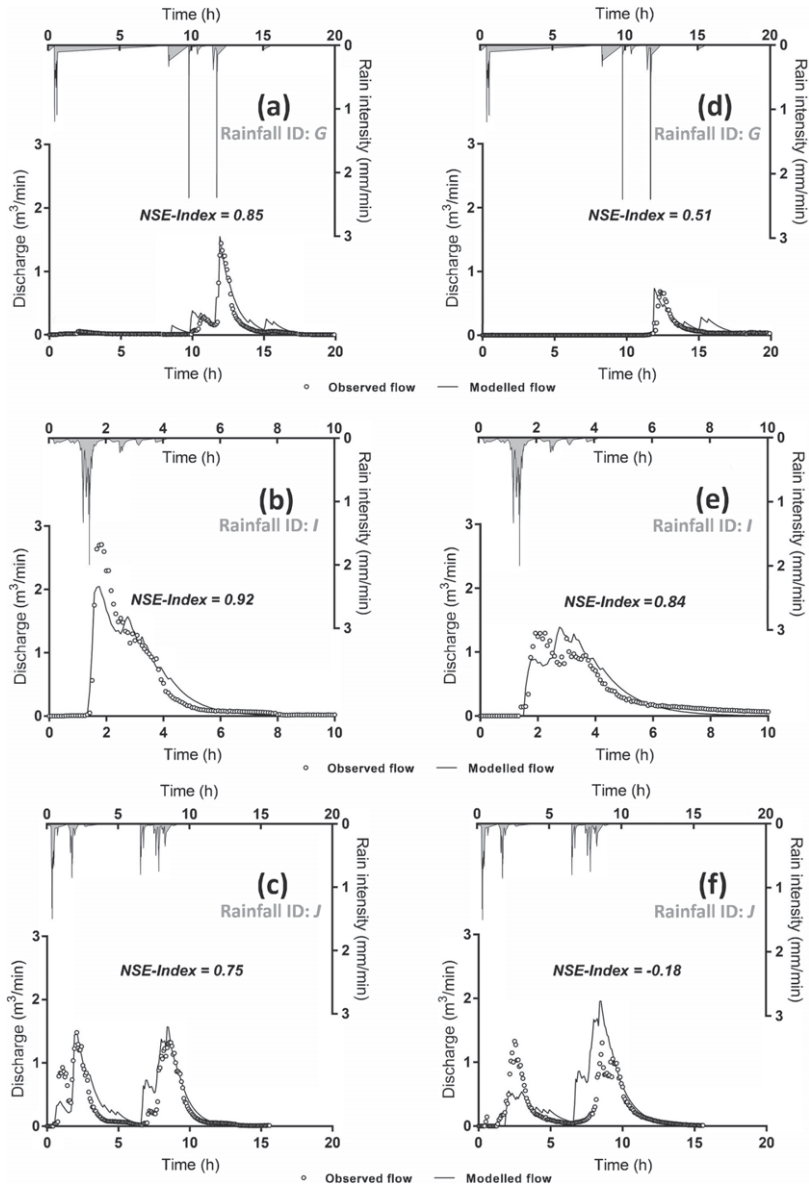


Fig. 6. Examples of the observed versus modelled discharges from the Northern (a, b, c: $k = 0.017 \text{ min}^{-1}$; $m = 1.00$) and Southern SuDS (d, e, f: $k = 0.014 \text{ min}^{-1}$, $m = 1.00$) in Augustenborg.

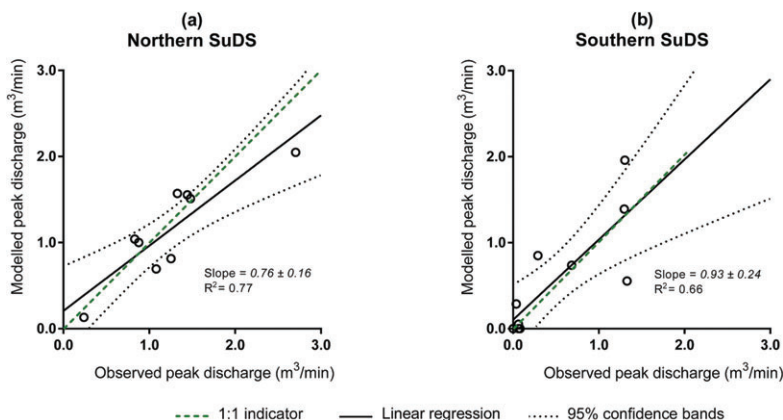


Fig. 7. Model performance with regard to peak discharge for (a) Northern SuDS (b) Southern SuDS in Augustenborg.

role in facilitating the communication between urban water engineers and urban planners who are supposed to design and implement SuDS through a mutual perspective and collaboration.

However, the current version of the model is designed and developed to simulate single rain events, since it does not take the relief in retention capacity through infiltration and evapotranspiration into account. Moreover, initial soil moisture and evapotranspiration processes for the permeable surfaces of the catchment are also excluded for simplicity as the model employs only DCIA as the contributing surface to runoff. It is possible, that in the future developments, such functions could be added to the description of the SCMs through employment of physically-based infiltration equations, e.g., nonlinear/linear reservoir models.

In order to extend the applicability of the model to nonexistent systems/unmonitored catchments with different configurations and outlet setups, it may be possible to relate the calibration parameters of the nonlinear reservoir model, i.e., k and m , to some physical characteristics of the system. For instance, the model parameters k and m could tentatively be estimated if the nonlinear reservoir model is interpreted as a weir equation (or bottom outlet equation) governing the discharge. The fact that the weir discharge from SuDS, as demonstrated for Augustenborg, in principle follows a linear reservoir dynamics (i.e.,

$m = 1$) makes the described process more convenient (only k needs to be estimated). In addition, the fact that the calibrated values of k for both systems (0.017 and 0.014 min^{-1} for Northern and Southern SuDS, respectively) are very close and have similar order of magnitude can be interpreted as an indication for the physical similarities in outlet setups of the systems. In this way, the number of coefficients to be estimated can be reduced, substituted with recommended values instead, while yielding a more robust and easy-to-use model.

4.4. Sensitivity analysis

To gain insights to how the different parts of the model affect its response, sensitivity analyses were performed for both the Northern and the Southern systems. These were carried out using the One-Factor-at-a-Time (OFAT) method, which entails perturbing one parameter (*ceteris paribus*) and studying the effect on the model output (Nolin et al., 2018). The OFAT method is simple to implement, and is helpful in understanding the dependency of the model on the investigated parameters (Delgarm et al., 2018). In this case, SCM properties (such as retention, SCM area, DCIA) as well as the nonlinear reservoir model parameters (k and m) were individually perturbed at three different levels, i.e., $\pm 10\%$, $\pm 25\%$ and $\pm 50\%$, representing reasonable,

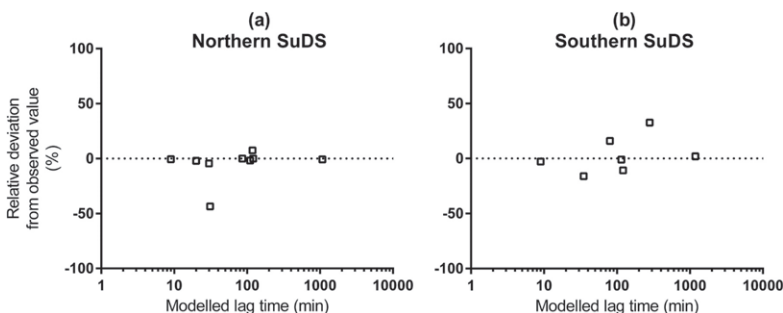


Fig. 8. Relative deviation of modelled lag times from observed values, normalized against the total duration of the rainfall.

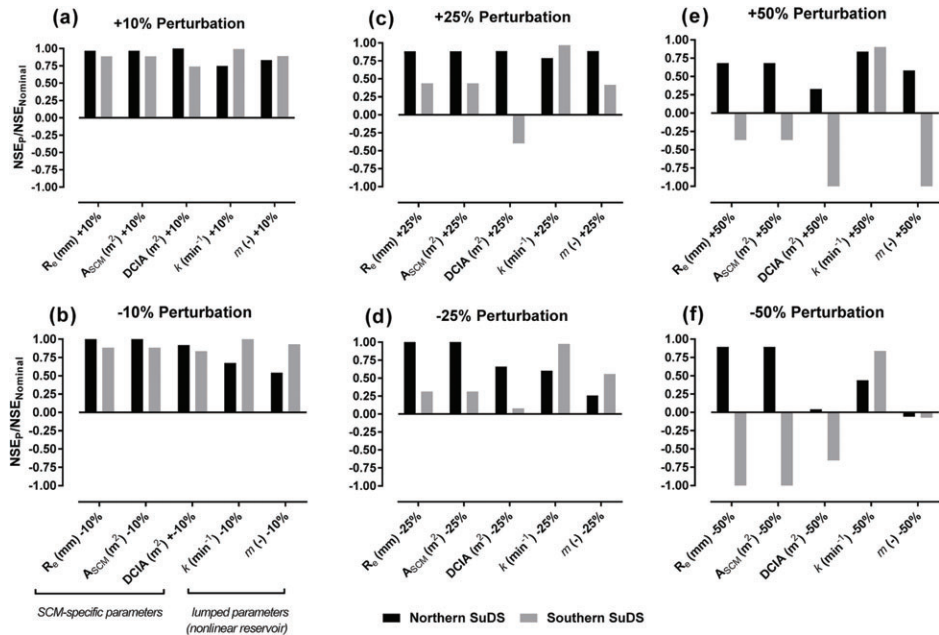


Fig. 9. Sensitivity analysis based on OFAT method showing the obtained NSE for the Northern and Southern SuDS in case of $\pm 50\%$ alteration in the model parameters.

moderate, and extreme perturbation scenarios, respectively. Note that no recalibration of the model was performed during this investigation, and the k values of 0.017 min^{-1} and 0.014 min^{-1} for the Northern and Southern SuDS, respectively, were used when not perturbed themselves. The results from the OFAT sensitivity studies for the Northern and Southern SuDS when perturbing the aforementioned parameters are presented in Fig. 9, in which the relative variation of the achieved NSE after perturbation (NSE_p) against the calibrated/nominal NSE ($\text{NSE}_{\text{Nominal}} = 0.92$ [Northern SuDS]; 0.84 [Southern SuDS]) is used as an indicator for model sensitivity.

The results show impact from all perturbations, making the NSE lower than or equal to the nominal case; this is expected since the nominal case is calibrated to maximize the NSE. However, $\pm 10\%$ perturbations (Fig. 9a and b) for all parameters result in acceptable NSE values, retaining 75%–100% of the nominal NSE for $+10\%$ perturbation for both Northern and Southern SuDS, whereas in case of -10% perturbation, model performance slightly deteriorates for k and m for the Northern SuDS. In general, regarding the lumped parameters, the model is found to be more sensitive to perturbations of m compared to those of k , but this has a negligible significance since the model behavior is rather linear, which means m is in general equal to 1.0.

In case of $\pm 25\%$ perturbations, the model performance deteriorates considerably for the Southern SuDS, while the Northern SuDS tends to retain acceptable results. It is also important to note that the SCM-specific parameters (R_e , A_{SCM} and DCIA) are relatively easily quantifiable; thus, $\pm 10\%$ perturbations is assessed to be more realistic for them than $\pm 25\%$ and $\pm 50\%$ perturbations.

There is a clear difference in the effect of the perturbations on the two systems, where the response of the Southern model is impacted to a

higher degree for all perturbations except for those on k . Furthermore, varying k by $\pm 50\%$ has a relatively small effect for the Southern SuDS, whereas it has a similar effect as the other parameters for the Northern SuDS. Combined, the low effect of k and the difference in effects between the two systems indicate that the physically based model is robust and captures system behavior quite well, since the lumped parameters do not change the solution substantially. It also highlights the importance of proper quantification of the SCM-specific parameters – tolerating an error of about $\pm 10\%$ – as these can have a large influence on the model output.

5. Concluding remarks

The event-based model developed in this study fulfills the overall objective, which was to predict the discharge pattern (hydrograph) from mesoscale SuDS at low computational costs and with acceptable accuracy. The complete hydrograph from a mesoscale SuDS for a 10-h rainfall event is generated in a matter of seconds. This model property facilitates large-scale/city-wide optimization studies that are essential for long-term, sustainable performance of urban drainage networks. Such city-wide optimization using the developed rapid simulation tool could be regarded as a preliminary screening stage after which more complex models can be employed for further investigation at selected sites and locations for prospective SuDS retrofits. Presently, the model uses the nonlinear reservoir equation only to characterize the last compartment in the SuDS. A more detailed and representative approach would be to apply the nonlinear reservoir model to the discharges from all the upstream SCMs as well, i.e., $q^{1,t}$, $q^{2,t}$, ..., $q^{n-1,t}$. It might also be desirable to introduce infiltration and evapotranspiration rates – as sink

functions – to the components (SCMs) to facilitate long-term continuous rainfall-runoff simulations. However, for validation this would require more extensive data collection at many discharge points from the SCMs. Furthermore, it means that the k and m constants have to be quantified for each compartment (SCM), which will make the model a more complicated tool to use. On the other hand, depending on the type of SCM, analytical or empirical expression may be developed for k and m .

Declarations of interest

None

Acknowledgements

This work was financially supported by J. Gustaf Richert Foundation at SWECO (grant number 2015-00181), Sweden's Innovation Agency (VINNOVA) via *Future City Flow* project (grant number 2017-01046) at Sweden Water Research as well as the Swedish Water and Wastewater Association (*Svenskt Vatten*) via *VA-teknik Södra*. The authors also acknowledge the personnel at the regional water and wastewater utility company (VA SYD) for their support with respect to measuring instrument and data collection. *Tomas Wolf* and *John Hågg* at VA SYD are especially thanked for their contribution to setup and maintenance of the instruments. Our colleagues *Miguel Sanchis Sebastia* and *Niklas Andersson* at the Department of Chemical Engineering, Lund University are also acknowledged for their input and advice during the course of code-development.

Appendix A. Supplementary data

Supplementary data associated with this article can be found, in the online version, at <https://doi.org/10.1016/j.jenvman.2019.03.037>.

References

- Adamowski, J., Prasher, S.O., 2012. Comparison of machine learning methods for runoff forecasting in mountainous watersheds with limited data. *J. Water Land Dev.* 17. <https://doi.org/10.2478/v10025-012-0038-4>.
- Brunetti, G., Šimůnek, J., Turco, M., Piro, P., 2017. On the Use of Surrogate-Based Modeling for the Numerical Analysis of Low Impact Development Techniques. <https://doi.org/10.1016/j.jhydrol.2017.03.013>.
- Delgarm, N., Sejjadi, B., Azarbad, K., Delgarm, S., 2018. Sensitivity analysis of building energy performance: a simulation-based approach using OFAT and variance-based sensitivity analysis methods. *J. Build. Eng.* 15, 181–193. <https://doi.org/10.1016/j.jobe.2017.11.020>.
- Elliott, A.H., Trowsdale, S.A., Wadhwa, S., 2009. Effect of aggregation of on-site storm-water control devices in an urban catchment model. *J. Hydrol. Eng.* 14, 975–983. [https://doi.org/10.1061/\(ASCE\)1084-0699\(2009\)14:4\(975\)](https://doi.org/10.1061/(ASCE)1084-0699(2009)14:4(975)).
- Fiener, P., Auerwald, K., 2009. Spatial variability of rainfall on a sub-kilometre scale. *Earth Surf. Process. Landforms* 34, 848–859. <https://doi.org/10.1002/esp.1779>.
- Freni, G., La Loggia, G., Notaro, V., 2010. Uncertainty in urban flood damage assessment due to urban drainage modelling and depth-damage curve estimation. *Water Sci. Technol.* 61, 2979–2993. <https://doi.org/10.2166/wst.2010.177>.
- García-Serrana, M., Gulliver, J.S., Nieber, J.L., 2017. Non-uniform overland flow-infiltration model for roadside swales. *J. Hydrol.* 552, 586–599. <https://doi.org/10.1016/j.jhydrol.2017.07.014>.
- Gerice, O.J., Smithers, J.C., 2018. An improved and consistent approach to estimate catchment response time parameters: case study in the C5 drainage region, South Africa. *J. Flood Risk Manag.* 11, S284–S301. <https://doi.org/10.1111/jfr3.12206>.
- Gerice, O.J., Smithers, J.C., 2014. Review of methods used to estimate catchment response time for the purpose of peak discharge estimation. *Hydrol. Sci. J.* 59, 1935–1971. <https://doi.org/10.1080/02626667.2013.866712>.
- Géron, A., 2017. *Hands-On Machine Learning with Scikit-Learn and TensorFlow - Concepts, Tools, and Techniques to Build Intelligent Systems*. O'Reilly Media.
- Golden, H.E., Hough, N., 2018. Green infrastructure and its catchment-scale effects: an emerging science. *Wiley Interdiscip. Rev. Water* 5, e1254. <https://doi.org/10.1002/wat2.1254>.
- Grayson, R., Holden, J., Rose, R., 2010. Long-term change in storm hydrographs in response to peatland vegetation change. *J. Hydrol.* 389, 336–343. <https://doi.org/10.1016/j.jhydrol.2010.06.012>.
- Haghighatafshar, S., la Cour Jansen, J., Aspegren, H., Jönsson, K., 2018a. Conceptualization and schematization of mesoscale sustainable drainage systems: a full-scale study. *Water* 10, 1041. <https://doi.org/10.3390/w10081041>.
- Haghighatafshar, S., Nordlöf, B., Roldin, M., Gustafsson, L.-G., la Cour Jansen, J., Jönsson, K., 2018b. Efficiency of blue-green stormwater retrofits for flood mitigation – conclusions drawn from a case study in Malmö, Sweden. *J. Environ. Manag.* 207, 60–69. <https://doi.org/10.1016/j.jenvman.2017.11.018>.
- Halevy, A., Norvig, P., Pereira, F., 2009. The unreasonable effectiveness of data. *IEEE Intell. Syst.* 24, 8–12. <https://doi.org/10.1109/MIS.2009.36>.
- Hu, C., Wu, Q., Li, H., Jian, S., Li, N., Lou, Z., Hu, C., Wu, Q., Li, H., Jian, S., Li, N., Lou, Z., 2018. Deep learning with a long short-term memory networks approach for rainfall-runoff simulation. *Water* 10, 1543. <https://doi.org/10.3390/w10111543>.
- Jain, S.K., Sudheer, K.P., 2008. Fitting of hydrologic models: a close look at the Nash–Sutcliffe Index. *J. Hydrol. Eng.* 13, 981–986. [https://doi.org/10.1061/\(ASCE\)1084-0699\(2008\)13:10\(981\)](https://doi.org/10.1061/(ASCE)1084-0699(2008)13:10(981)).
- Jato-Espino, D., Charlesworth, S., Bayon, J., Warwick, F., 2016. Rainfall-runoff simulations to assess the potential of SuDS for mitigating flooding in highly urbanized catchments. *Int. J. Environ. Res. Public Health* 13, 149. <https://doi.org/10.3390/ijerph13010149>.
- Jayasooriya, V.M., Ng, A.W.M., 2014. Tools for modeling of stormwater management and economics of green infrastructure practices: a review. *Water, Air, Soil Pollut.* 225, 2055. <https://doi.org/10.1007/s11270-014-2055-1>.
- Krebs, G., Kokkonen, T., Valtanen, M., Seitälä, H., Koivusalo, H., 2014. Spatial resolution considerations for urban hydrological modelling. *J. Hydrol.* 512, 482–497. <https://doi.org/10.1016/j.jhydrol.2014.03.013>.
- Locatelli, L., Mark, O., Mikkelsen, P.S., Arbjerg-Nielsen, K., Bergen Jensen, M., Binning, P.J., 2014. Modelling of green roof hydrological performance for urban drainage applications. *J. Hydrol.* 519, 3237–3248. <https://doi.org/10.1016/j.jhydrol.2014.10.030>.
- Loperfido, J.V., Noe, G.B., Jarnagin, S.T., Hogan, D.M., 2014. Effects of distributed and centralized stormwater best management practices and land cover on urban stream hydrology at the catchment scale. *J. Hydrol.* 519, 2584–2595. <https://doi.org/10.1016/j.jhydrol.2014.07.007>.
- Mansell, M.G., 2003. *Rural and Urban Hydrology*. Thomas Telford Publishing. <https://doi.org/10.1680/rauh.32309>.
- Moriasi, D.N., Arnold, J.G., Liew, M.W., Van, Bingner, R.L., Harmel, R.D., Veith, T.L., 2007. Model evaluation guidelines for systematic quantification of accuracy in watershed simulations. *Trans. ASABE* 50, 885–900.
- Mosavi, A., Ozturk, F., Chau, K., 2018. Flood prediction using machine learning models: literature review. *Water* 10, 1536. <https://doi.org/10.3390/w10111536>.
- Nash, J.E., Sutcliffe, J.V., 1970. River flow forecasting through conceptual models part I – a discussion of principles. *J. Hydrol.* 10, 282–290.
- Nolin, M., Andersson, N., Nilsson, B., Max, M., Pajalic, O., 2018. Analysis of an oscillating two-stage evaporator system through modelling and Simulation: an industrial case study. *Chem. Eng. Trans.* 69.
- Nordlöf, B., 2016. 1D/2D Modeling of the Open Stormwater System of Augustenborg Using MIKE FLOOD by DHI. Project report available at: Water and Environmental Engineering at the Department of Chemical Engineering, Lund University, Lund, Sweden.
- Palla, A., Gneco, I., 2015. Hydrologic modeling of Low Impact Development systems at the urban catchment scale. *J. Hydrol.* 528, 361–368. <https://doi.org/10.1016/j.jhydrol.2015.06.050>.
- Roldin, M., Locatelli, L., Mark, O., Mikkelsen, P.S., Binning, P.J., 2013. A simplified model of soakaway infiltration interaction with a shallow groundwater table. *J. Hydrol.* 497. <https://doi.org/10.1016/j.jhydrol.2013.06.005>.
- Rujner, H., Leonhardt, G., Marsalek, J., Vilkander, M., 2018. High-resolution modelling of the grass swale response to runoff inflows with Mike SHE. *J. Hydrol.* 562, 411–422. <https://doi.org/10.1016/j.jhydrol.2018.05.024>.
- Schulz, E.F., Lopez, G., 1974. Determination of Urban Watershed Response Time.
- Singh, V.P., 1997. Effect of spatial and temporal variability in rainfall and watershed characteristics on stream flow hydrograph. *Hydrol. Process.* 11, 1649–1669. [https://doi.org/10.1002/\(SICI\)1099-1085\(199710\)11:12<1649::AID-HYP495>3.0.CO;2-1](https://doi.org/10.1002/(SICI)1099-1085(199710)11:12<1649::AID-HYP495>3.0.CO;2-1).
- Souls, K.X., Valiantzas, J.D., Ntoulas, N., Kargas, G., Nektarios, P.A., 2017. Simulation of Green Roof Runoff under Different Substrate Depths and Vegetation Covers by Coupling a Simple Conceptual and a Physically Based Hydrological Model. <https://doi.org/10.1016/j.jenvman.2017.06.012>.
- Zhang, X., Shen, L., Tam, V.W.Y., Lee, W.W.Y., 2012. Barriers to implement extensive green roof systems: a Hong Kong study. *Renew. Sustain. Energy Rev.* 16, 314–319. <https://doi.org/10.1016/j.rser.2011.07.157>.
- Zoppou, C., 2001. Review of urban storm water models. *Environ. Model. Softw.* 16, 195–231. [https://doi.org/10.1016/S1364-8152\(00\)00084-0](https://doi.org/10.1016/S1364-8152(00)00084-0).

Paper IV

Hydroeconomic optimization of mesoscale blue-green stormwater systems at the city level

IV

Salar Haghighatafshar^{a*}

Mikael Yamanee-Nolin^b

Anders Klinting^c

Maria Roldin^d

Lars-Göran Gustafsson^d

Henrik Aspegren^{a,e}

Karin Jönsson^a

Journal of Hydrology, 578, Article 124125
(2019)

^a Water and Environmental Engineering, Department of Chemical Engineering,
Lund University, P.O. Box 124 SE-22100, Lund, Sweden

^b Department of Chemical Engineering, Lund University,
P.O. Box 124, SE-22100 Lund, Sweden

^c DHI Denmark (Head Office), DHI A/S - DHI Water Environment Health,
Agern Allé 5, DK-2970 Hørsholm, Denmark

^d DHI Sweden, Södra Tullgatan 3, SE-21140 Malmö, Sweden

^e Sweden Water Research AB,
Ideon Science Park, Scheelevägen 15, SE-22370 Lund, Sweden

* Corresponding author



Contents lists available at ScienceDirect

Journal of Hydrology

journal homepage: www.elsevier.com/locate/jhydrol

Research papers

Hydroeconomic optimization of mesoscale blue-green stormwater systems at the city level

Salar Haghighatafshar^{a,*}, Mikael Yamanee-Nolin^b, Anders Klinting^c, Maria Roldin^d, Lars-Göran Gustafsson^d, Henrik Aspegren^{a,e}, Karin Jönsson^a^a Water and Environmental Engineering, Department of Chemical Engineering, Lund University, P.O. Box 124, SE-22100 Lund, Sweden^b Department of Chemical Engineering, Lund University, P.O. Box 124, SE-22100 Lund, Sweden^c DHI Denmark (Head Office), DHI A/S – DHI Water Environment Health, Artens Allé 5, DK-2970 Hørsholm, Denmark^d DHI Sweden, Södra Tullgatan 3, SE-21140 Malmö, Sweden^e Sweden Water Research AB, Ideon Science Park, Scheelevägen 15, SE-22370 Lund, Sweden

ARTICLE INFO

This manuscript was handled by G. Syme,
Editor-in-Chief

Keywords:
Blue-green stormwater
Mesoscale
Macroscale
Urban drainage
Urban infrastructure
Optimization
Hybrid modeling
Cosimulation

ABSTRACT

The development of tools to help cities and water utility authorities communicate and plan for long-term sustainable solutions is of utmost importance in the era of a changing and uncertain climate. This study introduces a hybrid modeling concept for the cosimulation of mesoscale blue-green stormwater systems and conventional urban sewer networks. The hybrid model successfully introduces the retention/detention effects of mesoscale blue-green stormwater systems to the hydraulic dynamics of the sewer network. The cosimulation package was further facilitated with a cost-oriented multiobjective optimization algorithm. The aim of the scalar multi-objective optimization was to minimize the total cost comprising both *flooding costs* and *action costs* – both parameters solely representing the financial components of cost – through optimal placement of mesoscale blue-green systems of optimal size. The suggested methodology provides a useful platform for sustainable management of the existing sewer networks in cities from a hydroeconomic perspective.

1. Introduction

The limitation in drainage capacity and its consequent outcomes have been discussed among urban engineers since the late 19th century (Kuichling, 1889; Lloyd-Davies, 1906). The focus on urban flooding as a serious challenge has been intensified due to the observed increase in the frequency of rainfall events/pluvial floods as a result of climate change. Cities have struggled with the mitigation of urban flooding ever since and have recently become interested in the notion of blue-green stormwater solutions, also known as stormwater control measures (SCM). However, there is still no consensus in the scientific community or among the city authorities on how, where and to what extent these solutions shall be implemented.

Many large and old cities have inherited a larger proportion of their infrastructure from the far past. In a changing climate, it is highly desirable to sustain the functionality of the existing infrastructure and to maintain resilience in the case of natural catastrophes. This is especially desirable from an economic point of view, as the intensity and frequency of extreme rain events are increasing. This can be done by introducing flexibility to urban infrastructure, avoiding a technical lock-

in to solely pipe-based drainage systems. In addition, further urbanization in terms of altered land use and further densification leads to increased impermeable surfaces compared to the situation for which the drainage system was designed. This means that even under a constant climate scenario, elevated flooding will still be a serious challenge considering the current urban planning and engineering practices (Berndtsson et al., 2019). Cities are trying to enhance the capacity of the drainage system by increasing the safety margins in the design criteria as well as by replacing the existing pipes with larger culverts. This is done, for instance, by introducing climate factors to design criteria (Arnbjerg-Nielsen, 2012; SWWA, 2016; Watt et al., 2003), updating intensity-duration-frequency (IDF) curves (Guo, 2006; Hailegeorgis et al., 2013; Lima et al., 2018; Mailhot et al., 2007) and construction of large stormwater tunnels in cities (Dolowitz et al., 2018; VA SYD, 2019). Such measures might be effective to some extent, but in the era of a nonstationary climate – as demonstrated and argued by Milly et al. (2008), Vogel et al. (2011), and Liu et al. (2017b) – manipulation of drainage capacity might not be an optimal solution. A parallel solution would be to manipulate the contributing catchments – by introducing retention/detention capacities, e.g., via blue-green

* Corresponding author.

E-mail address: Salar.Haghighatafshar@chemeng.lth.se (S. Haghighatafshar).<https://doi.org/10.1016/j.jhydrol.2019.124125>

Received 23 July 2019; Received in revised form 29 August 2019; Accepted 6 September 2019

Available online 09 September 2019

0022-1694/ © 2019 Elsevier B.V. All rights reserved.

stormwater systems – to modify the volume and the flow of the generated runoff (Azzout et al., 1995; Fletcher et al., 2015; Stahre, 2006, 1993).

Blue-green stormwater systems aim to mimic a naturally-oriented water cycle as well as introducing amenity by juxtaposing water and greenery in urban environments (Everett et al., 2015). These systems combine natural hydrological and ecological values and are shown to have considerable contributions to flood mitigation (BlueGreenCities, 2019). This is done by slowing down runoff and by improving infiltration, evapotranspiration, detention, and surface storage. Green roofs, wet and dry ponds, swales, biofilters (raingardens), and infiltration basins are all individual solutions (SCMs) within the context of blue-green stormwater management. In this paper, however, a *blue-green system* is defined as an interconnected group of blue-green stormwater solutions or SCMs, which can be implemented on different scales depending on the effect they are expected to deliver (Demuzere et al., 2014). The presented definition for the blue-green stormwater systems – as used within the context of this paper – is also regarded as sustainable drainage systems (SuDS) (Fletcher et al., 2015). According to a classification by Haghighatafshar et al. (2018b), blue-green stormwater systems can be implemented at:

- *microscale*, where single and discrete blue-green stormwater solutions or SCMs are implemented locally and the discharge from each SCM is directly connected to the urban drainage network;
- *mesoscale*, where the blue-green stormwater system is implemented as a group of tree-structured SCMs, in which the discharge from one (or more) SCM(s) flows into the next immediate SCM lying downstream and eventually to the recipient/urban drainage network. This configuration of SCMs is frequently referred to as “SuDS management train” (Kirby, 2005). A detailed conceptualization of mesoscale systems is presented and discussed by Haghighatafshar et al. (2018a) as a definition for blue-green stormwater systems;
- *macroscale*, where blue-green stormwater systems are upscaled to the city level and in a hydraulic context, might have considerable effects on the functionality of the existing urban drainage network.

Whilst acknowledging all legal and institutional obstacles (Berndtsson et al., 2019; Wahlborg et al., 2019), one of the possible scenarios with respect to the realization of the macroscale blue-green stormwater systems is to upscale the mesoscale blue-green stormwater system, i.e., to replicate the mesoscale blue-green stormwater system in multiple locations of the city (Haghighatafshar et al., 2018a). The replication of mesoscale blue-green stormwater systems in multiple locations in the city could result in the concept of *sponge cities* – a concept and practice developed in China (Liu et al., 2017a; Ren et al., 2017; Zhang et al., 2018) – or a macroscale blue-green stormwater system (Haghighatafshar et al., 2018a) in which city surfaces are designed to contain enough infiltration, retention or detention volume to overcome the consequences of flooding along with stormwater management, rainwater harvesting and stormwater quality improvement (Zhang et al., 2018). The collection of these services in the cities could potentially help survival of the highly contrasted wet and dry seasons (Trenberth et al., 2014) that lead to floods and droughts, respectively. The literature available concerning the macroscale implementation of blue-green stormwater systems within the context of sponge cities is increasing, and different aspects of the challenge are addressed (Fenner and Richard, 2017; Li et al., 2019; Ren et al., 2017; Zhang et al., 2018). For instance, land availability, land use, population density, topology and geological characteristics have been addressed for the implementation of stormwater control measures by investigating the urban morphology (Bach et al., 2013; Romnée et al., 2015). There are also studies that have looked into biophysical factors as well as the sociodemographic status of urban districts for the likely implementation of blue-green stormwater systems (Kuller et al., 2016). Zischg et al. (2018) and Cunha et al. (2016) have studied how microscale SCMs

(single blue-green stormwater measures) and underground storage units along the pipes affect the performance of the local pipe network under design storm scenarios, and have consequently recommended a placement strategy. A similar study was carried out by Wang et al. (2017), who have optimized placement of storage tanks using a two-stage approach for flood mitigation. Zischg et al. (2019) take a step further and develop a methodology for assessing the influence of different sociotechnical pathways on the future transitions of urban drainage systems. There are also studies through which microscale implementations of blue-green measures in smaller urban districts are optimized (Eckart et al., 2018; Huang et al., 2018; Leimgruber et al., 2019). Furthermore, investigations regarding the macroscale hydro-economic optimization of multiple mesoscale blue-green stormwater systems in interaction with the existing and mostly underground urban drainage infrastructure have recently been drawing attention in the scientific community (e.g., Bakhshipour et al., 2019; Glenis et al., 2018; Zhou et al., 2018). Sustaining the functionality of the existing drainage network, especially the combined sewer network, which is associated with basement flooding and higher health risks, is a crucial subject in cities worldwide.

Such upscaling of mesoscale blue-green stormwater systems has hypothetically the potential to prevent the hydraulic overloading of the drainage network. However, economic consequences should also be taken into consideration since economy – along with ecology and society – is one of the fundamental pillars of sustainability (Wilkins, 2008). This means that both the quantity (retention volume) and location of the mesoscale blue-green stormwater systems (i.e., distribution of retention volumes) with respect to the existing drainage network must be investigated and optimized with regard to costs and benefits. Costs and benefits may, in a broad context, include a range of different socio-ecological factors in addition to monetary/financial aspects. However, in order to delimit the study boundaries in this paper, we focus on strictly financial costs related to the implementation of blue-green systems and flood hydraulics.

Therefore, the aim of this study is to develop and introduce a methodology to systematically locate mesoscale blue-green stormwater systems throughout the city to achieve the lowest possible flooding-damage related costs through a cost-effective implementation scenario. Having the methodology development in focus at a large-scale view, a generic transfer of mesoscale blue-green systems is applied in order to facilitate the theoretical siting and sizing of these systems throughout cities. It should be noted that practical implementation with regard to detailed design and choice of SCMs according to local circumstances in each catchment – e.g. land availability, land ownership, and physical characteristics of the area – is left for complementing studies.

2. Software architecture

To perform the optimization study, cosimulation of physical rainfall-runoff processes encompassing three different domains was structured. These domains were:

- D₁* Hydrological simulation of conventional catchments
- D₂* Hydrological and hydraulic simulation of blue-green catchments
- D₃* Hydrodynamic simulation of the sewer system loaded by the results from domains *D₁* and *D₂*.

To manage the cosimulation of these three domains, a hybrid model consisting of two modules, *hydrological* and *hydraulic*, was constructed. Domains *D₁* and *D₂* are included in the *hydrological module*, whereas domain *D₃* is simulated under the *hydraulic module*.

The model concerning the simulation of the mesoscale blue-green system (Domain *D₂*) is the model developed and presented in detail by Haghighatafshar et al. (2019), while the rainfall-runoff engine of MIKE Urban by DHI was employed for the hydrological simulation of conventional catchments (Domain *D₁*). The mesoscale blue-green model

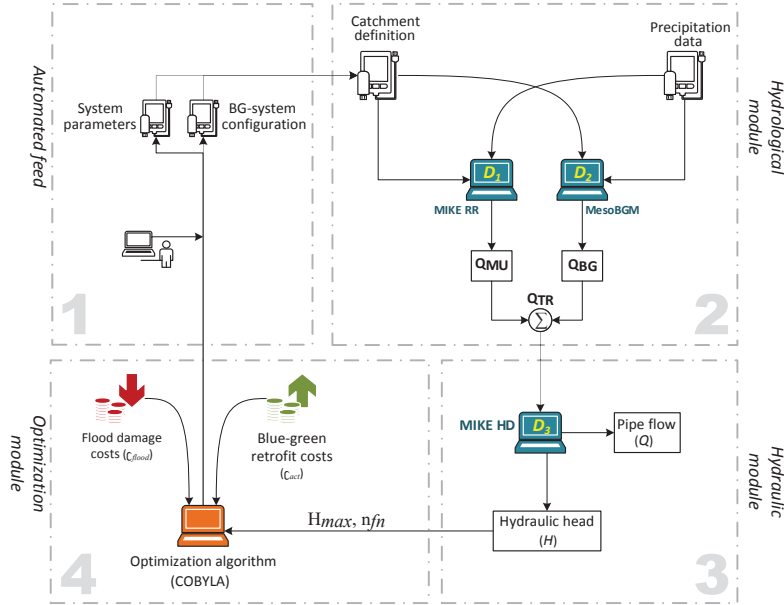


Fig. 1. The modeling and optimization logics (encompassing four major modules) were implemented in MIKE Operations to couple MIKE Urban and MesoBGM.

(*MesoBGM*) – introduced by Haghighatafshar et al. (2019) – simulates the hydrograph of the discharge from a mesoscale blue-green stormwater system. This discharge is then accumulated with MIKE Urban's rainfall-runoff (MIKE RR) output and is introduced as the input to the 1D MIKE Urban hydrodynamic simulation model (MIKE HD). MIKE Operations by DHI were employed as the cosimulation platform to facilitate communication between the three models, i.e., *MesoBGM*, MIKE RR, and MIKE HD. The suggested algorithm implemented in MIKE Operations is presented in Fig. 1, encompassing four major modules:

- User-defined/automated feed* where the parameter sets for the definition of catchments as well as the system parameters are managed.
- Hydrological module* for calculation of the hydrological load (D_1 and D_2).
- Hydraulic module* for assessing the performance of the drainage network (D_3).
- Optimization module* for performing the optimization based on the cost-benefit assessment,

The characteristics of the urban catchment in the joint model are defined in the user-defined/automated feed block, which is in turn fed into the hydrological module. The estimation of model parameters for D_1 is performed according to the standard procedure recommended by the Swedish Water and Wastewater Association (SWWA, 2016), whereas the characteristics of the mesoscale blue-green stormwater system (D_2) are defined according to Haghighatafshar et al. (2019). In addition to network setup, runoff coefficients, time-area curves, retention volumes, etc., the introduced feed also consists of the blue-green retrofit area (ABG,i) in the i^{th} subcatchment with a total area of ASC,i . Based on the introduced feed, D_1 and D_2 generate hydrological load schemes, denoted as $Q_{MU,i}$ and $Q_{BG,i}$ (time series), respectively, in which

the contributing area to $Q_{MU,i}$ is $ASC,i - ABG,i$.

In the next stage, the overall hydrologic load (total runoff, Q_{TR}) – as a cumulated time series – is calculated according to Eq. (1).

$$Q_{TR} = \sum_{i=1}^n (Q_{MU,i} + Q_{BG,i}) \quad (1)$$

This means that the discharge from the mesoscale blue-green system is still connected to the sewer network. The cumulative total flow, Q_{TR} , is then introduced as the network load to the MIKE HD model (D_3), through which 1D Saint-Venant's mass and momentum equations are applied for the computation of flow (Q) and piezometric pressure (hydraulic head, H) in the pipes (DHI, 2017). The ground level – in the context of a separate sewer network – and the basement level – in the context of a combined sewer network – for each manhole can be used to define a critical hydraulic head, h_c , at which exceedance can be interpreted as flooding. It should also be noted that the 0D/1D nature of the hybrid model made it appropriate for performing numerous large-scale simulations in terms of simulation time and computational costs.

2.1. The optimization module

As shown in Fig. 1, optimization is performed with regard to flood economics. The basic idea is that the investment in flood mitigation measures would lead to lower flood damage costs, hence these two parameters, i.e., investment in measures and maintenance (cost of action, C_{act}) and flood damage cost (C_{flood}) can be incorporated into a scalar cost function. However, it is necessary that these costs are quantified according to the specific perspective of the stakeholder who performs the optimization, e.g., insurance companies, water utility companies, municipalities, or government. Note that additional socio-ecological



Fig. 2. The catchment area, encompassing 954.35 ha, connected to the combined sewer network in Malmö, Sweden, drained through the Turbinen pump station. Background picture: GSD-Orthophoto, courtesy of The Swedish Mapping, Cadastral and Land Registration Authority, ©Lantmäteriet.

benefits associated with blue-green stormwater systems are not included in this study. Incorporation of monetized and quantified added socio-ecological values would presumably have strong impacts on optimization results.

The annual cost of action and flood damage cost are calculated according to Eqs. (2) and (3), respectively as follows:

$$C_{act} = f\left(\sum A_{BG}(u), c_{BG}, i, L\right) \\ = \sum A_{BG} \left(c_{BG} \cdot \left[\frac{i(1+i)^L}{(1+i)^L - 1} \right] + \frac{M}{L} \cdot \sum_{j=0}^{L-1} (1+\alpha)^j \right) \quad (2)$$

where $\sum A_{BG}(u)$ is the total area of the retrofitted blue-green stormwater system (ha) according to scenario u , c_{BG} is the average cost of blue-green stormwater retrofits per hectare (SEK/ha), L is the technical lifespan of the constructed system (50 years, which is the local standard assumption in infrastructure investments), M is the annual maintenance cost, α is the average annual pay raise ($\sim 2\%$), and i is the average interest rate ($\sim 3\%$). A similar approach for computing the annual cost of action was also adopted by Huang et al. (2018).

$$C_{flood} = f(n_m(u), c_m, i, T) = (c_m \cdot n_m(u)) \left[\frac{i}{(1+i)^T - 1} \right] \quad (3)$$

where $n_m(u)$ is the number of flooded manholes in scenario u , c_m is the average damage cost per flooded manhole (SEK/manhole), T is the recurrence interval of the optimization storm (years), and i is the average interest rate ($\sim 3\%$). Eq. (2) represents the uniform annual worth of the investment in year 0 through the lifespan of the blue-green stormwater system by using a capital recovery factor, and Eq. (3) represents the uniform annual cost of a total future fund (i.e., future cost of flood damage) during T years (assuming that the flood recurrence follows the recurrence period of the rainfall event) using a sinking fund factor (Blank and Tarquin, 2012). Subsequently, a scalar total cost function can be introduced (Eq. (4)). This total cost function (Eq. (4)) is later incorporated in the scalar multiobjective to determine a scenario matrix (u) resulting in the minimum possible cost.

$$\Phi(u) = C_{act}(u) + C_{flood}(u) \quad (4)$$

where u is the scenario matrix representing the implementation extent of the blue-green stormwater system in different sub-catchments. For instance, in a drainage model with k subcatchments, u can be specified according to Eq. (5).

$$u = [\mathcal{F}_{BG,1}, \mathcal{F}_{BG,2}, \dots, \mathcal{F}_{BG,k}] \quad (5)$$

where $\mathcal{F}_{BG,i}$ is the implementation extent, i.e., the ratio of the blue-green retrofitted area in subcatchment i ($A_{BG,i}$) to the total subcatchment area ($A_{SC,i}$), defined according to Eq. (6).

$$\mathcal{F}_{BG,i} = \frac{A_{BG,i}}{A_{SC,i}} \in [0, 1] \quad (6)$$

3. Case study

The general methodology adopted in this study is to employ hydrodynamic modeling to systematically optimize the distribution of blue-green stormwater systems in an urban catchment drained through a combined sewer network. This case study presents an example of how the developed methodology can be employed to enhance and understand the functionality of urban drainage systems.

3.1. Study area: Malmö, Sweden

Malmö is the 3rd largest city in Sweden located in the southern part of the country and is populated by over 330,000 people (Malmö stad, 2018). The drainage network in the city is mainly dominated by a combined sewer system in densely built central areas, while in the suburbs, mainly separate sewer networks are functional. This study focuses specifically on the combined sewer network and its corresponding catchment. The reason is that the city has been struck by extreme rainfall events several times and has undergone a relatively large burden of expenses due to basement flooding in the combined sewer network catchments (Haghighatafshar et al., 2014; Sørensen and

Mobini, 2017).

For this study, part of the combined sewer network and its corresponding catchment, which is drained into the *Turbinen* pump station in Malmö, was selected as shown in Fig. 2. The pump station receives combined sewer flows from two separate catchments, namely, the West catchment and the East catchment, drained from the south and south-east, respectively, toward the pump station. More information about the distribution of the combined and separate sewer networks in Malmö can be found in Haghighatafshar et al. (2018b) and Sörensen and Mobini (2017).

The fundamental approach in this study is to replicate the mesoscale blue-green system in Augustenborg – as the reference mesoscale retrofit described in Haghighatafshar et al. (2019, 2018a) – to achieve an optimized upscaling scenario. Augustenborg comprises two major mesoscale blue-green stormwater systems: one each in the south (Southern system, implemented 1999–2001), with a drainage area of roughly 9.6 ha, and north (Northern system, implemented 2002–2003), with a drainage area of approximately 6.3 ha. In addition, a separate local stormwater pipe system was constructed in 2003, covering a drainage area of about 3.5 ha. These three subsystems of Augustenborg are

illustrated in Fig. 3. For more information about the configuration of the mesoscale blue-green stormwater systems in Augustenborg refer to Haghighatafshar et al. (2019, 2018a). In this study, it is assumed that the Southern system in Augustenborg, accounting for a total drainage area of 9.6 ha ($= A_{Aug}$) can be replicated as a scaled retrofit depending on the area of the target catchment. In other words, the configuration in Augustenborg with regard to the drainage area, retention/detention volumes, and infiltration capacities can be linearly upsized/downsized to fit in the target catchment at various implementation extents ($\mathcal{F}_{BG,i}$). In this way, two major simplifications are introduced into the modeling process. First, there is no need to design and simulate specific systems based on local circumstances for each and every target catchment. Second, the original shape and form of the output hydrograph from Augustenborg (Q_{Aug}) is retained intact while values are manipulated by factor ξ_i . Upsizing and downsizing the Augustenborg system is performed according to the equations below:

$$\xi_i = \frac{A_{BG,i}}{A_{Aug}} \quad (7)$$

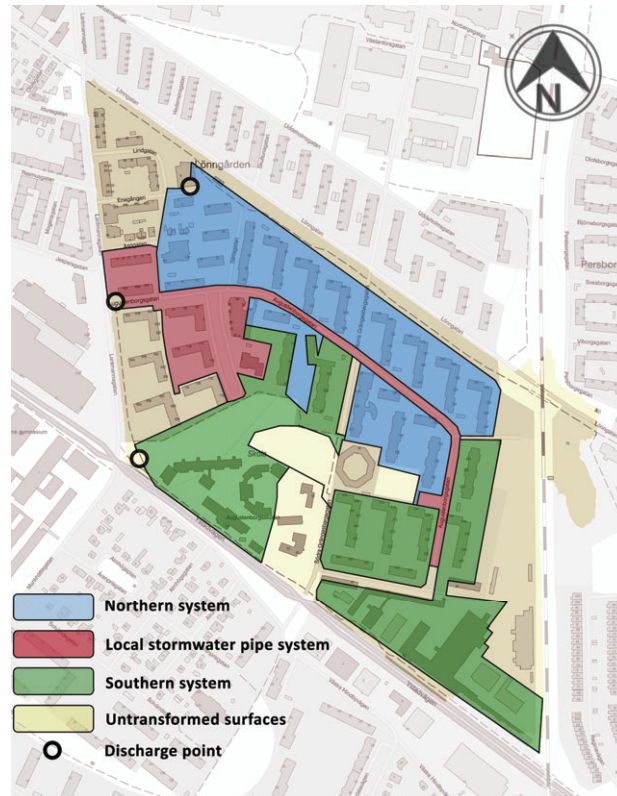


Fig. 3. Subsystems of Augustenborg, including two blue-green stormwater retrofits and the local pipe system. The figure also shows the discharge points from the subsystems to the sewer network.

Table 1

The subcatchments in the optimization study, totaling 954.35 ha (see Fig. 4 for the graphic illustration).

| ID | District name | Area (ha) | ID | District name | Area (ha) |
|-----|----------------|-----------|-----|-----------------|-----------|
| 1 | Fridhem N | 18.09 | 14 | Djupadal NV | 48.93 |
| 2 | Ribersborg | 18.52 | 15 | Kroksbäck | 63.97 |
| 3 | Rönneholm | 58.85 | 16 | Djupadal S | 91.59 |
| 4 | Fägelbacken | 17.20 | 17 | Möllevången | 21.02 |
| 5 | Fridhem Ö | 18.88 | 18 | Södervärn | 26.61 |
| 6 | Rönneholm SV | 12.33 | 19 | Södra Sofielund | 13.28 |
| 7 | Dammfri | 58.16 | 20 | Gröndal | 61.21 |
| 8 | Lorensborg | 33.28 | 21 | Kulladal | 56.91 |
| 9 | Västervång | 10.22 | 22 | Heleneholm | 24.35 |
| 10 | Fridhem SÖ | 8.31 | 23a | Eriksfält V | 7.97 |
| 11a | Mellanheden V | 24.57 | 23b | Eriksfält Ö | 21.48 |
| 11b | Mellanheden Ö | 25.93 | 24 | Almhög | 32.30 |
| 12a | Nya Bellevue V | 15.39 | 25 | Hindby | 27.38 |
| 12b | Nya Bellevue Ö | 46.11 | 26 | Gullvik N | 11.50 |
| 13 | Rosenvång | 37.29 | 27 | Gullvik S | 42.72 |

$$Q_{TR,i} = Q_{MU} + Q_{BG} = Q_{FRC,i}(1 - \mathcal{F}_{BG,i}) + Q_{SRC,i} + Q_{ww,i} + \xi_i Q_{Aug} \quad (8)$$

where A_{BG} is the area occupied by the blue-green retrofit (ha), A_{SC} : target subcatchment area (ha), \mathcal{F}_{BG} : implementation extent in the target catchment ($0 \leq \mathcal{F}_{BG} \leq 1$), $A_{Aug} = 9.6$ ha = area of the existing retrofit in Augustenborg in Malmö (the Southern retrofit), ξ_i : retrofit scale compared to the reference, i.e., the Southern retrofit in Augustenborg, Q_{MU} : runoff from the conventional catchment simulated in MIKE Urban, Q_{BG} : runoff (discharge) from the blue-green system, Q_{FRC} : fast runoff component of the flow (stormwater), Q_{Aug} : discharge from the Southern retrofit in Augustenborg, Q_{ww} : domestic wastewater flow, Q_{SRC} : slow runoff component of the flow (groundwater infiltration), and Q_{TR} : total runoff to be handled by the pipe network.

3.2. The optimization problem

The goal of the unconstrained, bounded optimization problem was to minimize the total cost of flooded nodes, C_{flood} , and the cost of implementation of the blue-green systems based on the Augustenborg system, C_{act} . The cost of flooded nodes was expressed using the average cost per flooded node, C_{fn} , based on a rough assessment of the available data from the extensive flooding in Malmö in 2014. Thus, C_{flood} , in the case of a 10-year rainfall event (as employed in this study), was estimated at 47,000 SEK/(year-flooded node), and C_{act} (including maintenance) was estimated to be 110,000 SEK/(year-retrofitted area) during the 50-year lifespan of the built system. It should be noted that these values are preliminary assessments and cannot be considered as verified template costs in other contexts.

The cost of action was assumed to be linear with respect to the area of the constructed blue-green systems, as described in Eqs. (2) and (3), and the costs were then combined according to Eq. (4). A performance indicator (PI) was then constructed and used as the objective for the optimization to more easily discern whether a tested solution is cheaper than the reference case ($PI < 0$) or worse ($PI > 0$).

The 1D model area was divided into 30 different subcatchments, as presented in Table 1 and Fig. 4. In other words, the optimization space to be investigated was a high-dimensional space with 30 dimensions corresponding to the 30 decision variables that the subcatchments constitute.

The implementation extent of each catchment ($\mathcal{F}_{BG,i}$, defined in Eqs. (5) and (6)) was used as decision variables. The decision variables were bounded by the characteristics of the catchments by setting the bounds to $[0, 1]$, representing catchments that are empty or full (or in between) with regards to the blue-green systems. With the reference case of no implemented blue-green solutions, i.e., $\Phi_{Ref} = C_{flood}(0)$, the full

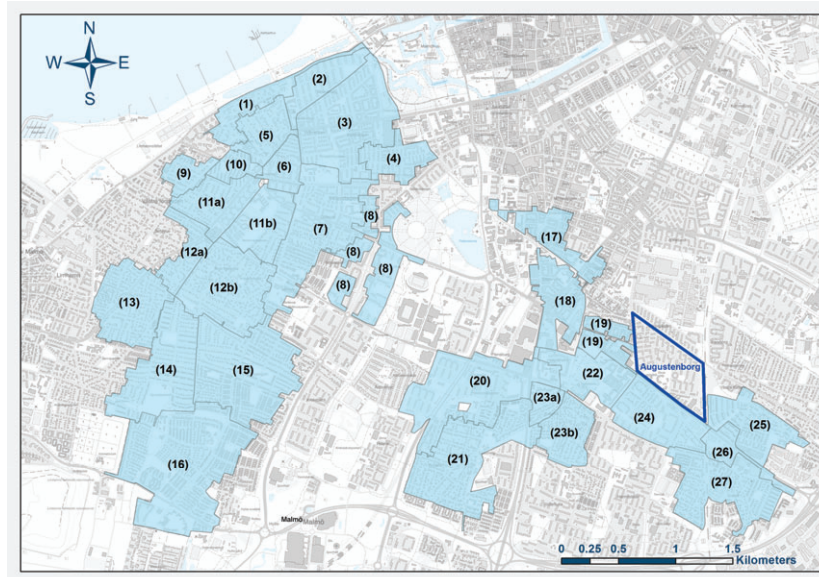


Fig. 4. The spatial distribution of model subcatchments in the city of Malmö, Sweden. Background picture: dimmed topographic web map, courtesy of The Swedish Mapping, Cadastral and Land Registration Authority, ©Lantmäteriet.

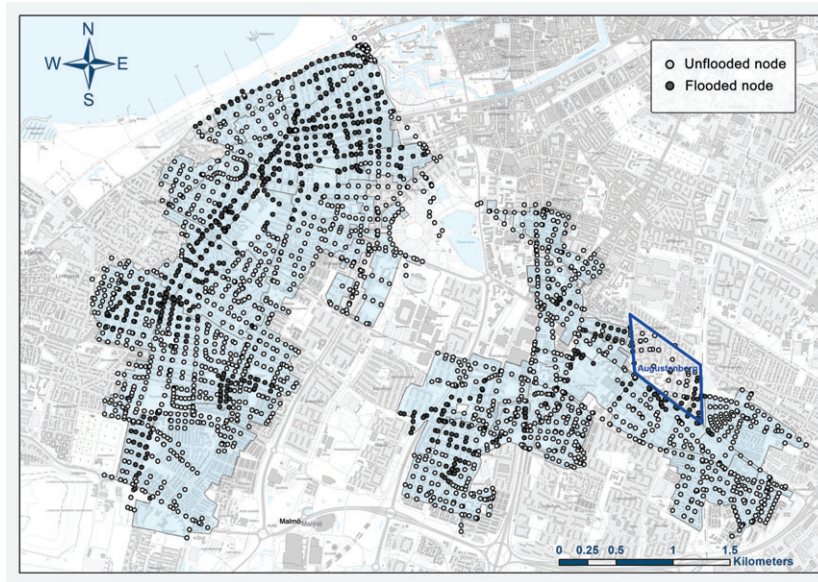


Fig. 5. Flooded nodes (filled markers, ●) and unflooded nodes (unfilled markers, ○) under the reference scenario, i.e., $10y\text{-}CDS$; $\mathcal{F}_{BG,i} = 0$. Background picture: dimmed topographic web map, courtesy of The Swedish Mapping, Cadastral and Land Registration Authority, ©Lantmäteriet.

optimization problem was expressed as:

$$\min \quad PI = \frac{\Phi(u) - \Phi_{Ref}}{\Phi_{Ref}}$$

$$\text{w.r.t. } u = [\mathcal{F}_{BG,1}, \dots, \mathcal{F}_{BG,k}]$$

$$\text{s.t. } \mathcal{F}_{BG,i} \in [0, 1] \quad \text{for } i \in [1, 2, \dots, k]$$

4. Results and discussion

The optimization problem was solved using the SciPy implementation of the algorithm known as constrained optimization by linear approximation (COBYLA), which is a derivative free method (Conn et al., 1997; Powell, 1994). The optimization was performed for a Chicago Design Storm (CDS) (Keifer and Chu, 1957) with a recurrence interval of 10 years, denoted as $10y\text{-}CDS$. The initial values for the decision variables were the reference case, i.e., $\mathcal{F}_{BG,i} = 0$. In the reference case, the water level in 779 manholes was over the average basement level (assumed to be 1.3 m below the ground level), leading to basement flooding. The spatial distribution of the flooded manholes (model nodes) is illustrated in Fig. 5.

After the simulation of the reference case scenario, the optimization process under the $10y\text{-}CDS$ continues to locate an optimum (local minimum for $\Phi(u)$) according to the design of the COBYLA-algorithm. Fig. 6 is a two-dimensional illustration of approximately 100 iterations.

As shown in Fig. 6, the optimization started with the reference scenario, and all subsequent iterations are presented in the clockwise order. The first 30 iterations have an average PI value of approximately +0.04 (increased costs). The optimization continues with systematic alterations in the implementation extents and moves toward an average PI of approximately -0.01 (decreased costs) and ultimately

finds an optimal solution with a PI of almost -0.03 and 714 flooded nodes. The results of the optimization process suggested that sub-catchments 1 and 19 should be transformed to mesoscale blue-green stormwater systems at 56.6% (≈ 10 ha) and 63.6% (8.5 ha), respectively. Based on this optimization, the total cost of a $10y\text{-}CDS$ event will be 3% lower than the cost of flooding under the reference case scenario. This shows that there is at least one scenario through which implementation of blue-green stormwater systems would lead to less overall costs, i.e., the sum of action and flood costs, than the reference case scenario.

Although the financial benefit is limited in the optimized scenario, the total number of the flooded nodes is decreased by approximately 8.5%. The green nodes in Fig. 7 show the spatial distribution of 65 nodes that do not flood in the optimized scenario compared to the reference. It is also interesting to note that the majority of the saved nodes (44 nodes) lie within the boundaries of the optimally retrofitted sub-catchments, i.e., 1 and 19, while the rest (21 nodes) are in other sub-catchments with $\mathcal{F}_{BG,i}=0$. This shows that the benefits of mesoscale blue-green retrofits are not limited to the retrofit boundaries.

Although economic savings ($\sim 3\%$) are modest, it should be noted that this value exclusively represents the monetary and financial aspects of the action. However, from a cost-benefit perspective, the value of the blue-green systems is much more comprehensive and may include aesthetics, societal add-ons in terms of human well-being, amenity, and promoted biodiversity. In this respect, tools for monetization and quantification of multiple benefits of blue-green stormwater systems, such as BeST (Ashley et al., 2016, 2018), are becoming widely available. These tools can be employed and adapted to local contexts in order to enhance the decision-making process.

As seen in Fig. 6, there is one iteration – marked with (D) – that despite introduced blue-green retrofits – leading to elevated costs by

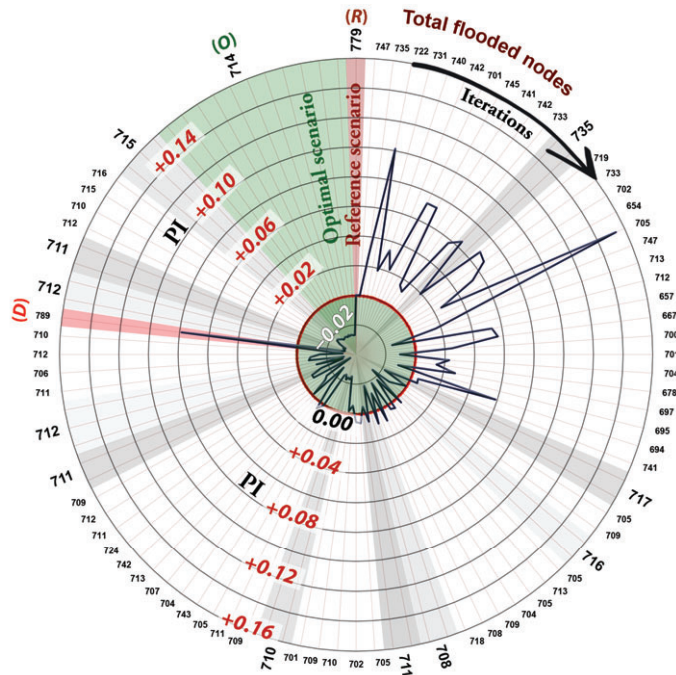


Fig. 6. Convergence map of 100 iterations (out of 325) using COBYLA. Angular axes show the total number of flooded nodes, and the radial axes show the performance indicator (PI) for each iteration. (R): Reference scenario, (D): Deteriorated scenario, and (O): Optimal scenario.

approximately 8% – the number of flooded nodes has increased to 789 compared to the reference scenario (779 flooded nodes). An explanation for this deteriorated behavior is that in the complex system of catchment-sewer interactions, even detained and retained discharges from catchments can possibly coincide with some peak discharge along the way causing elevated hydraulic head and, hence, flooding. This agrees with the recommendation by Haghighatafshar et al. (2018b), who advise the implementation of blue-green stormwater retrofits in the upstream areas of a city catchment to avoid (or decrease the risk of) deteriorative flow coincidences. The deteriorated flood situation, despite the introduction of blue-green stormwater systems, is an indication that unoptimized retrofits of blue-green systems in which the discharge is connected to the same sewer network do not necessarily improve the hydraulic performance of the network. The same phenomenon could also occur when rainfalls other than the optimization rainfall, with different hyetograph characteristics, strike. Thus, there might be situations through which a different rainfall would lead to different times of concentration and lag times so that the aforementioned unprecedented flow coincidences and flooding occur. A safe retrofitting strategy would thus be the total separation of the blue-green stormwater retrofits through which the overflow from the system does not enter the original sewer network but is diverted into a separate stormwater pipe network, as is the case for Augustenborg (see Fig. 4). Further research must be performed to achieve a better understanding of the complex behavior of sewer networks.

A sensitivity analysis was conducted according to the one-factor-at-a-time (OFAT) method with respect to C_{act} and C_{flood} in order to

demonstrate the sensitivity of the PI to the quality of the cost estimation. It should be noted that different perturbations to c_{fn} , c_{BG} and M were performed as C_{flood} is directly proportional to c_{fn} and C_{act} is directly proportional to $c_{BG} + M$ (provided c_{BG} and M are simultaneously and identically perturbed, all else unchanged). In effect, perturbations to the action cost and flooding cost, as well as their simultaneous perturbation (i.e. $\Phi(u)$), were performed ranging from -50% to $+50\%$. All other parameters, such as the hydrological characteristics of the toolchain, total retrofitted blue-green area, and number of flooded manholes, were kept unchanged. The resulting outcomes of these perturbations with regard to the delivered PI are shown in Fig. 8.

As shown in Fig. 8, the PI is extremely sensitive to the estimation of C_{flood} rather than C_{act} . For instance, it is observed that a reduced cost of flooding by 30% would enhance the PI by a factor of 10 (from -0.03 to -0.3), while the corresponding PI change in the case of perturbations in C_{act} is negligible. This is also reflected in the simultaneous perturbation of the costs (both cost of action and cost of flood), as it is in strong agreement with the sensitivity to C_{flood} only. However, the provided results do not necessarily imply that the quality of the estimated cost of action (implementation and maintenance of the blue-green systems) has a trivial impact on the optimization outcome. The small impact of C_{act} on the PI is mainly due to the fixed blue-green scenario (the scenario presented in Fig. 7) under which all perturbations are tested. As noted in Fig. 7, the retrofitted area is relatively small in comparison to the reference case (approximately 2% of the total modeled catchment area), while the proportion of the flooded manholes in the optimized scenario compared to the reference scenario is

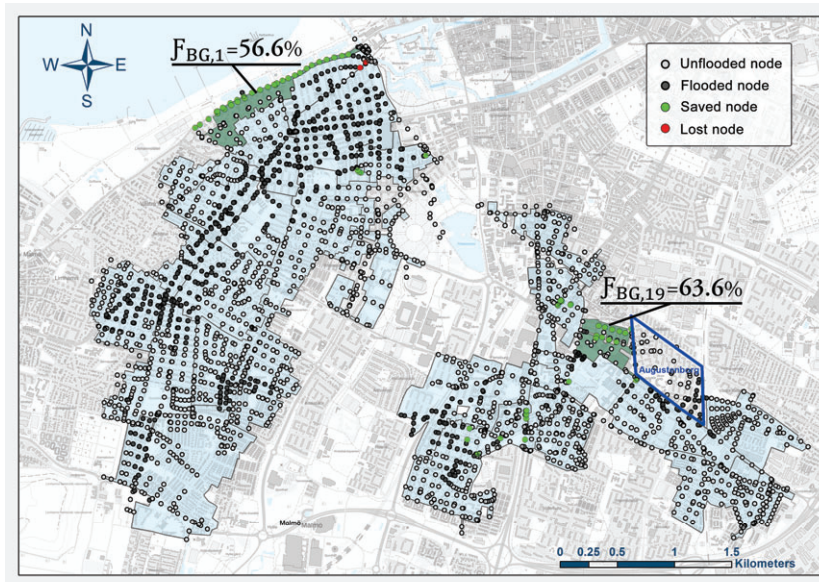


Fig. 7. Optimized scenario with respect to implementation extents, flooded (filled markers, ●), unflooded (unfilled markers, ○), saved (green-filled markers, ●), and lost (red-filled markers, ●) nodes. Background picture: dimmed topographic web map, courtesy of The Swedish Mapping, Cadastral and Land Registration Authority, ©Lantmäteriet.

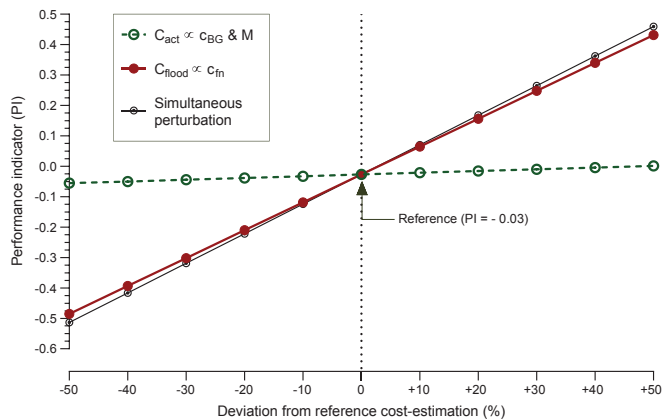


Fig. 8. The sensitivity of PI to the perturbations in the cost estimations associated with the optimization study.

approximately 92%. This specific optimized setup thus underlines the importance of estimation of C_{flood} opposed to C_{act} . However, it is highly anticipated that perturbations in either of the associated costs (or both) would result in substantial changes in the outcome of the optimization process regarding the returned optimal \mathcal{F}_{BGJ} -matrix as well as the PI. Further investigations must be carried out to study the direct sensitivity

of the optimization process to deviations and errors in the estimated cost components.

5. Concluding remarks

A hybrid model was structured to run cosimulations of mesoscale

blue-green stormwater systems and the pipe-bound sewerage network. The model was subsequently facilitated with an optimization algorithm to suggest hydroeconomically optimal solutions for citywide siting and sizing of mesoscale blue-green stormwater systems. The developed software package was tested on a city-scale catchment drained through a combined sewer system. The model delivered satisfactory results concerning promoted hydraulic performance of the sewer network (in terms of decreased flooded nodes) and financial gains. However, locating the global optimum remains a challenge due to the extremely high dimensionality of the optimization space. Given these circumstances, the model performance was shown to fulfill the general aim of the study. Further research is required to improve the optimization process and move the solution toward a global optimum. This can be done by employment of different gradient-free optimization techniques, such as evolutionary or simulated annealing algorithms, or by employing algorithms that make use of formulated analytical Jacobians. There is also the possibility to implement decision variable selection techniques to decrease the dimensionality of the decision space.

Moreover, there are indications that the performance of the optimized scenario might be specifically valid for the exact rainfall hyetograph for which the model is optimized. This also remains a serious challenge considering the stochastic nature of rainfalls and the complexity of sewer networks. It is also implied that random sizing and siting of blue-green retrofits without investigating the hydraulic consequences on the existing sewer network could lead to deterioration in the performance of the sewer network in terms of the number of flooded nodes.

CRedit authorship contribution statement

Salar Haghighatafshar: Conceptualization, Investigation, Funding acquisition, Methodology, Project administration, Formal analysis, Visualization. **Mikael Yamane-Nolin:** Methodology, Software, Visualization. **Anders Klinting:** Methodology, Software. **Maria Roldin:** Supervision, Methodology, Software. **Lars-Göran Gustafsson:** Methodology, Software. **Henrik Aspegren:** Supervision, Investigation, Resources, Funding acquisition. **Karin Jönsson:** Supervision, Investigation, Resources, Funding acquisition.

Declaration of Competing Interest

The authors declare that they have no known competing financial interests or personal relationships that could have appeared to influence the work reported in this paper.

Acknowledgements

This project was financially supported by the J. Gustaf Richert Foundation at SWECO (grant number 2018-00430), Sweden Water Research and the Swedish Water and Wastewater Association via *VA-teknik Södra*. The authors are thankful to *Susanne Steen Kronborg* and *Emma Falk* at VA SYD for their contributions to the setup of the MIKE model for Malmö. All background maps (either orthophoto or topographic web map) used in the figures of this article are courtesy of the Swedish Mapping, Cadastral and Land Registration Authority, ©Lantmäteriet.

References

- Arnbjerg-Nielsen, K., 2012. Quantification of climate change effects on extreme precipitation used for high resolution hydrologic design. *Urban Water J.* 9, 57–65. <https://doi.org/10.1080/1573062X.2011.630091>.
- Ashley, R., Dugman, C., Horton, B., Gersonius, B., Smith, B., Baylis, A., 2016. Using the multiple benefits of SuDS tool (BeST) to deliver long-term benefits. In: The 9th International Conference on Planning and Technologies for Sustainable Management of Water in the City, 28 June–1 July 2016. NOVATECH, Lyon, France.
- Ashley, R.M., Gersonius, B., Dugman, C., Horton, B., Bacchin, T., Smith, B., Shaffer, P., Baylis, A., 2018. Demonstrating and monetizing the multiple benefits from using SuDS. *J. Sustain. Water Built Environ.* 4. <https://doi.org/10.1061/JSWBAY.00000848>.
- Azzout, Y., Barraud, S., Cres, F.N., Alfallah, E., 1995. Decision aids for alternative techniques in urban storm management. *Water Sci. Technol.* 32, 41–48. <https://doi.org/10.2166/wst.1995.0011>.
- Bach, P.M., McCarthy, D.T., Ulrich, C., Sitzenfrei, R., Kleidorfer, M., Rauch, W., Deletic, A., 2013. A planning algorithm for quantifying decentralised water management opportunities in urban environments. *Water Sci. Technol.* 68, 1857–1865. <https://doi.org/10.2166/wst.2013.437>.
- Bakhsipour, A.E., Dittmer, U., Haghighi, A., Nowak, W., 2019. Hybrid green-blue-gray decentralized urban drainage systems design, a simulation-optimization framework. *J. Environ. Manage.* 249, 109364. <https://doi.org/10.1016/j.jenvman.2019.109364>.
- Bernidsson, R., Becker, P., Persson, A., Aspegren, H., Haghighatafshar, S., Jönsson, K., Larsson, R., Mobini, S., Mottaghi, M., Nilsson, J., Nordström, J., Pilejaj, P., Scholz, M., Sternudd, C., Sörensen, J., Tussupova, K., 2019. Drivers of changing urban flood risk: a framework for action. *J. Environ. Manage.* 240, 47–56. <https://doi.org/10.1016/j.jenvman.2019.03.094>.
- Blank, L., Tarquin, A., 2012. *Engineering Economy*, seventh ed. McGraw-Hill, New York, USA.
- BlueGreenCities, 2019. What is a Blue-Green City? [WWW Document]. URL <http://www.bluegreencities.ac.uk/about/bluegreencitiesdefinition.aspx> (accessed 8.23.19).
- Conn, A.R., Scheinberg, K., Toint, P., 1997. On the convergence of derivative-free methods for unconstrained optimization. In: Iserles, A., Buhmann, M. (Eds.), *Approximation Theory and Optimization: Tributes to M. Cambridge University Press*, Cambridge, UK. J. D. Powell, pp. 83–108.
- Cunha, M.C., Zeferino, J.A., Simões, N.E., Saldarriaga, J.G., 2016. Optimal location and sizing of storage units in a drainage system. *Environ. Model. Softw.* 83, 155–166. <https://doi.org/10.1016/j.envsoft.2016.05.015>.
- Demuzere, M., Orru, K., Heidrich, O., Olazabal, E., Geneletti, D., Orru, H., Bhawe, A.G., Mittal, N., Feliu, E., Faehle, M., 2014. Mitigating and adapting to climate change: multi-functional and multi-scale assessment of green urban infrastructure. *J. Environ. Manage.* 146. <https://doi.org/10.1016/j.jenvman.2014.07.025>.
- DHI, 2017. MIKE Urban Collection System – Modelling of storm water drainage networks and sewer collection systems (User guide). MIKE Powered by DHI.
- Dolowitz, D.P., Bell, S., Keeley, M., 2018. Retrofitting urban drainage infrastructure: green or grey? *Urban Water J.* 15, 83–91. <https://doi.org/10.1080/1573062X.2017.1396352>.
- Eckart, K., McPhee, Z., Bolisetti, T., 2018. Multiobjective optimization of low impact development stormwater controls. *J. Hydrol.* 562, 564–576. <https://doi.org/10.1016/j.jhydrol.2018.04.068>.
- Everett, G., Lawson, E., Lamond, J., 2015. Green infrastructure and urban water management. In: Sinnett, D., Smith, N., Burgess, S. (Eds.), *Handbook on Green Infrastructure: Planning Design and Implementation*. Edward Elgar Publishing.
- Fenner Richard, R., 2017. Spatial evaluation of multiple benefits to encourage multi-functional design of sustainable drainage in blue-green cities. *Water* 9, 953. <https://doi.org/10.3390/w9120953>.
- Fletcher, T.D., Shuster, W., Hunt, W.F., Ashley, R., Butler, D., Arthur, S., Trowsdale, S., Barraud, S., Semadeni-Davies, A., Bertrand-Krajewski, J.-L., Mikkelsen, P.S., Rivard, G., Uhl, M., Dagenais, D., Viklander, M., 2015. SUDS, LID, BMPs, WSUD and more – The evolution and application of terminology surrounding urban drainage. *Urban Water J.* 12, 525–542. <https://doi.org/10.1080/1573062X.2014.916314>.
- Glenis, V., Kutija, V., Kisly, C.G., 2018. A fully hydrodynamic urban flood modelling system representing buildings, green space and interventions. *Environ. Model. Softw.* 109, 272–292. <https://doi.org/10.1016/j.envsoft.2018.07.018>.
- Guo, Y., 2006. Updating rainfall IDF relationships to maintain urban drainage design standards. *J. Hydrol. Eng.* 11, 506–509. [https://doi.org/10.1061/\(ASCE\)1084-0699\(2006\)11:5\(506\)](https://doi.org/10.1061/(ASCE)1084-0699(2006)11:5(506)).
- Haghighatafshar, S., la Cour Jansen, J., Aspegren, H., Jönsson, K., 2018a. Conceptualization and schematization of mesoscale sustainable drainage systems: a full-scale study. *Water* 10, 1041. <https://doi.org/10.3390/w10081041>.
- Haghighatafshar, S., la Cour Jansen, J., Aspegren, H., Lidström, V., Mattsson, A., Jönsson, K., 2014. Storm-water management in Malmö and Copenhagen with regard to climate change scenarios. *VATTEN. J. Water Manage. Res.* 70, 159–168.
- Haghighatafshar, S., Nordlöf, B., Roldin, M., Gustafsson, L.-G., la Cour Jansen, J., Jönsson, K., 2018b. Efficiency of blue-green stormwater retrofits for flood mitigation – Conclusions drawn from a case study in Malmö, Sweden. *J. Environ. Manage.* 207, 60–69. <https://doi.org/10.1016/j.jenvman.2017.11.018>.
- Haghighatafshar, S., Yamane-Nolin, M., Larson, M., 2019. A physically based model for mesoscale SuDS – an alternative to large-scale urban drainage simulations. *J. Environ. Manage.* 240, 527–536. <https://doi.org/10.1016/j.jenvman.2019.03.037>.
- Hailegeorgis, T.T., Thorolfsson, S.T., Alfredsen, K., 2013. Regional frequency analysis of extreme precipitation with consideration of uncertainties to update IDF curves for the city of Trondheim. *J. Hydrol.* 498, 305–318. <https://doi.org/10.1016/j.jhydrol.2013.06.019>.
- Huang, C.L., Hsu, N.S., Liu, H.J., Huang, Y.H., 2018. Optimization of low impact development layout designs for megacity flood mitigation. *J. Hydrol.* 564, 542–558. <https://doi.org/10.1016/j.jhydrol.2018.07.044>.
- Keifer, C.J., Chu, H.H., 1957. Synthetic storm pattern for drainage design. *J. Hydraul. Div.* 83, 1–25.
- Kirby, A., 2005. SuDS – Innovation or a tried and tested practice?. In: Proceedings of the Institution of Civil Engineers: Municipal Engineer. pp. 115–122. doi: 10.1680/muen.2005.158.2.115.
- Kuichling, E., 1889. The relation between the rainfall and the discharge of sewers in populous districts. *Trans. Am. Soc. Civ. Eng.* 20, 1–56.
- Kuller, M., Bach, P., Ramirez-Lovering, D., Deletic, A., 2016. The Location Choice of Water Sensitive Urban Design Within a City: A Case Study of Melbourne. *IWA World*

- Water Congress and Exhibition, Brisbane, Australia.
- Leimgruber, J., Krebs, G., Camhy, D., Muschalla, D., 2019. Model-based selection of cost-effective low impact development strategies to control water balance. *Sustainability* 11, 20. <https://doi.org/10.3390/su11082440>.
- Li, C., Peng, C., Chiang, P.C., Cai, Y., Wang, X., Yang, Z., 2019. Mechanisms and applications of green infrastructure practices for stormwater control: a review. *J. Hydrol.* <https://doi.org/10.1016/j.jhydrol.2018.10.074>.
- Lima, C.H.R., Kwon, H.-H., Kim, Y.-T., 2018. A local-regional scaling-invariant Bayesian GEV model for estimating rainfall IDF curves in a future climate. *J. Hydrol.* 566, 73–88. <https://doi.org/10.1016/j.jhydrol.2018.08.075>.
- Liu, H., Jia, Y., Niu, C., 2017a. "Sponge city" concept helps solve China's urban water problems. *Environ. Earth Sci.* 76, 473. <https://doi.org/10.1007/s12665-017-6652-3>.
- Liu, S., Huang, S., Huang, Q., Xie, Y., Leng, G., Luan, J., Song, X., Wei, X., Li, X., 2017b. Identification of the non-stationarity of extreme precipitation events and correlations with large-scale ocean-atmospheric circulation patterns: a case study in the Wei River Basin, China. *J. Hydrol.* 548, 184–195. <https://doi.org/10.1016/j.jhydrol.2017.03.012>.
- Lloyd-Davies, D.E., 1906. The elimination of storm-water from sewerage systems. *Minutes Proc. Inst. Civ. Eng.* 164, 41–67. <https://doi.org/10.1680/imotp.1906.16637>.
- Mailhot, A., Duchesne, S., Caya, D., Talbot, G., 2007. Assessment of future change in intensity-duration-frequency (IDF) curves for Southern Quebec using the Canadian Regional Climate Model (CRCM). *J. Hydrol.* 347, 197–210. <https://doi.org/10.1016/j.jhydrol.2007.09.019>.
- Malmö stad, 2018. Malmö – Sweden's fastest-growing city [WWW Document]. URL <https://malmo.se/Kommun-politik/Fakta-och-statistik/In-english/Demographics/Population-growth.html> (accessed 12.04.18).
- Milly, P.C.D., Betancourt, J., Falkenmark, M., Hirsch, R.M., Kundzewicz, Z.W., Lettenmaier, D.P., Stouffer, R.J., 2008. Climate Change. Stationarity is dead: whither water management? *Science* 319, 573–574. <https://doi.org/10.1126/science.1151915>.
- Powell, M.J.D., 1994. A direct search optimization method that models the objective and constraint functions by linear interpolation. In: *Advances in Optimization and Numerical Analysis*. Springer, Netherlands, Dordrecht, pp. 51–67. https://doi.org/10.1007/978-94-015-8330-5_4.
- Ren, N., Wang, Qian, Wang, Qiuru, Huang, H., Wang, X., 2017. Upgrading to urban water system 3.0 through sponge city construction. *Front. Environ. Sci. Eng.* 11, 9. <https://doi.org/10.1007/s11783-017-0960-4>.
- Romn e, A., Evrard, A., Trachte, S., 2015. Methodology for a stormwater sensitive urban watershed design. *J. Hydrol.* 530, 87–102. <https://doi.org/10.1016/j.jhydrol.2015.09.054>.
- S rensen, J., Mobini, S., 2017. Pluvial, urban flood mechanisms and characteristics – Assessment based on insurance claims. *J. Hydrol.* 555, 51–67. <https://doi.org/10.1016/j.jhydrol.2017.09.039>.
- Stahre, P., 2006. Sustainability in Urban Storm Drainage – Planning and Examples, first ed. Svenskt Vatten, Stockholm, Sweden.
- Stahre, P., 1993. Assessment of BMPs Being Used in Scandinavia. Proceedings of the Sixth International Conference on Urban Storm Drainage. Seapoint Publishers, Niagara Falls, Ontario, Canada.
- SWWA, 2016. Drainage of Runoff and Wastewater – Functional Requirements, Hydraulic Dimensioning and Design of Public Sewer Systems (in Swedish). Publication P110, Swedish Water and Wastewater Association (Svenskt Vatten), Bromma, Sweden.
- Trenberth, K.E., Dai, A., van der Schrier, G., Jones, P.D., Barichivich, J., Briffa, K.R., Sheffield, J., 2014. Global warming and changes in drought. *Nat. Clim. Change* 4, 17–22. <https://doi.org/10.1038/nclimate2067>.
- VA SYD, 2019. Ett s krare och effektivare avloppssystem [A safer and more efficient wastewater system] [WWW Document]. URL <https://www.vasyd.se/Artiklar/Tunnel/Malmo-avloppstunnel> (accessed 08.27.19).
- Vogel, R.M., Yaindi, C., Walter, M., 2011. Nonstationarity: flood magnification and recurrence reduction factors in the United States. *JAWRA J. Am. Water Resour. Assoc.* 47, 464–474. <https://doi.org/10.1111/j.1752-1688.2011.00541.x>.
- Wang, M., Sun, Y., Sweetapple, C., 2017. Optimization of storage tank locations in an urban stormwater drainage system using a two-stage approach. *J. Environ. Manage.* 204, 31–38. <https://doi.org/10.1016/j.jenvman.2017.08.024>.
- Watt, E.W., Waters, D., McLean, R., 2003. Climate Change and Urban Stormwater Infrastructure in Canada: Context and Case Studies Climate Change and Urban Stormwater Infrastructure in Canada: Context and Case Studies CONTENTS PAGE. Toronto-Niagara Reg. Study Rep. Work. Pap. Ser. Rep. No. 2003-1, Meteorol. Serv. Canada, Waterloo, Ontario. 27.
- Wihlborg, M., S rensen, J., Alkan Olsson, J., 2019. Assessment of barriers and drivers for implementation of blue-green solutions in Swedish municipalities. *J. Environ. Manage.* 233, 706–718. <https://doi.org/10.1016/j.jenvman.2018.12.018>.
- Wilkins, H., 2008. The integration of the pillars of sustainable development: a work in progress. McGill Int J. Sustain. Dev. Law Policy/Rev. Int. droit Polit. du d veloppement durable McGill. <https://doi.org/10.2307/24352601>.
- Zhang, S., Li, Y., Ma, M., Song, T., Song, R., Zhang, S., Li, Y., Ma, M., Song, T., Song, R., 2018. Storm water management and flood control in sponge city construction of Beijing. *Water* 10, 1040. <https://doi.org/10.3390/w10081040>.
- Zhou, Q., Lai, Z., Blohm, A., 2018. Optimising the combination strategies for pipe and infiltration-based low impact development measures using a multiobjective evolution approach. *J. Flood Risk Manage.* 12. <https://doi.org/10.1111/jfr3.12457>.
- Zischg, J., Rogers, B., Gunn, A., Rauch, W., Sitzenfrie, R., 2019. Future trajectories of urban drainage systems: a simple exploratory modeling approach for assessing socio-technical transitions. *Sci. Total Environ.* 651, 1709–1719. <https://doi.org/10.1016/j.scitotenv.2018.10.061>.
- Zischg, J., Zeisl, P., Winkler, D., Rauch, W., Sitzenfrie, R., 2018. On the sensitivity of geospatial low impact development locations to the centralized sewer network. *Water Sci. Technol.* 77, 1851–1860. <https://doi.org/10.2166/wst.2018.060>.

Drainage channel and the *Gate of All Nations* in Persepolis, Iran



This thesis addresses an ancient challenge. Since the establishment of early civilizations, stormwater management has been an issue. Over centuries, a few paradigms of urban drainage have evolved. Open channel systems have likely been the most primitive solution, as seen in many excavations worldwide. With the growth of cities and populations, the management of human feces and domestic waste also became an issue. Having stormwater channels already in place, domestic waste(water) was also thrown into the open channel system. Not so thoughtful, right? Subsequently, to overcome the hygiene issues and discomfort due to odors, it was decided that the entire system be lowered to underground levels. This event is likely when combined sewer systems were born.

In the modern era, as hydrology and hydraulic sciences advanced, separate sewer systems were introduced, solving some of the challenges, such as basement flooding, but not all. The development of rain gauges, flow measurement techniques, and computational tools have contributed substantially to our understanding of how rainfall turns into runoff and how this runoff should be managed. In the past few decades, a “new” paradigm emerged: blue-green stormwater management, representing a call for looking to and learning from Mother Nature. This thesis is an attempt to embrace that call, as many others have, and examine today's complex drainage systems using modern knowledge and tools.

ISBN: 978-91-7422-681-2

Department of Chemical Engineering
Faculty of Engineering, LTH
Lund University